LEABHARLANN CHOLÁISTE NA TRÍONÓIDE, BAILE ÁTHA CLIATH | TRINITY COLLEGE LIBRARY DUBLIN
Ollscoil Átha Cliath | The University of Dublin

Terms and Conditions of Use of Digitised Theses from Trinity College Library Dublin

Copyright statement

All material supplied by Trinity College Library is protected by copyright (under the Copyright and Related Rights Act, 2000 as amended) and other relevant Intellectual Property Rights. By accessing and using a Digitised Thesis from Trinity College Library you acknowledge that all Intellectual Property Rights in any Works supplied are the sole and exclusive property of the copyright and/or other IPR holder. Specific copyright holders may not be explicitly identified. Use of materials from other sources within a thesis should not be construed as a claim over them.

A non-exclusive, non-transferable licence is hereby granted to those using or reproducing, in whole or in part, the material for valid purposes, providing the copyright owners are acknowledged using the normal conventions. Where specific permission to use material is required, this is identified and such permission must be sought from the copyright holder or agency cited.

Liability statement

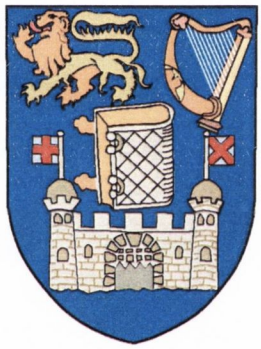
By using a Digitised Thesis, I accept that Trinity College Dublin bears no legal responsibility for the accuracy, legality or comprehensiveness of materials contained within the thesis, and that Trinity College Dublin accepts no liability for indirect, consequential, or incidental, damages or losses arising from use of the thesis for whatever reason. Information located in a thesis may be subject to specific use constraints, details of which may not be explicitly described. It is the responsibility of potential and actual users to be aware of such constraints and to abide by them. By making use of material from a digitised thesis, you accept these copyright and disclaimer provisions. Where it is brought to the attention of Trinity College Library that there may be a breach of copyright or other restraint, it is the policy to withdraw or take down access to a thesis while the issue is being resolved.

Access Agreement

By using a Digitised Thesis from Trinity College Library you are bound by the following Terms & Conditions. Please read them carefully.

I have read and I understand the following statement: All material supplied via a Digitised Thesis from Trinity College Library is protected by copyright and other intellectual property rights, and duplication or sale of all or part of any of a thesis is not permitted, except that material may be duplicated by you for your research use or for educational purposes in electronic or print form providing the copyright owners are acknowledged using the normal conventions. You must obtain permission for any other use. Electronic or print copies may not be offered, whether for sale or otherwise to anyone. This copy has been supplied on the understanding that it is copyright material and that no quotation from the thesis may be published without proper acknowledgement.

Drug-Induced Veno-Occlusive Disease of the Liver: Unravelling the Role of the Inflammatory and Coagulation Pathways



A thesis submitted for the degree of

Doctor of Philosophy

by

Johanna C. Bruneau, B.A., M.Sc., P.Grad.Dip.

Trinity College,

University of Dublin

December 2007

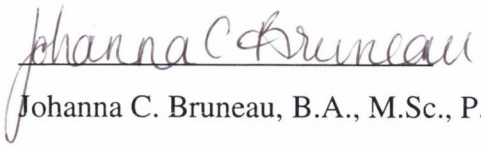
TRINITY COLLEGE
0 8 JAN 2009
LIBRARY DUBLIN
THESIS
8681

To Mom and Richie

Declaration

I hereby certify that this thesis submitted for the degree of Doctor of Philosophy to the University of Dublin, Trinity College, has not previously been submitted for a degree or diploma to this or any other University. The work here is entirely my own, except where stated.

This thesis may be made available for consultation within the University library and may be photocopied or lent to other libraries for the purpose of consultation.



Johanna C. Bruneau, B.A., M.Sc., P.Grad.Dip.

SUMMARY

The thiopurines thioguanine (6TG) and mercaptopurine (6MP), along with Mylotarg (an antibody targeted agent), are used in the treatment of acute leukaemias. These drugs are more commonly associated with the development of Veno-Occlusive Disease (VOD) than any other therapeutic agent used in this patient group. Since VOD is known to be a pro-coagulant and pro-inflammatory syndrome, we investigated the effect of these three drugs on the expression of Tissue Factor (TF), the initiator of blood coagulation, as well as the secretion of Tumour Necrosis Factor alpha (TNF-α) and Interleukin 8 (IL-8) *in vitro*. TF expression was determined by flow cytometry and cytokine secretion was quantified by sandwich ELISA. The cytotoxic effects of Mylotarg, 6TG and 6MP were investigated *via* the WST-1 assay. The apoptotic effects of 6TG and 6MP were measured by BrdU incorporation; the apoptotic effects of Mylotarg have been studied in detail previously, therefore were not repeated herein. The thiopurines were tested on three different leukaemic cell lines, representative of the different types of leukaemia that these agents would be used to treat: THP1 (acute myeloid leukaemia), Jurkat E6.1 (T lymphoblastic leukaemia), and 697 (B cell precursor acute lymphoblastc leukaemia). HepG2, a hepatocyte cell line, was also used to determine the effect of these drugs on the liver. Mylotarg, a Cluster of Differentiation (CD) 33 specific antibody conjugated to the cytotoxic molecule calicheamicin, is used in the treatment of acute myelogenous and other CD33+ leukaemias. It was tested on the CD33+ THP1 cell line and the HepG2 cell line (CD33-).

6-thioguanine and 6MP had a significant ($P<0.001$) effect on the secretion of IL-8 by THP1 and HepG2 cells, but not Jurkat E6.1 and 697 cells. Neither drug had an effect on the secretion of TNF-α by any of the cell lines tested. Mylotarg did not have any significant effect on the secretion of IL-8 or TNF-α. 6-thioguanine and 6MP had varied

effects on TF expression. In THP1 cells, 6TG caused a significant ($P<0.01$) decrease in TF expression, however 6MP had no effect. Jurkat E6.1 cells showed a significant ($P<0.001$) increase in TF expression after incubation with 6TG, but a significant ($P<0.001$) decrease in TF expression after 6MP treatment. Both 6TG and 6MP significantly increased TF expression in HepG2 cells ($P<0.01$ and $P\leq0.05$, respectively). Mylotarg significantly ($P<0.001$) increased TF in THP1 cells but not HepG2 cells. 6-thioguanine and 6MP both significantly ($P<0.001$) decreased viability in THP1 and Jurkat E6.1 cells. Neither thiopurine had a significant effect on the viability of HepG2 or 697 cells. Both 6TG and 6MP increased apoptosis in Jurkat E6.1 cells ($P<0.001$ and $P<0.01$, respectively). However, only 6TG increased apoptosis in THP1 cells ($P\leq0.05$). Neither drug significantly increased the proportion of apoptotic cells in the HepG2 or 697 cell line. Mylotarg did not significantly decrease the viability of either THP1 or HepG2 cells.

Both 6TG and 6MP are demonstrated to be pro-inflammatory and pro-coagulant, particularly in hepatocytes. IL-8 is the predominant chemo-attractant secreted by the hepatocytes, and initiates autocrine and paracrine loops in the injured liver that perpetuate inflammation and lead to the development of fibrosis.

Mylotarg elicited a pro-coagulant response in THP1 cells at the highest dose studied (100 ng/ml), but did not affect the secretion of TNF-α or IL-8. This could explain the clinical findings that patients treated with 9 mg/m^2 are more likely to develop VOD than those treated with a dose of $6mg/m^2$. High doses of Mylotarg may exert a pro-coagulant state *in vivo*, as it does *in vitro*, predisposing the patient to the development of VOD. In contrast to the thiopurines, Mylotarg had no effect on HepG2 cells. Mylotarg is a CD33 specific drug, and HepG2 cells do not express CD33. Hepatocytes may be involved in the development of VOD, but they are not the site of initiation with this drug.

ACKNOWLEDGEMENTS

Firstly, I would like to thank my supervisor, Professor Owen P. Smith, for guidance throughout the project. Also, thanks Dr. James O'Donnell for allowing me to finish the work in his lab, and Dr. Aengus O'Marcaigh for supporting the grant that made this work possible.

Special thanks to all lab members past and present, who were there in good times and bad: Catriona, Gail, Ciarán, Hélène, Joanna, Helen, Jen, Leeona, Wendy, Vince, Moya, Shona, Deirdre, Roger, and Virginie. Also, heartfelt thanks to Amanda Kiely, who always managed to somehow squeeze me into Owen's busy schedule; Dr. Sean Rooney at Our Lady's Children's Hospital, Crumlin, for assistance with FACS and supplying cells; and Dr. Tony Davies for assistance with HCS technologies. No one could get through their PhD without friends to lean on, especially those who know how you are feeling (and know not to ask when you are finishing!): Fiona, Anne, Erica, Catriona and Gail again; all Drs. themselves now! Of course, the support of all the people in the IMM who answered questions and lent supplies in times of crisis, your help is appreciated too, even if it is not named.

Last, but not least, to my friends and family on the other side of the pond, it is finally done! This thesis exists now especially because of my husband Richie and my mom Ann Marie, without whose support I would not have been able to return to the lab after my leave of absence. Thanks to you I have been able to finish my lab work, but more importantly, complete the write up as well. I owe you two more than I will ever be able repay you.

TABLE OF CONTENTS

1 INTRODUCTION
1.1 Coagulation 1
1.1.1 Tissue Factor 3
1.1.2 Protein C 3
1.1.3 Protein S 3
1.1.4 Thrombomodulin 4
1.1.5 Thrombin 4
1.2 Inflammation 5
1.2.1 Chemokines 5
1.2.2 Cytokines 5
1.3 The Coagulation and Inflammation Interface 6
1.4 Veno-Occlusive Disease 7
1.4.1 Introduction 7
1.4.2 Pathogenesis 8
1.4.3 Inflammation and Coagulation in VOD 10
1.4.4 Anti-Leukaemic Drugs and VOD 11

2 MATERIAL & METHODS
2.1 Materials 15
2.1.1 Reagents and Supplies 15
2.1.2 Cell Lines 16
2.2 Methods 21
2.2.1 Tissue Culture 21
2.2.2 Flow Cytometry 23
2.2.3 Quantitation of Apoptosis 25
2.2.4 Proliferation 25
2.2.5 ELISA 26
2.2.6 DNA Techniques 28
2.2.7 High Content Screening 30
2.2.8 Statistics 31

3 INVESTIGATION OF THE INFLAMMATORY, APOPTOTIC AND ANTI-PROLIFERATIVE EFFECTS OF 6-THIOGUANINE AND 6-MERCAPTOPURINE
3.1 Introduction 33
3.2 Thioguanine and Mercaptopurine Experiments 40
3.3 Results 43
3.3.1 Cytokine Release 43
3.3.2 Viability 49
3.3.3 Apoptosis 55
3.3.4 Tissue Factor Expression 61
3.3.5 TPMT Polymorphism 65
3.4 Discussion 67

4 DESIGN AND DEVELOPMENT OF ASSAYS FOR THE INTRACELLULAR DETECTION OF 6-THIOGUANINE AND 6-MERCAPTOPURINE
4.1 Introduction 77
4.2 Thiopurine ELISA Experimental Design 81
4.2.1 ELISA Protocol 81
4.2.2 Primary Antibody Selection 82
4.2.3 Generation of Plate Conjugate 83
4.2.4 Optimisation of Sample and Plate Preparation 84
4.2.5 Defining Limits of Sensitivity 87
4.2.6 Quantitation of 6TG and 6MP in Experimental Samples 90
4.3 Intracellular Staining for 6TG and 6MP 93
4.3.1 Fluorescent Staining Protocol 93
4.3.2 Optimisation of Assay Parameters 94
4.3.2.1 *Antibody Concentration* 94
4.3.2.2 *Blocking Experiments* 96
4.3.3 Results 99
4.4 Discussion 101

5 PRO-INFLAMMATORY AND PRO-COAGULANT PROPERTIES OF MYLOTARG
5.1 Introduction 105
5.2 Materials and Methods 109
5.2.1 Materials 109
5.2.2 Methods 109
5.3 Results 111
5.3.1 CD33 Expression 111
5.3.2 Cytokine Release 113
5.3.3 Viability 117
5.3.4 Tissue Factor 121
5.4 Discussion 121

6 CONCLUSIONS AND FUTURE WORK 127

REFERENCES 133

TABLES

		Page
Table 2.1	Cell line origins and characteristics	19
Table 2.2	Medium Formulations	19
Table 4.1	Cell Lysis Buffers	85
Table 4.2	Antibody and Plate Conjugate ELISA Plate Layout	85
Table 4.3	Results of Optimisation ELISA	86
Table 4.4	Plate Layout for Fluorescent Antibody Optimisation	94

FIGURES

		Page
Figure 1.1	Coagulation Pathway	2
Figure 1.2	Regulation of Coagulation	2
Figure 1.3	Organisation of Zones in the Liver	8
Figure 2.1	Photograph of THP1 cells	17
Figure 2.2	Photograph of Jurkat E6.1 cells	17
Figure 2.3	Photograph of HepG2 cells	18
Figure 2.4	Photograph of 697 cells	18
Figure 3.1	Chemical Structure of 6TG and 6MP	34
Figure 3.2	Thiopurine Metabolic Pathway	34
Figure 3.3	Oxidative Metabolic Pathway	35
Figure 3.4	THP1 Cytokine Response to 6TG or 6MP	45
Figure 3.5	Jurkat E6.1 Cytokine Response to 6TG or 6MP	46
Figure 3.6	HepG2 Cytokine Response to 6TG or 6MP	47
Figure 3.7	697 Cytokine Response to 6TG or 6MP	48
Figure 3.8	Viability of THP1 cells after treatment with 6TG or 6MP	51
Figure 3.9	Viability of Jurkat E6.1 cells after treatment with 6TG or 6MP	52
Figure 3.10	Viability of HepG2 cells after treatment with 6TG or 6MP	53
Figure 3.11	Viability of 697 cells after treatment with 6TG or 6MP	54
Figure 3.12	Apoptosis in THP1 cells after treatment with 6TG or 6MP	57
Figure 3.13	Apoptosis in Jurkat E6.1 cells after treatment with 6TG or 6MP	58
Figure 3.14	Apoptosis in HepG2 cells after treatment with 6TG or 6MP	59
Figure 3.15	Apoptosis in 697 cells after treatment with 6TG or 6MP	60
Figure 3.16	Effect of 6TG or 6MP on Tissue Factor expression in THP1 cells	62
Figure 3.17	Effect of 6TG or 6MP on Tissue Factor expression in Jurkat E6.1 cells	62
Figure 3.18	Effect of 6TG or 6MP on Tissue Factor expression in HepG2 cells	63
Figure 3.19	Histogram of Tissue Factor Expression in 697 cells	63
Figure 3.20	TPMT Polymorphism G238C	65
Figure 3.21	TPMT Polymorphism G460A	66
Figure 3.22	TPMT Polymorphism A719G	66

		Page
Figure 4.1	Maleimide Reaction	83
Figure 4.2	Bradford Standard Curve	84
Figure 4.3	Inhibition Curve for 6TG Antibody Sensitivity Assay	88
Figure 4.4	Percent Inhibition for 6TG Antibody Sensitivity Assay	89
Figure 4.5	Quantitation of Intracellular Accumulation of 6TG and 6MP	91
Figure 4.6	Intracellular Concentration of 6TG and 6MP normalised to protein content	92
Figure 4.7	Optimisation of Antibody Concentrations for Fluorescent Staining	95
Figure 4.8	Intensity of the Hoechst 33342 stain in THP1 cells	97
Figure 4.9	Intensity of Cytoplasmic stain in THP1 cells	97
Figure 4.10	Results of Blocking Experiment	98
Figure 4.11	Cytoplasmic versus nuclear localisation of 6TG	99
Figure 4.12	Cytoplasmic versus Nuclear localisation of 6TG or 6MP in THP1 cells, with and without NBMPR.	100
Figure 5.1	Structure of Gemtuzumab Ozogamicin	106
Figure5.2	CD33 expression in THP1 cells	111
Figure 5.3	CD33 expression in HepG2 cells	111
Figure 5.4	THP1 Cytokine Secretion Levels after Treatment with Mylotarg	114
Figure 5.5	HepG2 Cytokine Secretion Levels after treatment with Mylotarg	115
Figure 5.6	Viability of THP1 cells after treatment with Mylotarg	118
Figure 5.7	Viability of HepG2 cells after treatment with Mylotarg	118
Figure5.8	Tissue Factor expression in THP1 cells after treatment with Mylotarg	120
Figure 5.9	Tissue Factor expression in HepG2 cells after treatment with Mylotarg	120

ABBREVIATIONS

1°	Primary
2°	Secondary
6MP	6-mercaptopurine
6-TdGTP	6-thio-2'deoxyguanine 5' diphosphate
6TG	6-thioguanine
Ab	Antibody
ADP	Adenosine Diphosphate
ALL	Acute Lymphocytic Leukemia
ANOVA	Analysis of Variance
AML	Acute Myelogenous Leukemia
APC	Activated Protein C
AT	AntiThrombin
ATP	Adenosine Triphosphate
AZA	Azathioprine
BCP-ALL	B cell Precursor ALL
BMT	Bone Marrow Transplant
BSA	Bovine Serum Albumin
CD	Cluster of Differentiation
cib	CNT insensitive to NBMPR, broad range of permeants
cif	CNT insensitive to NBMPR, formycin B permeant
cit	CNT insensitive to NBMPR, permeant to thymidine
CNT	Concentrative Nucleoside Transporter
CR	Complete Remission
CSA	Cyclosporin
DMSO	Dimethyl Sulphoxide
DNA	Deoxyribo-Nucleic Acid
dNTP	DeoxyriboNucleotide TriPhosphate
dUTP	DeoxyUridine TriPhosphate
ei	Equilibrative nucleoside transporter insensitive to NBMPR
ELISA	Enzyme-Linked ImmunoSorbent Assay
ENT	Equilibrative Nucleoside Transporter
es	Equilibrative nucleoside transporter sensitive to NBMPR
FACS	Fluorescence Activated Cell Sorting
FBS	Foetal Bovine Serum
FITC	Fluorescein Isothiocyanate
FSC	Forward Scatter Characteristics
GO	Gemtuzumab Ozogamicin
HCS	High Content Screening
HEPES	4-(2-hydroxyethyl)-1-piperazine ethanesulfonic acid
HGPRT	Hypoxanthine Guanine PhosphoRibosyl Transferase
HPLC	High Pressure Liquid Chromatography
HRP	Horse Radish Peroxidase
IBD	Inflammatory Bowel Disease
IFN	Interferon
Ig	Immunoglobulin
IgG4	Immunoglobulin G4
IL	Interleukin 8
ITIM	Immunomodulatory Tyrosine-based Inhibitory Motifs
LAL	Limulus Amebocyte Lysate

L-Glut	L-glutamine
LPS	LipoPolySaccharide
LSD	Least Significant Diffference
MDS	MyeloDysplastic Syndrome
MDR	MultiDrug Resistance protein
MEM	Minimum Essential Medium
MMR	MisMatch Repair
NBMPR	Nitrobenzylthioinosine
NEAA	Non-Essential Amino Acids
NGS	Normal Goat Serum
NLM	National Library of Medicine
nm	Nanometer
OD	Optical Density
PAI-1	Plasminogen Activator Inhibitor-1
PBS	Phosphate Buffered Saline
PC	Protein C
PCR	Polymerase Chain Reaction
PDNS	Purine *de novo* synthesis
PE	PhycoErythrin
PFA	Paraformaldehyde
Pgp	Permeability GlycoProtein
PMA	Phorbol-12-Myristate-13-Acetate
PPD	Purified Protein Derivative of tuberculin
PRPP	PhosphoRibosylPyroPhosphate
PS	Protein S
P/S	Penicillin/Streptomycin
RBC	Red Blood Cell
RFLP	Restriction Fragment Length Polymorphism
RNA	Ribo-Nucleic Acid
ROS	Reactive Oxygen Species
RPMI	Roswell Park Memorial Institute medium
SCT	Stem Cell Transplantation
SEC	Sinusoidal Endothelial Cells
SEM	Standard Error of the Mean
Siglecs	Sialic acid binding Ig-like lectins
SOS	Sinusoidal Obstructive Syndrome
SSC	Side Scatter Characteristics
TGN	Thioguanine nucleotides
TF	Tissue Factor
TFPI	Tissue Factor Pathway Inhibitor
TM	Thrombomodulin
TMB	TetraMethylBenzidine
TNF	Tumour Necrosis Factor
tPA	Tissue Plasminogen Activator
TPMT	ThioPurine Methyl Transferase
TPMT+	CCRF-CEM leukaemic cells over expressing TPMT
TUNEL	Terminal deoxynucleotidyltransferase dUTP Nick End Labelling
UC	Ulcerative Colitis
UV	UltraViolet
VEGF	Vascular Endothelial Growth Factor
VOD	Veno-Occlusive Disease
vWF	von Willebrand Factor

WST-1	4-[3-(4-iodophenyl)-2-(4-nitrophenyl)-2H-5-tetrazolio]-1,3-benzene disulfonate
XO	Xanthine Oxidase

CHAPTER 1
INTRODUCTION

1.1 COAGULATION

Coagulation is a critical defence mechanism in the body. Tissue damage initiates the coagulation process, which involves a series of enzymatic reactions, as shown in Figure 1.1, and results in the formation of a fibrin clot. Many of the critical proteins in the system circulate in the blood as zymogens, which must be enzymatically activated. The coagulation cascade is regulated by feedback pathways, cofactor requirements, and signalling cascades. When there is an alteration in this balance, known as haemostasis, excessive clotting or bleeding can occur (Roberts and Tabares, 1995).

The coagulation cascade is a complex process that cannot be reviewed in detail here. The involvement of critical factors for this study, Protein C, Protein S, Tissue Factor, Thrombin and Thrombomodulin, will be discussed. The association between these proteins and their pro-coagulant and anti-coagulant effects are detailed in Figure 1.2.

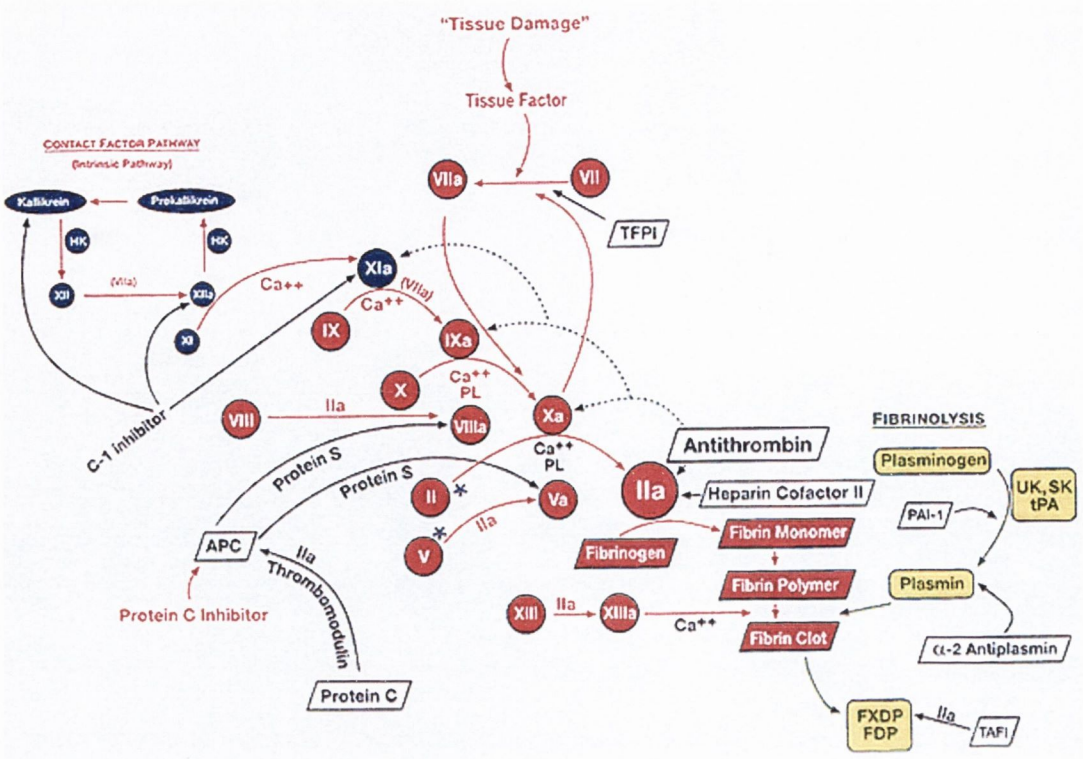


Figure 1.1 The Coagulation Pathway. Diagram taken from the American Diagnostica Inc. website, http://www.americandiagnostica.com/

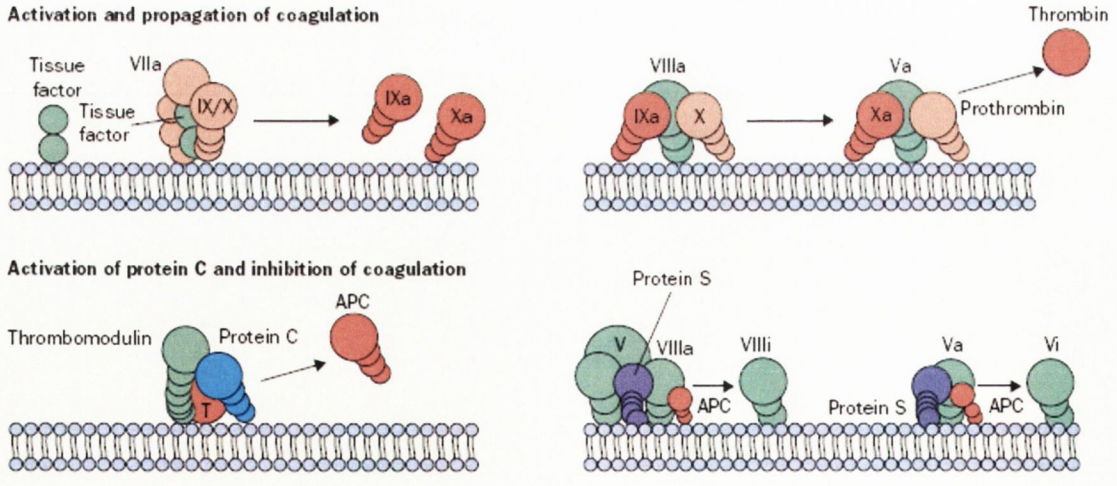


Figure 1.2 Regulation of Coagulation. T=thrombin. Taken from Dahlbäck (2000) *The Lancet* 355: 1627-32.

1.1.1 Tissue Factor

Tissue Factor (TF) is a membrane bound protein that is abundant in the cells surrounding the vascular endothelium. When the endothelium is disrupted by injury, the TF is exposed and initiates coagulation. TF binds to factor VII in both its active (VIIa) and inactive forms. When TF binds factor VII, it is converted into its active form. The TF/factorVIIa complex initiates the coagulation cascade by converting factors IX and X to their active forms (IXa and Xa, respectively) (Dahlbäck, 2000). The TF pathway is inhibited by the Tissue Factor pathway inhibitor (TFPI), which inactivates the TF-factor VIIa complex (Esmon, 2001).

1.1.2 Protein C

Protein C (PC) is the critical component of the protein C anticoagulant pathway. PC is activated by thrombin bound to thrombomodulin (TM) on the surface of endothelial cells. Activated Protein C (APC) inhibits coagulation by cleaving and inactivating actors Va and VIIIa (Esmon, 2001). PC is synthesised by hepatocytes (Roberts and Tabares, 1995).

1.1.3 Protein S

Protein S (PS) is a vitamin K dependent plasma protein that acts as a cofactor for APC. PS improves the anti-coagulant activity APC and APC-mediated inactivation of factor Va. APC and PS associate to form a membrane bound complex that can inactivate factors VIIIa and Va even when they are part of the tenase or prothrombinase complexes (Dahlbäck, 2000). PS is synthesised by hepatocytes (Roberts and Tabares, 1995).

1.1.4 Thrombomodulin

Thrombomodulin (TM) is a membrane bound protein expressed on the surface of endothelial cells. Thrombin complexed with TM is able to activate PC at a much higher rate than thrombin alone (Roberts and Tabares, 1995).

1.1.5 Thrombin

Thrombin is a key enzyme in the coagulation cascade. It is generated when prothrombin is cleaved by the prothrombinase complex on the phospholipid surface. The prothrombinase complex is composed of factor Xa and its cofactor, factor Va. Thrombin generation feeds back into the system by activating factors V, VIII and XI. Thrombin has both pro-coagulant and anti-coagulant properties, depending on the manner in which it is generated. In the PC system, it acts as an anti-coagulant by activating PC. Thrombin mediates it pro-coagulant activity *via* activation of factors V and VIII (Dahlback, 2000).

1.2 INFLAMMATION

Inflammation is another of the body's defence mechanisms. The process of inflammation involves the recruitment of immune cells, in particular neutrophils, to the site of injury within the body. This is mediated in part by the release of chemokines and cytokines in response to infection and injury (Kuby, 1997).

1.2.1 Chemokines

Chemokines are small polypeptides that attract leukocytes to the site of inflammation. They are known as chemotactic cytokines because unlike other chemotactic agents, they are specific to certain cell types. Apart from leukocyte recruitment, they are also involved in lymphocyte maturation, angiogenesis and tumour growth. The ability of chemokines to attract certain cell types is dependent on the cell surface expression of specific receptors (Rottman, 1999).

1.2.2 Cytokines

Cytokines are low molecular weight proteins secreted by leukocytes and other cells in the body. Like chemokines, they bind to specific receptors on the surface of the target cell. When a cytokine binds to its receptor, signal transduction pathways are activated that alter the gene expression in the cell. Cytokines regulate the intensity of the immune response to injury or infection by controlling the activation, proliferation and differentiation of the cells of the immune response. The major cytokine producing cells are macrophages and T_H cells (Kuby, 1997).

1.3 THE INFLAMMATION AND COAGULATION INTERFACE

The coagulation and inflammation systems do not exist independently; there is cross talk between the two. It has also become clear that inflammation enhances coagulation and vice versa. For example, venous thrombi contain a large number of leukocytes, which express TF, the expression of which is upregulated by the inflammatory cytokine TNF-α. In addition, APC has anti-inflammatory activity (Esmon, 2004). Numerous other components overlap between the two systems, further underlining their interrelationship in the development of certain syndromes such as VOD.

1.4 VENO-OCCLUSIVE DISEASE

1.4.1 Introduction

Hepatic veno-occlusive disease (VOD) is a major side effect of cytotoxic therapy. It is characterised by weight gain, painful hepatomegaly, abdominal ascites and jaundice. The pathogenesis of the disease is complex, involving inflammation, coagulation, and fibrosis (Bearman, 2001). Typically the initiating factor for developing VOD is stem cell transplantation (SCT) (Coppell. 2003), however there have been observations of VOD following the intake of liver toxic substances or drugs without prior SCT or Bone Marrow Transplantation (BMT) (Faioni, 1997). VOD is also known as Sinusoidal Obstructive Syndrome (SOS).

The severity of VOD is diagnosed retrospectively. Mild VOD is self-limiting and normally does not require treatment. Moderate VOD does require treatment, but most patients will recover. Severe VOD is defined as liver damage that does not resolve by 100 days post SCT or prior to death. It is associated with multiorgan failure, which is usually the cause of death (Coppell, 2003).

There is no standard therapy for VOD. Heparin, tissue plasminogen activator (tPA) and defibrotide have been reported as active. Defibrotide stimulates fibrinolysis by increasing the activity of tPA and at the same time decreasing activity of Plasminogen Activator Inhibitor (PAI-1). It also stimulates the expression of thrombomodulin (TM) on endothelial cells. However, unlike heparin and tPA, defibrotide lacks systemic anticoagulant activity (Bearman, 2000).

1.4.2 Pathogenesis

The pathogenesis of VOD is still unclear. The site of injury is zone 3 of the liver (Figure 1.3) (Bearman, 2000), with fibrosis in the central veins of the liver or extended into the sinusoids. The fibrosis is often accompanied by hepatocyte necrosis (Faioni, 1997). Material found within the sinusoids has been identified as fibrin and von Willebrand factor (vWF) by immunohistochemical staining, indicating that at some point in the development of VOD, endothelial damage and clotting occur (Faioni, 1997). Cytokines have also been implicated in the pathogenesis of VOD. Soluble Interleukin (IL) -2 receptor, interferon (IFN)-γ, IL-6 and TNF-α have all been found at increased levels in patients who develop VOD (Faioni, 1997).

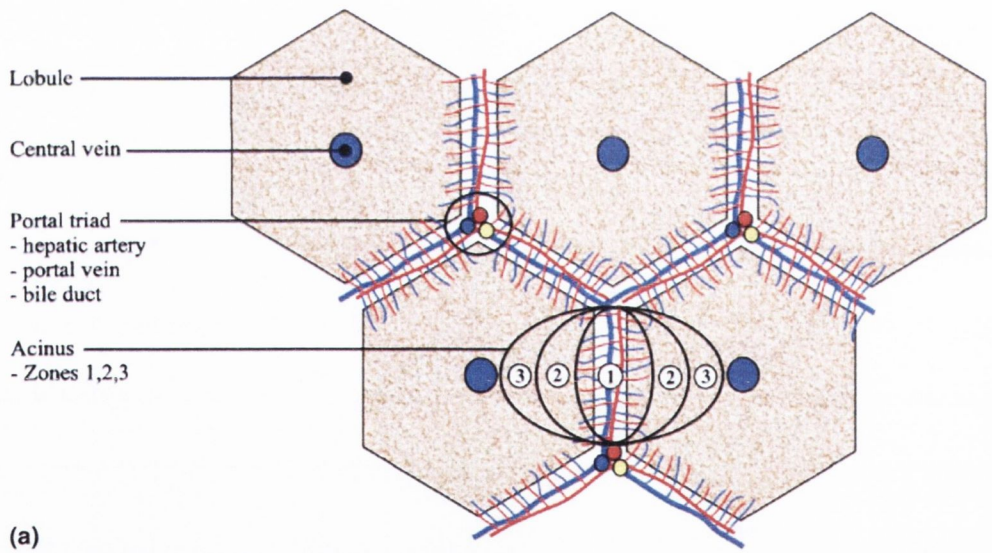


Figure 1.3 Organisation of Zones in the Liver. The acinus is the functional unit of the liver; the zones are determined by distance from the afferent blood supply. Zone 1 surrounds the portal tract and is termed the periportal area; Zone 2 is intermediate; and Zone 3 surrounds the central vein in the centrilobular region. Within each lobule, hepatocytes are arranged in one cell thick layers, creating the sinusoids. The sinusoids are lined by the sinusoidal endothelial cells, which are fenestrated to allow the plasma to bathe the hepatocytes. Diagram taken from Coppell *et al,* Blood Reviews (2003) 17, 63-70.

The location of the damage in zone 3 of the liver appears to be related to its metabolism of drugs and other toxic substances. Drugs must be converted into a water soluble form by cytochrome P450 in order to be eliminated. While most metabolites are stable, some are not, and these are detoxified by glutathione. Zone 3 hepatocytes are rich in cytochrome P450 but have reduced levels of glutathione, which makes this area a target for toxic metabolites (Carreras, 2000). The initial site of injury in VOD appears to be the sinusoidal endothelial cells (SEC) (Bearman, 2000). *In vitro* studies have shown that damage to SECs is mediated by depletion of glutathione (DeLeve, 1996).

Hepatic stellate cells are the most important mediators of fibrosis. They are located in the subendothelial space between the hepatocytes and the sinusoidal endothelial cells, arranged circumferentially. Activated stellate cells express smooth muscle specific α-actin which provides the cells with contractile ability (Bearman, 2001).

Macrophages have also been implicated in the development of VOD. Histopathological analysis of liver biopsies from VOD patients shows endothelial cell damage, activation and proliferation of stellate cells, and collagen deposition in the central vein wall. Activated macrophages have also been identified within the central vein wall and lumen. Most likely, these were monocytes that were activated by the endothelial damage in the liver and matured into macrophages (Tang, 2003).

1.4.3 Inflammation and Coagulation in VOD

Disturbances in normal coagulation parameters which predispose individuals to hypercoaguability are well documented in VOD patients. Hypercoaguability has also been identified as a contributor to the development of VOD. Several studies have shown that decreased levels of the anticoagulant proteins Protein C and anti-thrombin predispose individuals to developing VOD (Bearman, 2001). The liver synthesises or modifies PC, PS and factor VII, therefore liver impairment will affect their levels in the plasma, (especially PC and factor VII, which have a short half life) and contribute to a hypercoaguable state (Faioni, 1997).

The inflammatory mediators TNF-α, IL-1β and IL-2 have been implicated in the pathogenesis of VOD. TNF-α levels are significantly elevated in patients prior to the clinical development of VOD, and peripheral blood mononuclear cells of patients with VOD show increased expression of TNF-α and IL-1β genes. Patients with VOD also had higher circulating levels of the IL-2 receptor (Bearman, 2001). Vascular endothelial growth factor (VEGF) was significantly increased in patients who developed VOD after SCT ($P<0.01$). VEGF was also significantly increased in patients whose plasma PC activity was below 40%. In addition, VEGF stimulates the expression of TF on the surface of circulating monocytes, thereby increasing hypercoaguability (Iguchi, 2001).

Markers of endothelial damage are also increased in patients with VOD. Plasminogen activator inhibitor-1 (PAI-1) was increased after high dose cytoreductive therapy in patients with VOD. Endothelial cell marker vWF increased after bone marrow transplant (Bearman, 2001). Endothelial damage would result in local activation of coagulation by internalisation of TM and expression of TF on the cell surface (Faioni, 1997).

1.4.4 Anti-Leukaemic Drugs and VOD

An increased incidence of hepatic Veno-Occlusive Disease following treatment with Mylotarg (Gemtuzumab Ozogamicin, GO) has been documented following stem cell transplantation (SCT) (Rajvanshi, 2002). Cases have also been reported in patients who have not received SCT either before or after GO. VOD may also occur when GO is given as a single agent or in combination with other cytotoxic agents, especially thioguanine. It can also occur in patients who have not received any prior cytotoxic therapy (Giles, 2001). The incidence of this complication is more often associated with GO than any other treatment in this patient group.

A number of studies have been published on the incidence of VOD following GO exposure, the results of which have been mixed. In a paper by Arceci *et al* (2005), one paediatric patient (of 29 total) developed VOD after being treated with GO at a dosage of $9mg/m^2$. Of the 29 patients enrolled in the study, 13 went on to receive SCT within 3.5 months of the last GO infusion. Six (40%) of the patients who received SCT following GO treatment developed VOD (Arceci, 2005). Similar results were reported by McKoy *et al* from the Research on Adverse Drug Events Reports (RADAR) group. Their review of the clinical results in adults revealed that when GO was given at dosages $\leq 6mg/m^2$, either alone or with other non-hepatotoxic agents, the incidence of SOS was 3%. However, SOS incidence increased to 15% when GO was administered alone at a dosage of $9mg/m^2$ and 28% when given in combination with 6-thioguanine. If patients underwent SCT within 3 months of GO therapy, the frequency of SOS was 15-40% (McKoy, 2007).

In a retrospective study by Nabhan et al (2004), only 1 patient out of 47 developed VOD, while 31% displayed GO-related liver toxicity. In this patient group, GO was administered at a dosage of $9mg/m^2$ in two infusions 14 days apart, as a single agent for initial treatment

or in relapsed/refractory acute myelogenous leukaemia (AML) (Nabhan, 2004). Another retrospective study examined the incidence of VOD in 62 patients with previously treated AML or myelodysplastic syndrome (MDS) who then underwent SCT (Wadleigh, 2003). This study found a statistically significant difference in the incidence of VOD between patients with and without prior GO treatment (Wadleigh, 2003). Of the 62 patients, 14 had prior GO treatment. Thirteen (21%) patients overall developed VOD; 9 (64%) patients with prior GO exposure compared to 4 (8%) without prior GO treatment ($P<0.0001$) (Wadleigh, 2003).

Reviewing the results of these studies, it is clear that while GO is hepatotoxic, the incidence of VOD is low when the approved treatment schedule is followed. Increasing the intensity or dosage schedule, or combining GO with other hepatotoxic agents, (including SCT 3 months prior to or post GO administration), increases the incidence of VOD. Combination of GO with 6-thioguanine (6TG), a known hepatotoxin, significantly increases the incidence of VOD (McKoy, 2007).

6-thioguanine (6TG), along with 6-mercaptopurine (6MP) and azathioprine (AZA), are members of the thiopurine class of drugs. These compounds are used to treat a variety of ailments including inflammatory bowel disease (IBD), ulcerative colitis (UC) along with acute leukaemias (Cara, 2004). All of these agents, particularly 6TG, have been implicated in the development of VOD, in both acute lymphoblastic leukaemia (ALL) and IBD patients. A systematic review of the literature by Gisbert *et al* (2007) found that in a retrospective study, 3% of IBD patients treated with AZA/6MP developed VOD, compared to 10% in a prospective study (Gisbert, 2007). Individual case studies of VOD following AZA treatment have also been published (Russmann, 2001).

Similar VOD incidence rates have been reported in patients treated with 6TG for ALL. In one retrospective study, 12 (12%) children treated with 6TG developed VOD; 99 patients were included, 62 of whom received 6TG (versus 37 who received 6MP). All cases of VOD occurred in patients receiving 6TG therapy (Stoneham, 2003). In the recent ALL97 trial of 6TG and 6MP, 95 patients (6% of 1498 total) developed veno-occlusive disease of the liver. However, 82 of the VOD patients were randomised to receive 6TG, representing 11% of all 6-thioguanine recipients (Vora, 2006).

The pro-inflammatory and pro-coagulant nature of VOD has been well documented in clinical studies. However, there is still a lack of understanding of the basic mechanisms that initiate the development of the syndrome. The aim of this study was to examine the effects of 6TG, 6MP and GO *in vitro* on the expression and secretion of mediators of coagulation and inflammation in an attempt to gain a better understanding of the pathways involved in the development of VOD.

CHAPTER 2
MATERIALS AND METHODS

2.1 MATERIALS

2.1.1 Reagents and Supplies

All chemical reagents were supplied by Sigma (Dorset, UK) unless otherwise stated. Cell culture reagents were obtained from Gibco BRL/Invitrogen (Paisley, UK). Tissue culture plasticware was obtained from Nunc (Hereford, UK). Enzyme Linked Immunosorbent Assay (ELISA) kits were supplied by R&D Systems (Minneapolis, MN, USA); the tetramethyl benzidine (TMB) solution used to develop ELISAs was purchased from Pierce (Rockford, IL, USA). ELISA plates (96 well) were obtained from Sarstedt (Leicester, UK). PCR buffer and *Taq* were purchased from Promega (Madison, WI, USA). Stock deoxyribonucleotide triphosphate (dNTP) solutions were obtained from Roche (Mannheim, Germany). Primer synthesis was performed by Invitrogen (Paisley, UK). All reagents and buffers for Fluorescence Activated Cell Sorting (FACS) analysis were purchased from Becton Dickinson (Sunnyvale, CA, USA) unless otherwise stated. Fluorescent dyes and secondary antibodies for High Content Screening (HCS) were purchased from Molecular Probes (Eugene, OR, USA). Corning CellBIND plates (Corning, NY, USA) were used for HCS. Albumin conjugation kit for the thiopurine ELISA was purchased from Calbiochem (San Diego, CA, USA). Dialysis products were obtained from Pierce (Rockford, IL, USA). The anti-thioguanine antibody was purchased from the Antibody Shop (Gentofte, Denmark). The horseradish peroxidase (HRP)-conjugated rat anti-mouse secondary antibody was purchased from BD Pharmingen (Sunnyvale, CA, USA).

2.1.2 Cell Lines

The monocyte cell line THP-1 (TIB-202), T lymphocyte cell line Jurkat E6.1 (TIB-152), and hepatocyte line HepG2 (HB-8065), were obtained from the American Type Culture Collection (Manassas, VA, USA). The B-cell precursor acute lymphoblastic leukaemic (BCP-ALL) cell line 697 (also designated EU-3) was obtained from the DSMZ German Collection of Microorganisms and Cell Cultures (Braunschweig, Germany). Photographs of the four cell lines are shown in Figure 2.1-2.4, respectively. The origin and characteristics of all four cell lines are outlined in Table 2.1. THP-1, Jurkat E6.1 and 697 cells were grown in Roswell Park Memorial Institute (RPMI) medium supplemented with 2 mM L-glutamine (L-Glut), 10% foetal bovine serum (FBS), 50 U/ml Penicillin and 50 µg/ml Streptomycin (P/S). Jurkat E6.1 cells were additionally supplemented with 10 mM HEPES, 4.5 g/l glucose and 1 mM sodium pyruvate. HepG2 cells were grown in Minimum Essential Medium (MEM) with Earle's salts, also supplemented with 2 mM L-Glut, 10% FBS, 1% Non-Essential Amino Acids (NEAA) and 1 mM sodium pyruvate. Table 2.2 lists the medium and supplements for all cell lines. All cultures were maintained in a humidified atmosphere at 37°C, 5% CO_2.

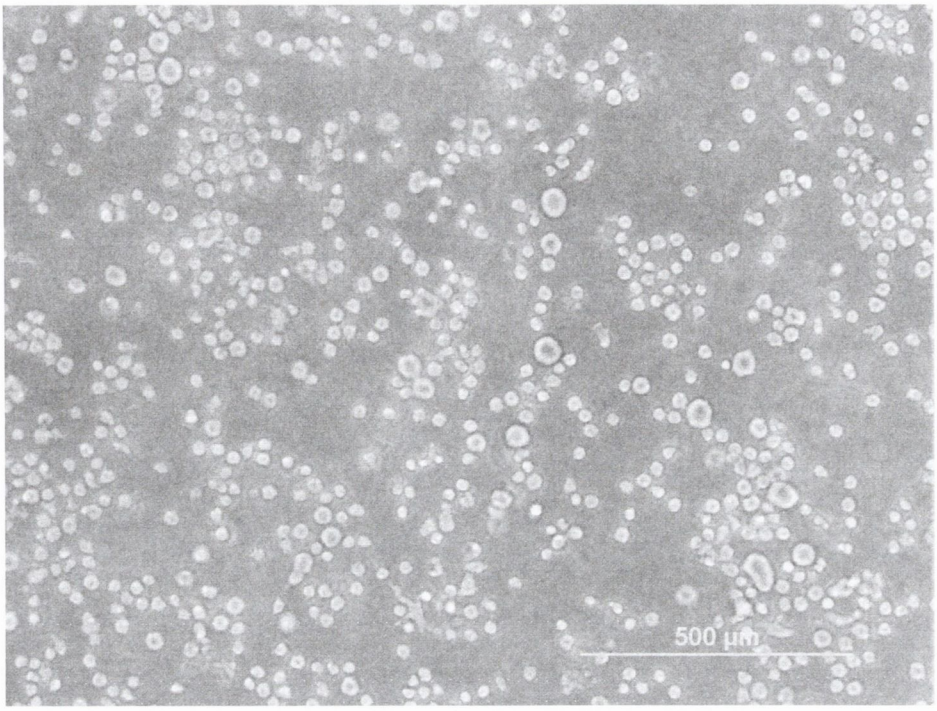


Figure 2.1 THP1 cells viewed under the 10X objective.

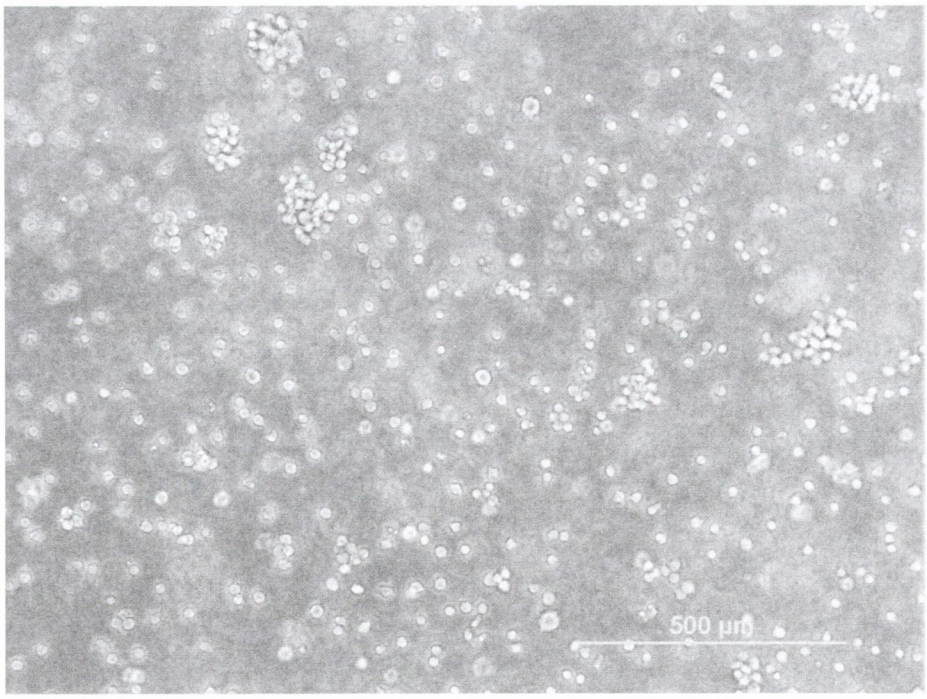


Figure 2.2 Jurkat E6.1 cells viewed under the 10X objective.

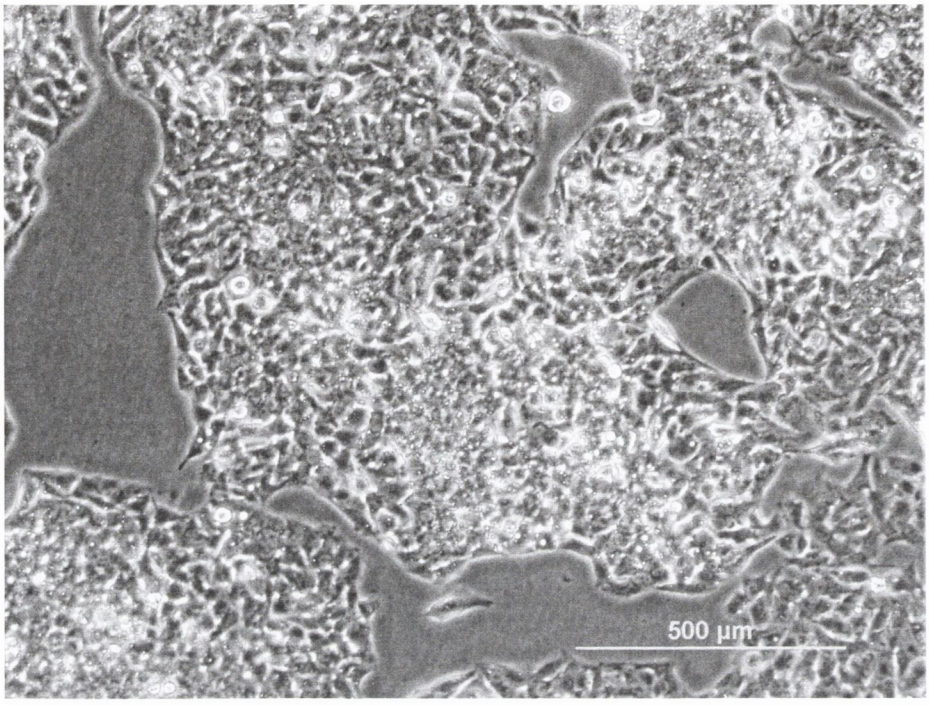


Figure 2.3 HepG2 cells viewed under the 10X objective.

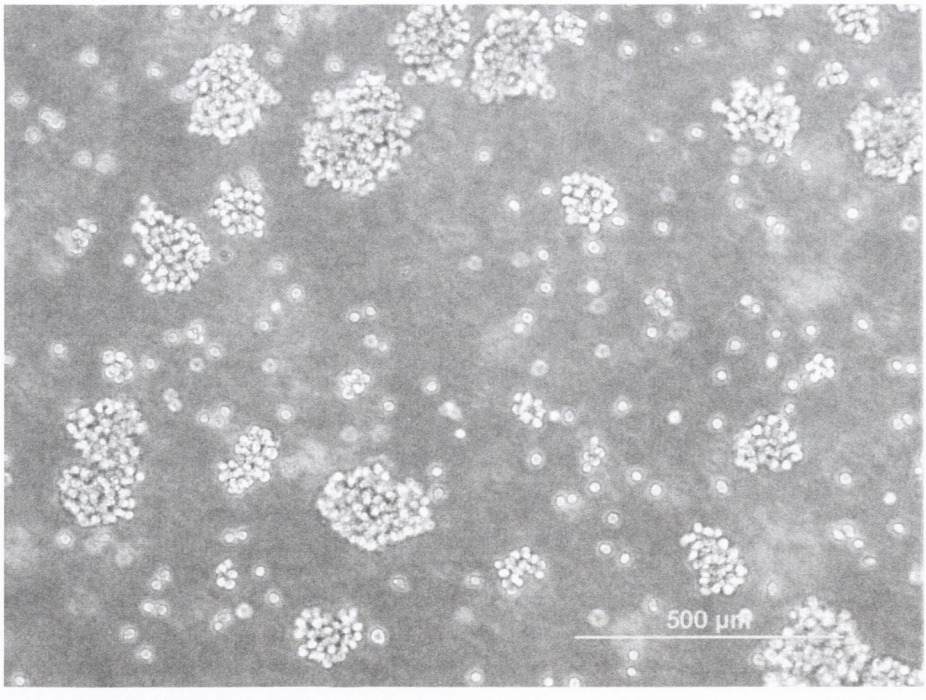


Figure 2.4 697 cells viewed under the 10X objective.

Table 2.1 Cell Line Characteristics

Cell Line	Tissue	Designation	Morphology	Growth Properties
HepG2	Liver	Hepatocellular Carcinoma	epithelial	Adherent
Jurkat E6.1	Peripheral Blood	Acute T cell Leukaemia (T-ALL)	lymphoblast	Suspension
THP1	Peripheral Blood	Acute Monocytic Leukaemia (AML)	monocyte	Suspension
697	Peripheral Blood	Precursor acute B cell Leukaemia (precursor B-ALL)	lymphoblast	Suspension

Table 2.2 Medium Formulations

Cell Line	Medium	L-Glutamine	Penicillin/ Streptomycin	Fetal Bovine Serum	Non-Essential Amino Acids	Sodium Pyruvate	HEPES	Glucose
HepG2	MEM	2 mM	-	10%	1%	1 mM	-	-
Jurkat E6.1	RPMI	2 mM	-	10%	-	1 mM	10 mM	4.5 g/l
THP1	RPMI	2 mM	50 U/ml / 50 µg/ml	10%	-	-	-	-
697	RPMI	2 mM	-	10%	-	-	-	-

2.2 METHODS

2.2.1 Tissue Culture

Culture of Cell Lines

Suspension cell lines were sub-cultured by aseptically diluting growing cells 1 to 3 with fresh medium in sterile 75cm^2 tissue culture flasks. Adherent cells were sub-cultured by twice washing the monolayer with ice cold PBS, then adding 5ml 0.25% trypsin to the cells and incubating the flask at 37°C for 10 minutes. The flask was gently tapped to dislodge the cells from the surface of the flask, then 10ml fresh medium was added to neutralise the trypsin. Cells were recovered by centrifugation at 400g for 5 minutes, diluted in fresh medium, and then transferred to sterile 75cm^2 tissue culture flasks for further growth. All work was carried out in a LaminAir flow cabinet (Holten, Allerød, Denmark) to ensure sterility.

Long-term Storage of Cell Lines

Vials of each cell line were stored a -70°C for long-term storage. Freeze medium consisted of 95% of the appropriate medium and 5% dimethyl sulfoxide (DMSO). Cells were stored in 1ml aliquots in cryovials at a concentration of 5-10 x 10^6 cells/ml. Once aliquoted, the vials were immediately transferred to ice then placed in the -70°C freezer in an ice box for slow freezing.

Resuscitation of Frozen Cell Line Stocks

One ampoule of cells was thawed when new cultures were required, or to assess the viability of the cells after cryopreservation. 10ml of the appropriate medium was pre-warmed to 37°C in a 25 cm^2 sterile tissue culture flask. The cryovial was warmed briefly at room temperature before thawing in a 37°C water bath. The contents of the vial were

slowly transferred to the pre-warmed medium, which was then placed in the incubator. Cell growth was monitored by examining the cells under the microscope. After 72-96 hours, the regular subculture routine was initiated to ensure that the optimal cell concentration and conditions were maintained.

Cell Counting

Cells were counted and their viability assessed by means of trypan blue exclusion. Trypan blue is negatively charged, so it is excluded from viable cells. Therefore, only the cells with damaged cell membranes (e.g. dead cells) will stain blue. To count the cells, 10 µl of cell suspension was added to 90 µl of 0.04% trypan blue solution. The sample was loaded into the chamber of an improved Neubauer haemocytometer. Using a light microscope, cells were counted in 5 squares of either side of the chamber (10 in total). The concentration of the cells in the suspension (cells/ml) was calculated by multiplying the total number of cells in all 10 squares x dilution factor x 1000.

Mycoplasma Testing

All cell lines were periodically tested for mycoplasma contamination using the Cambrex (Rockland, ME, USA) MycoAlert kit. Mycoplasm is a prokaryote that affects the proliferative ability of cell lines by competing with the cells for nutrients in the culture medium. The MycoAlert kit is a luminescence-based assay that uses the mycoplasmal enzymes as a marker of mycoplasma contamination. The mycoplasmal enzymes will convert ADP to ATP in the presence of a substrate. The kit works by measuring the ATP levels before the addition of the substrate (reading A) then after the addition of the substrate (reading B). If the ratio of reading B to reading A is greater than 2, then there is mycoplasma contamination in the cell culture. A ratio between 1 and 2 is considered

borderline, and should be retested, while a ratio less than 1 is a negative result. The kit was used according to the manufacturer's instructions.

Endotoxin Testing

To exclude the effect of endotoxin contamination on experimental results, all drug suspensions were routinely screened using the Limulus Amebocyte Lysate (LAL) test (Cambrex, Rockland, ME, USA). The test is performed by adding equal volumes of LAL solution and test solution to a pyrogen-free tube and incubating the sample at 37°C for 1 hour. Positive and negative controls are included to ensure that there is no LAL inhibitor or other contaminant in the kit contents. The negative control is reagent water that is used to reconstitute the lysate. A vial of endotoxin is included in the kit, to serve as a positive control. Gelation of the tube contents will occur after 1 hour if there is endotoxin present in the sample. If there is no endotoxin contamination, the sample will not gel. The assay was performed as per the manufacturer's instructions.

2.2.2 Flow Cytometry

Tissue Factor

To determine the expression levels of Tissue Factor (TF) on the cell surface, cells were analysed by Fluorescence Activated Cell Sorting (FACS). Following the appropriate treatment and incubation time as per the experiment, the cells (200,000/sample) were pelleted at 400g. The supernatant was saved for IL-8 quantitation to confirm that the cells had been activated. The cell pellet was washed twice with 1 ml ice cold Phosphate Buffered Saline (PBS). After the wash step, the pellet was resuspended in 100 µl of PBS, to which 10 µl of a 1:10 dilution of the Fluorescein Isothiocyanate (FITC) labelled anti-TF antibody (American Diagnostica, Stamford, CT, USA) was added. Controls included unstained cells, which were incubated with PBS only, and an isotype control where cells

were stained with a mouse IgG1 FITC (Dako Cytomation, Glostrup, Denmark) to confirm that there was no non-specific binding of the anti-tissue factor antibody. All samples were incubated on ice in the dark for 30 minutes. After this incubation, the samples were washed twice in PBS to remove any unbound antibody, then resuspended in PBS (1 ml) for analysis on a FACSCalibur flow cytometer (Becton Dickinson, Sunnyvale, CA, USA). Data analysis was performed using CellQuest software (Becton Dickinson). Percentage TF expression was calculated using the geometric mean of the histogram plot. The average of the geometric means from the untreated replicates was defined as 100%. The percentage TF expression on cell surface after treatment was calculated by dividing the average geometric mean of all replicates by the average geometric mean of the untreated cells, then multiplied by 100 to yield a percentage.

Cluster of Differentiation 33

Cluster of Differentiation 33 (CD33) expression on the cell surface was measured in a similar manner to TF. Briefly, 100 µl of the cell suspension was aliquoted into a 0.5 ml eppendorf tube. The cells were washed once with ice-cold PBS, then incubated with 10 µl of 1:8 dilution (1.5 µg/ml) of Phycoerythrin (PE)-conjugated mouse anti-human CD33 monoclonal antibody (BD Biosciences, San Jose, CA, USA). An isotope matched, PE conjugated mouse IgG1 monoclonal antibody (BD Biosciences) was used as a negative control; a sample of untreated, unstained cells was also included as a control. Samples were incubated at 4°C for 30 minutes in the dark. At the end of the incubation, samples were washed twice with ice cold PBS, then resuspended in 1ml PBS, before analysis on BD FACSCalibur. Data analysis was performed using the CellQuest software program.

2.2.3 Quantitation of Apoptosis

One of the later steps in the apoptotic pathway is DNA fragmentation. This fragmentation can be detected by template-independent incorporation of bromolated deoxyuridine triphosphates (Br-dUTP) to the 3' end of double and single stranded DNA. The addition of Br-dUTPs is catalysed by the terminal deoxynucleotidyltransferase (TdT) enzyme, hence the method is known as TUNEL (terminal deoxynucleotyltrasferase dUTP nick end labelling). The Br-dUTPs are detected using an anti-BrdU antibody labelled with FITC. The samples are then analysed on a BD FACS Calibur flow cytometer and compared to positive and negative controls to determine the level of apoptotic induction.

The Apo-BRDU kit (BD Biosciences) contains all of the reagents necessary to carry out this reaction as well as positive and negative control cells for comparison. Briefly, the cells are fixed in 1% paraformaldehyde and permeabilised in 70% ethanol. DNA ends are labelled by incubating the samples with TdT enzyme and Br-dUTP at 37°C for 1 hour. The incorporated Br-dUTPs are detected by incubating the sample with FITC tagged anti-Br-dUTP for 30 minutes in the dark at room temperature. The sample is resuspended in RNase buffer and analyzed on the FACSCalibur. The assay was performed as per the manufacturer's instructions.

2.2.4 Proliferation

Proliferation was detected using the WST-1 reagent (Roche). This is a colourimetric assay that quantifies the viability of cells based on the cleavage of the tetrazolium salt WST-1 to formazan by mitochondrial dehydrogenases. The amount of formazan in the sample can be measured spectrophotometrically at an absorbance of 450 nm. A higher number of viable cells in the sample will lead to increased cleavage of WST-1.

Cells (1 x 10^6 /ml) were treated with the appropriate amount of drug or control for the indicated time period. At the end of the experiment incubation time, 10µl WST-1 reagent was added to a 100 µl aliquot of the cell suspension. The samples were incubated for a further 1 hour at 37°C, at which time the absorbance was read on a SPECTRAFluor Plus spectrophotometer (TECAN, Crailsheim, Germany). Each sample was assayed in duplicate. The viability of the cells was calculated by comparing the absorbance of the treated cells to the absorbance of untreated control cells from the same time point, the viability level which was defined as 100%. The assay was performed according to the manufacturer's instructions.

2.2.5 ELISA

TNF-α and IL-8

TNF-α and IL-8 ELISA kits were obtained from R&D systems. Briefly, a 96 well polystyrene plate was coated with the capture antibody overnight. The plate was then washed and blocked with a BSA solution to coat any areas of the plate that did not bind the capture antibody. Again the plate was washed and the samples were loaded onto the plate along with an 8 point standard. All samples and standards were assayed in duplicate. The plate was washed and the detection antibody added. After incubation with detection antibody the plate was washed and streptavidin-conjugated horseradish peroxidase was added to each well. After 20 minutes, the plate was washed and blotted again, and the substrate solution was applied to the plate. The substrate solution consisted of a 1:1 dilution of H_2O_2 and TetraMethylBenzidine (TMB). The colour development reaction was stopped with 2N H_2SO_4. The absorbance of each well was read at 450nm with a reference measurement at 595nm. The concentration of the cytokines was calculated by plotting the concentration of the standards versus their absorbance and fitting a line through the points. The equation of the standard curve was used to calculate the values in the samples.

Thiopurine ELISA

The intracellular accumulation of the thiopurines 6TG and 6MP were assayed by a competitive ELISA. In this type of ELISA, the test plate has been coated with a carrier protein conjugated to the chemical of interest. The sample that is being assayed is pre-incubated with the primary (1°) antibody, then added to the plate. Any of the 1° antibody that does not bind to the target in the sample will bind to the target that is adhered to the plate. The amount of 1° antibody bound to the plate is detected by a secondary (2°) antibody conjugated to streptavidin HRP. The absorbance of the sample is inversely related to the amount of target in that sample.

For this assay, the ELISA plate was coated with the BSA-6TG conjugate solution at 4°C overnight. The plate was washed with wash buffer (PBS + 0.05% Tween 20), then blocked with 1% BSA in PBS for 1 hour at room temperature. While the plate was being blocked, 200µl of cell lysis solution was incubated with 200µl of antibody solution at room temperature. After the blocking step, the plate was washed and 100µl of sample (cell lysis solution plus antibody) was added to the appropriate well. An 8 point standard was also included and all samples were assayed in duplicate. After the samples had been incubated on the plate for 1 hour at room temperature, the plate was washed again. A 1:1000 dilution of the 2° antibody was made, 100µl added to each well, and the plate incubated for a further 1 hour at room temperature. The plate was washed, then 100µl of the substrate solution (1:1:2 of H_2O_2, TMB and H_2O) was added to each well. The reaction was stopped with 50µl 2N H_2SO4 after the colour had developed sufficiently. The absorbance of each sample was read at 450nm with a reference measurement at 595nm. The concentration of the thiopurines in the cell lysate was calculated by plotting the concentration of the standards versus their absorbance and fitting a line through the points. The equation of the standard curve was used to calculate the values in the unknown samples.

2.2.6 DNA Techniques

DNA Isolation

DNA was isolated from each of the four cell lines using the Qiagen QIAmp DNA Mini Kit (Qiagen, Sussex, UK). For each cell line, $5x10^6$ cells were pelleted in a 1.5 ml eppendorf tube and resuspended in 200 µl PBS. Once the cells had been resuspended, 20µl of proteinase K was added to each sample, then 200 µl of buffer AL, and the solution was mixed thoroughly. The samples were incubated in a 56°C water bath for one hour to lyse the cells. After this incubation period, 200 µl of 100% ethanol was added to each tube, the samples were mixed thoroughly and applied to a QIAamp spin column. The columns, with collection tubes, were centrifuged at 6000 x g for 1 minute. The collection tube and filtrate were discarded, and the column was fitted with a new collection tube. Next, 500 µl of buffer AW1 was added to each column, then the samples were centrifuged again for 1 minute at 6000 x g. Again, the collection tube and the filtrate were discarded, and a new collection tube fitted to the column. 500 µl of buffer AW2 was added to each of the columns, which were then centrifuged for 3 minutes at 20,000 x g for 3 minutes. The filtrate and collection tube were discarded. The purified DNA was eluted from the column by placing the column in sterile 1.5 eppendorf, adding 200 µl of distilled water to the column, incubating at room temperature for 5 minutes, then centrifuging the apparatus for 1 minute at 6000 x g. The DNA content of each sample was quantitated using the NanoDrop ND-1000 spectrophotometer (NanoDrop Technologies, Wilmington, DE, USA).

Polymerase Chain Reaction (PCR)

DNA samples were amplified by polymerase chain reaction in a PTC-200 DNA Engine (MJ Research, MA, USA). The total volume of each reaction was 50 µl. The final concentrations of the *Taq* polymerase buffer (Promega, Madison, WI, USA) constituents in each reaction was 50 mM KCl, 10 mM Tris-HCl, 0.1% Triton X-100, and 1.5 mM $MgCl_2$. The following reaction mix was used, with minor alterations to optimise the product content of each PCR:

Constituents:	Final Concentration
5 µl Forward Primer (3µM)	0.3 µM
5 µl Reverse Primer (3µM)	0.3 µM
5 µl 10X Buffer	1X
5 µL dNTP stock	10µM each
2 µL DNA	50 µg
0.2 µl *Taq* polymerase	1 U

Amplification of DNA samples was carried using the following reaction conditions, which were adjusted accordingly for each PCR reaction:

PCR Cycling Conditions:

Step 1: Initial Denaturation, 95°C, 2 minutes;
Step 2: Denaturation, 94°C, 30 seconds;
Step 3: Primer Annealing, 52°C, 30 seconds;
Step 4: Extension, 72°C, 30 seconds;
Step 5: Final Extension, 72°C, 7 minutes
Step 6: 4°C for ever.



repeat for 30 cycles

Restriction Fragment Length Polymorphism (RFLP)

RFLP analysis was employed to determine the genotype of the samples. This assay is based on the ability of some bacterial enzymes, termed restriction enzymes, to cleave DNA at a specific base sequence. Each restriction enzyme has a unique recognition site. When a DNA sample is incubated with a restriction enzyme, the enzyme will cleave the DNA at all restriction sites, yielding fragments of defined length dependent on the location of the restriction sites to one another. This can be exploited to analyse DNA samples for a

known genetic polymorphism. If there is an addition or deletion of a base or bases, a restriction site can be removed or added, depending on the particular base change. This may result in a change in the size of the fragments generated, the number fragments, or both. For example, if the wild type gene has three known recognition sites for a certain restriction enzyme, and there is a mutation of some kind at one of these sites, then the enzyme will no longer cleave the DNA sequence at the mutated site. The mutant allele will therefore have a different banding pattern, because one of the recognition sites has been removed.

2.2.7 High Content Screening

High Content Screening (HCS) combines the imaging capabilities of confocal microscopy and quantitative fluorescence in one platform. This developing technology has the ability to monitor cell motility and growth, nuclear translocation and target activation. Several different targets can be monitored at one time, restricted only by the number of dyes available. It is also possible to analyse samples in a variety of formats, as the machine can be adapted to scan specimens mounted on slides, 96 or 384 well plates. Since the platforms are automated and can analyse up to 384 well plates, it is possible to screen a number of compounds or conditions at one time.

We utilised this technology to quantify the transport of TGNs from the cytoplasm to the nucleus. Cells were fixed with 1% paraformaldehyde and permeabilised with Triton X to allow the fluorescent probes to enter the cell. Nuclei were stained with DNA binding dye Hoechst 33342 (Molecular Probes, Eugene, OR, USA), which fluoresces blue. Thioguanine, mercaptopurine and their metabolites were labelled with a primary anti-thioguanine mouse monoclonal antibody (Antibody Shop, Gentofte, Denmark). The primary antibody was detected with a goat anti-mouse $IgG2_a$ secondary antibody

(Molecular Probes, Eugene, OR, USA) which was conjugated to Alexa 488. Alexa 488 fluoresces in the green spectrum. The cells are analysed in black, 96-well flat optical bottom plates to maximise image quality and minimise background interference.

After fixation and staining, plates were analysed on the KineticScan platform (Cellomics Inc., Pittsburgh, PA, USA). Images were acquired in the two channels corresponding to the fluorescent dyes that were used. Channel 1, which corresponded to Hoechst 33342, was used as the focussing channel. Channel 2 corresponded to the Alexa 488 fluorophore (green) conjugated to the 2° antibody used to detect the anti-6TG antibody. Image analysis was performed with the Compartmental Analysis algorithm on the KineticScan platform.

2.2.8 Statistics

All data are expressed as mean ± standard error of the mean (SEM) from at least three separate experiments. Data from cytokine, apoptosis and viability experiments were analysed by two-way analysis of variance (ANOVA) using DataDesk 6.0 (Data Descriptions, Ithaca, N.Y., USA). If the ANOVA was significant, post hoc analysis of treatment versus untreated control at the same time point were made using the Least Significant Difference (LSD). The TF data sets were analysed by ANOVA on the statistical package JMP 4 (SAS Institute, Cary, N.C., USA). Post hoc analysis was performed with Dunnett's test if the ANOVA was significant. A p value of less than 0.05 was considered significant for all tests performed.

CHAPTER 3

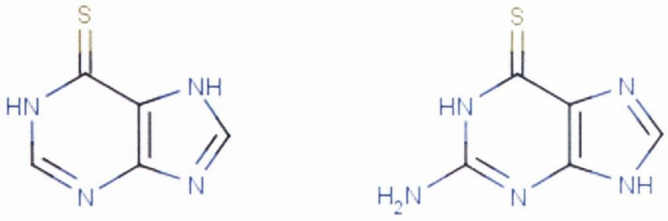
INVESTIGATION OF THE INFLAMMATORY, APOPTOTIC AND ANTI-PROLIFERATIVE EFFECTS OF 6-THIOGUANINE AND 6-MERCAPTOPURINE

3.1 INTRODUCTION

6-thioguanine (6TG) and 6-mercaptopurine (6MP) are members of the thiopurine class of compounds. This group of drugs has a wide range of clinical applications, varying from maintenance therapy of acute leukaemias, to treatment for inflammatory conditions such as rheumatoid arthritis, inflammatory bowel disease, and dermatologic conditions (McLeod and Siva, 2002). Thiopurines are inactive pro-drugs that require metabolic activation to exert their cytotoxic effects. The chemical structure of 6TG and 6MP and their metabolic pathway are shown in Figures 3.1 and 3.2, respectively.

The thiopurines are transported into the cell *via* concentrative and equilibrative nucleoside transporters. Both types of transporter are important for the regulation of key physiological processes, including cardiac contractility and platelet aggregation. Equilibrative nucleoside transporters (ENT) are ubiquitously expressed in mammalian tissues. The movement of the nucleobases across the membrane *via* these transporters is driven by their concentration gradient. ENTs can be divided into two groups: sensitive (*es*) or insensitive (*ei*) to nitrobenzylthioinosine (NBMPR). Both *es* and *ei* transporters have broad substrate specificity for purine and pyrimidine nucleobases (Baldwin, 1999).

Concentrative nucleoside transporters (CNT) are less widely distributed. They have been described in specialised epithelial cells such as renal, intestinal and liver. CNTs move nucleosides inward against their concentration gradient by coupling their transport to the



Mercaptopurine Thioguanine

Figure 3.1 Chemical structure of 6MP and 6TG, taken from the National Library of Medicine's ChemIDplus website, http://chem.sis.nlm.nih.gov/chemidplus/.

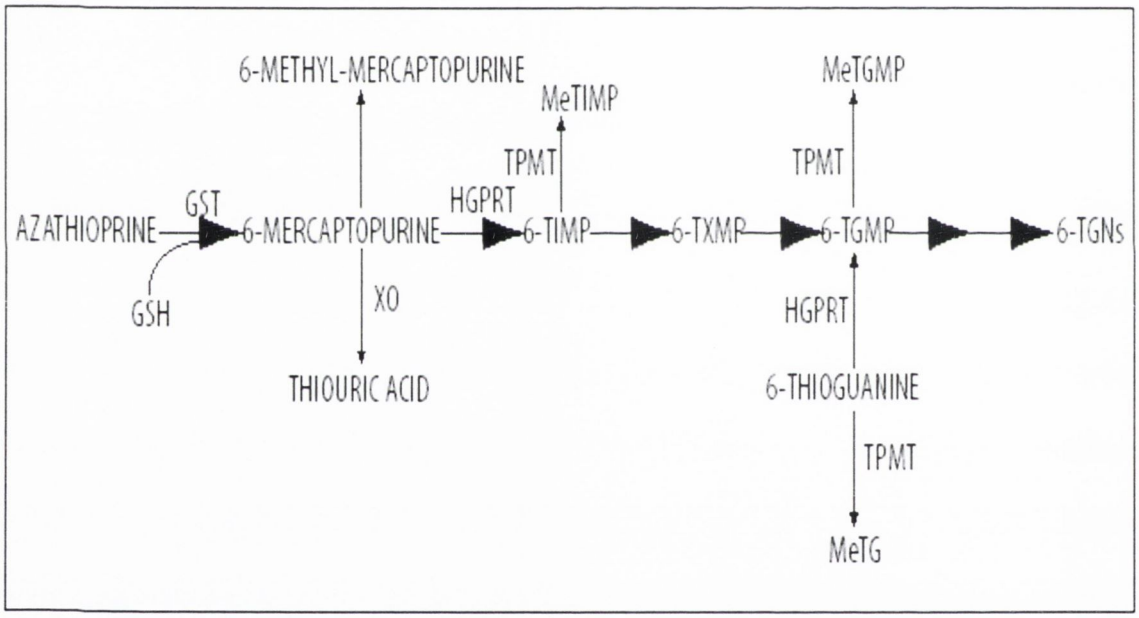


Figure 3.2 The Thiopurine Metabolic Pathway, taken from Cara *et al*, Med Sci Monit, 2004 10(11): RA247-254. GST, glutathione S-transferase; GSH, glutathione; XO, xanthine oxidase; HGPRT, hypoxanthine guanine phosphoribosyl transferase; TPMT, thiopurine methyltransferase; 6-TIMP, 6-thioinosine monophosphate; MeTIMP, methyl thioinosine monophosphate; 6-TXMP, 6-thioxanthine monophosphate; 6-TGMP, 6-thioguanine monophosphate; MeTG, methyl thioguanine; 6-TGNs, thioguanine nucleotides.

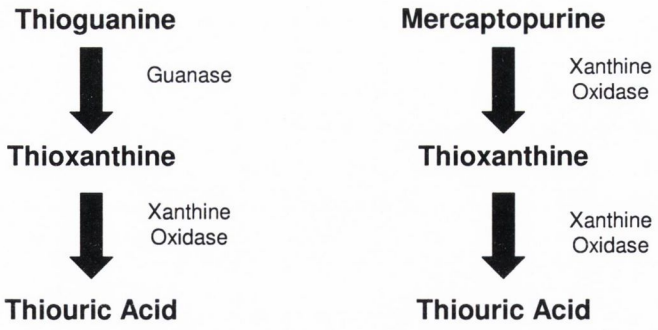


Figure 3.3 The Oxidative Metabolic Pathway of 6TG and 6MP, adapted from Lennard *et al*, 2006.

movement of sodium ions (Ritzel, 2001). There are three main types of CNTs which are classified on the basis of their sensitivity to NBMPR and their substrate specificity. The *cif* transporters accept purine nucleosides and uridine as substrates. They are insensitive to NBMPR and permeable to formycin B. The *cit* transporters are insensitive to NBMPR and permeable to thymidine. Their substrates are pyrimidine nucleosides and adenosine. The *cib* group or transporters are insensitive to NBMPR and permeant to a broad range of substances. Both purine and pyrimidine nucleosides are substrates for this group (Baldwin, 1999). The thiopurines are substrates for both ENT and CNT. It is probable that toxicity to these drugs is due in part to the expression levels of the nucleoside transporters. Inhibition of ENT1 with NBMPR has shown been shown to decrease the TGN level by 33-45% after *in vitro* 6MP treatment (Zaza, 2005).

Once the thiopurines have been transported into the cell by nucleoside transporters, they are converted into the active metabolites that exert the cytotoxic effects. The main active metabolites are thioguanine nucleotides (TGN), which are formed by hypoxanthine guanine phosphoribosyl transferase (HGPRT). These metabolites are thought to induce cytotoxicity by incorporation into DNA, triggering cell cycle arrest and apoptosis (Cara,

2004). Alternatively, the parent compounds can also be metabolised by thiopurine methyltransferase (TPMT) into methylated ribonucleotides. Methylated ribonucleotides inhibit purine *de novo* synthesis (PDNS), leading to metabolic arrest (Cara, 2004; Estlin, 2001). Therefore, it is probable that the cytotoxic effect of 6MP and 6TG is due to a balance between the apoptotic and anti-metabolic effects of their metabolites.

Expression levels of the TPMT and HGPRT enzymes are polymorphic. However, it appears that TPMT is the most important in determining patient sensitivity to treatment with either 6TG or 6MP (de Boer, 2006). The generation of TGNs is inversely related to TPMT activity. Low TPMT expression shunts the drug along the metabolic pathway toward TGN production. These metabolites are incorporated into DNA, causing extensive mismatch repair, eventually leading to apoptosis. If there is high TPMT expression, a larger proportion of the absorbed drug is converted into methylated ribonucleotides. The methylated ribonucleotides are inhibitors of PDNS, thereby contributing to the anti-metabolic effects of these drugs (de Boer, 2006).

An important difference between 6TG and 6MP is the additional metabolic steps that are required to activate 6MP. 6MP undergoes two additional metabolic activations in the pathway than 6TG (Figure 3.2). It can also be converted into 6-methylmercaptopurine by TPMT. 6-methylmercaptopurine is itself an inhibitor of PDNS. Therefore, 6MP has been proposed as a two in one drug with the dual activity of inhibiting proliferation on one hand and inducing apoptosis on the other (de Boer, 2006). TPMT activity levels play an important role in how the drug is metabolised. Patients with wild-type TPMT activity treated with 6MP were found to have more methylated ribonucleotides than TGN (Cara, 2004). *In vitro*, cells that express high levels of TPMT are more sensitive to 6MP than

6TG; conversely, cells that have low TPMT expression are more sensitive to 6TG than 6MP (Cara, 2004).

TPMT expression levels are polymorphic. In Caucasian populations, approximately 90% of individuals have high activity, 10% have intermediate activity, and around 1 in 300 individuals have low activity (Roberts, 2004). A patients' TPMT activity level influences treatment outcome; if there is low activity, the patient is at a severe risk for haematopoietic toxicity due to the accumulation of TGNs (Song, 2006).

Three major point mutations that reduce function have been identified in the TPMT gene. These are G238C, G460A, and A719G. The wild type allele is designated TPMT*1. The mutant alleles are TPMT*2 (G238C), TPMT*3A (G460A and A719G), TPMT*3B (G460A) and TPMT*3C (A719G). Ten alleles in total have been identified, but each of the other alleles has only been found in one individual (Roberts, 2004). The frequency of the polymorphisms varies among ethnic populations, however these four have been detected in over 80% of Caucasians with low to intermediate activity (Song, 2006).

The route of oxidative metabolism is also different for 6TG and 6MP. Oxidative metabolism is the manner through which the drugs are inactivated. Both 6TG and 6MP both require xanthine oxidase activity to be transformed into thiouric acid. But 6TG must first be deaminated by guanase before it can be inactivated by xanthine oxidase (XO) (Figure 3.3) (Lennard, 2006). This metabolic route appears to be more important for 6MP than 6TG. The addition of allopurinol, an XO inhibitor, to the treatment regimen of individuals with IBD on mercaptopurine therapy optimised the TGN metabolite levels by blocking the inactivation of 6MP (Sparrow, 2005). However, 6TG is not a direct substrate for XO, therefore a XO inhibitor will not have the same effect. 6TG dosage reduction is

not necessary with concomitant allopurinol (Grem, 2002). XO activity levels in the bone marrow are low, therefore this enzymatic pathway is unlikely to affect the activity of 6MP or 6TG at their main site of action (Coulthard, 2005).

There are two mechanism of action proposed for 6TG and 6MP. One is the inhibition of PDNS by methylated ribonucleotides. The other is induction of apoptosis *via* the incorporation of TGNs into DNA (Cara, 2004). TPMT can methylate the bases 6TG and 6MP, as well as the nucleotide form of the drug. The methylated bases themselves are not cytotoxic. However, if 6TG and 6MP are first converted into their nucleotide form (base + sugar + phosphate) by HGPRT, then methylated by TPMT, the end products are methylated ribonucleotides. Methylated ribonucleotides strongly inhibit PDNS by triggering the build up of phosphoribosyl pyrophosphate (PRPP). In the *de novo* pathway, purines are formed in a stepwise manner where PRPP serves as the phosphoribosyl donor. This pathway is subject to feedback regulation. However, there is also a salvage pathway that recycles preformed bases or nucleotides. One of the enzymes involved in purine salvage is HGPRT (Grem, 2002).

It has been proposed that TGN-induced apoptosis occurs *via* recognition of the faulty bases by the mismatch repair (MMR) pathway (Swann, 1996). The TGN 6-thio-2'-deoxyguanine triphosphate (6-TdGTP) is mis-incorporated in place of adenine, opposite thymine. If this incorporation is not corrected, in the next replication cycle a cytosine will be incorporated as complimentary to the 6-TdGTP, resulting in a T→C point mutation (Grem, 2002). The MMR system recognises and repairs mismatches after DNA replication, as well as triggering cell cycle arrest and apoptosis following certain types of DNA damage (O'Brien, 2006). MMR will recognise and cleave the mis-paired base from the daughter strand, but does not remove the 6-TdGTP from the parent strand. In the next

cycle of replication, the MMR system will be recruited to process the same site again. If there is considerable TGN incorporation into DNA, there will be several sites of single strand breaks in the DNA that will activate the checkpoint signalling, ending in apoptosis of the affected cell (Yan, 2003). Deficiencies in MMR are associated with genomic instability, creating a 'mutator phenotype' cell with a high rate of spontaneous mutations (O'Brien, 2006). MMR deficient cells also show variable resistance to thiopurines therapy, both *in vivo* and *in vitro* (Yan, 2003).

Another mechanism through which the thiopurines may induce apoptosis is recognition of structural changes in the DNA double helix. Incorporation of 6-TdGTP opposite cytosine causes a subtle change in the DNA structure because of changes in the hydrogen bonding. This structural alteration affects the thermal stability of the altered DNA sequence, decreasing the melting temperature by approximately 6°C. The effects were localised to the affected base pair (Somerville, 2003). However subtle these changes in DNA structure may be, the structural changes are recognised by a protein complex distinct from MMR. It is hypothesised that this protein complex triggers another series of biochemical events that induce a cytotoxic response to 6TG or 6MP (Krynetski, 2001). This may account for the thiopurines sensitivity observed in cell lines that lack vital components of the MMR system (Cara, 2004).

3.2 THIOGUANINE AND MERCAPTOPURINE EXPERIMENTS

For suspension cell cultures, the cells were passed the day before use to ensure that they were in the log phase of growth. The cells were centrifuged at 400g for 5 minutes and the supernatant discarded. The cell pellet was washed in the appropriate medium without FBS. The cells were counted and diluted accordingly for a final concentration of $1x10^6$ cells/ml. 990 ul of the cell suspension was aliquoted into each well of a 24-well sterile tissue culture plate. 10ul of the appropriate dilution of drug or control were then added to bring the final volume to 1000ul. Experiments involving HepG2 cells, 2 ml of 1×10^6 cells/ml cell suspension was added to each well of a 6-well sterile tissue culture plate and cells were allowed to adhere overnight in the incubator. On the day of the experiment, the monolayer was washed twice in PBS, then 1ml of serum free medium with the appropriate concentration of drug or control was aliquoted. All experiments were performed at 37°C, 5% CO_2, in the absence of FBS.

After the designated time period, the plate was removed from the incubator and the medium was removed from the wells to labelled 1.5ml eppendorf tubes. Adherent cells were scraped from the bottom of the plate with a sterile rubber policeman, then removed with the medium and pipetted into labelled 1.5 ml eppendorfs. The cells were centrifuged at 400g, 4°C for 5 minutes, and the supernatant removed. The cells were fixed and stored in ethanol -20°C for ApoBrdU labelling to measure induction of apoptosis, while the supernatant was stored at -70°C for ELISA quantitation of TNF-α and IL-8 cytokine concentrations.

Analysis of proliferation of suspension cell lines was performed as described in Chapter 2.2.4. For the HepG2 cell lines, cells were plated as described for the apoptosis assay, but 200µl of a $1x\ 10^6$ cells per ml solution was aliquoted into each well of a 96 well plate.

TF expression on the surface of THP1, Jurkat E6.1, and HepG2 cells was quantitated as described in Chapter 2.2.2. The geometric mean was used for all calculations; percentages are relative to the untreated cells, which were used to define the 100% expression level.

TPMT polymorphisms were determined as described in Chapter 2.2.6. Primer sequences and cycling conditions were used as described in Yates *et al.* (1997). A temperature curve was performed for the annealing temperature for each polymorphism in order to optimise product concentration. The temperatures chosen for the curve were based on the melting temperatures of the primer pairs. For the TMPT*2 reaction, the annealing temperature was increased from 48°C to 51°C in 1°C increments. The best results were obtained with an annealing temperature of 49°C. The G460A reaction was run with an annealing temperature curve from 48°C to 59°C, increasing in 1°C increments. For the G460A primer set an annealing temperature of 55°C achieved the best results. A magnesium concentration curve was also performed on the G460C polymorphism reaction conditions. The concentration of $MgCl_2$ was increased stepwise from 1.25 mM to 2.0 mM in 0.25 mM increments. The 55°C annealing temperature was used. At this annealing temperature, the strongest band was obtained with the reaction mixture containing 1.25 mM $MgCl_2$. The A719G annealing temperature curve was run from 65 °C to 73 °C in 1°C increments, and 52°C to 60°C in 2°C increments. The clearest product band was obtained with an annealing temperature of 52°C.

3.3 RESULTS

3.3.1 Cytokine Release

IL-8 was the predominant cytokine secreted by THP1 (Figure 3.3) and HepG2 (Figure 3.5) cells after treatment with 6TG or 6MP. After 24 hours, there was a significant ($P<0.001$) increase in IL-8 levels in the supernatant of THP1 cells treated with 6TG or 6MP. However, in the cells treated with 6TG the IL-8 concentration peaked at the 50μM treatment level and then decreased with higher doses of 6TG, whereas in the 6MP treated cells the IL-8 levels continuously increased. HepG2 cells secreted significant ($P<0.001$) levels of IL-8 after 2, 6 and 24 hour incubations with 6TG. The response to 6MP was different, however, showing a significant ($P<0.001$) increase in IL-8 only after 2 and 6 hour incubations. This may be due to the high level of IL-8 secreted by the untreated HepG2 cells at 24hours. In contrast to the THP1 response to 6TG, the IL-8 levels in HepG2 supernatant peaked at the 25 μM treatment and then remained constant at all three time points. The same response was seen in HepG2 cells after 6 hours 6MP treatment. Neither 6TG nor 6MP stimulated significant TNF-α secretion in THP1 or HepG2 cells. Jurkat E6.1 (Figure 3.4) and 697 cells (Figure 3.5) did not release significant amounts of TNF-α or IL-8 in response to either 6TG or 6MP.

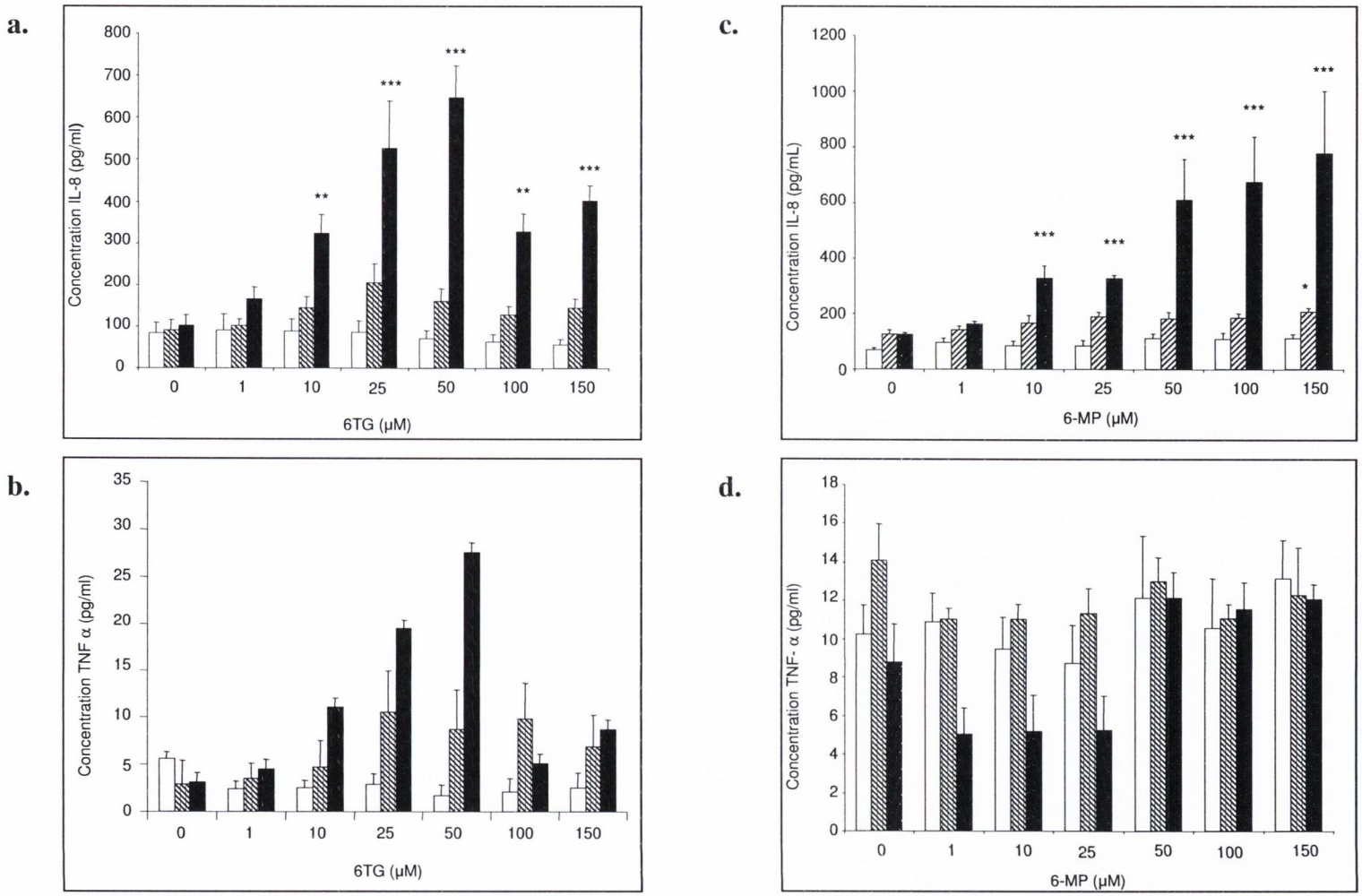


Figure 3.4 THP-1 Cytokine Response to 6TG or 6MP. IL-8 (a and c) and TNF-α (b and d) levels in the supernatant were measured at 2 (□), 6 (▨) or 24 (■) hours, after cells ($1x10^6$) were incubated with 6TG (a and b) or 6MP (c and d). Results shown are the average + SEM of at least 3 independent experiments assayed in duplicate. Significance was determined by 2-way ANOVA; if this was significant ($P<0.05$), *a posteriori* comparison of treatment to untreated control at the same time point were made by Least Significant Difference. * $P<0.5$, ** $P<0.01$, *** $P<0.001$.

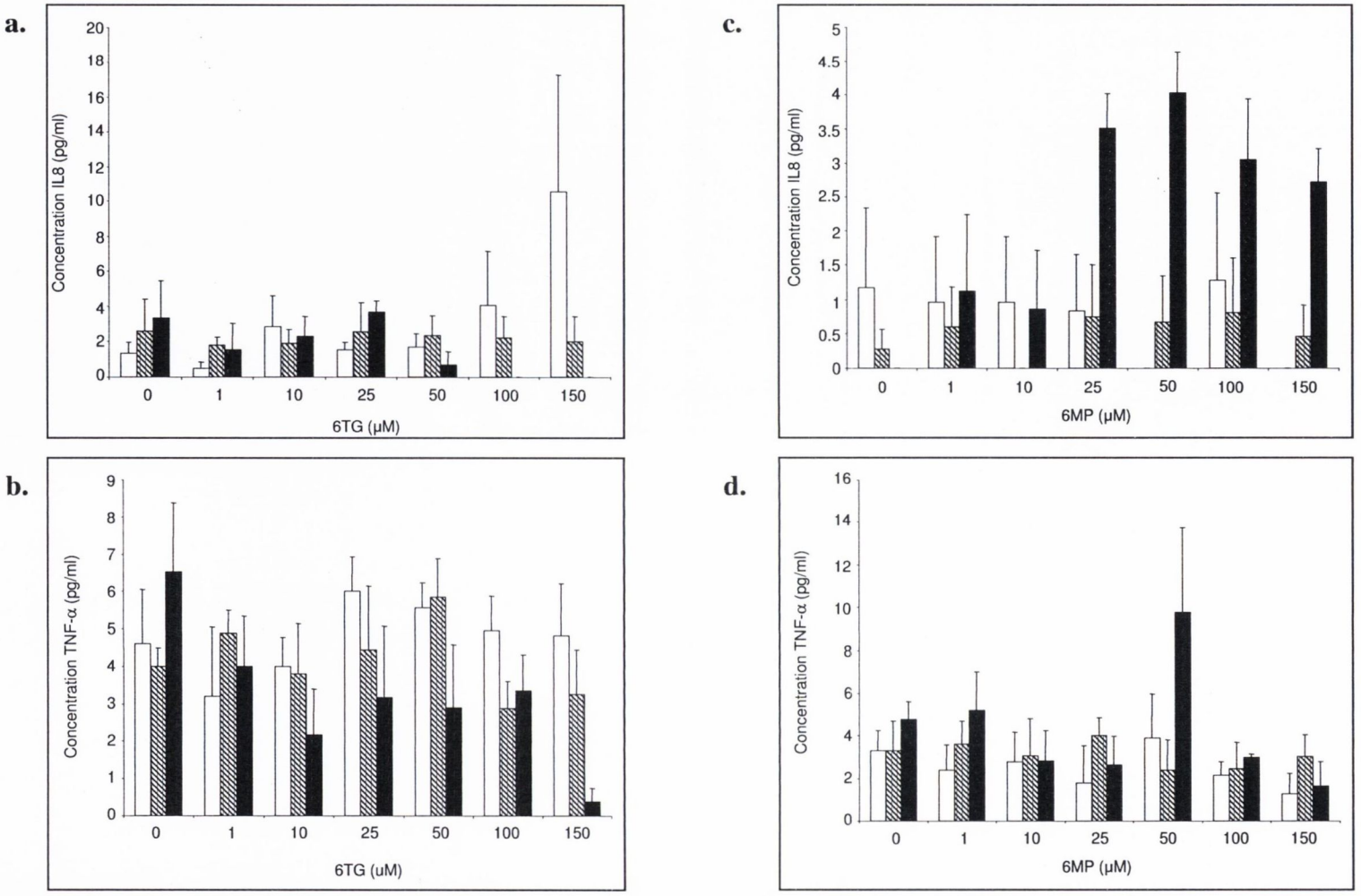


Figure 3.5 Jurkat E6.1 Cytokine Response to 6TG or 6MP. IL-8 (a and c) and TNF-α (b and d) levels in the supernatant were measured at 2 (□), 6 (▨) or 24 (■) hours, after cells ($1x10^6$) were incubated with 6TG (a and b) or 6MP (c and d). Results shown are the average + SEM of at least 3 independent experiments assayed in duplicate. Significance was determined by 2-way ANOVA; if this was significant ($P<0.05$), *a posteriori* comparison of treatment to untreated control at the same time point were made by LSD. * $P<0.5$, ** $P<0.01$, *** $P<0.001$.

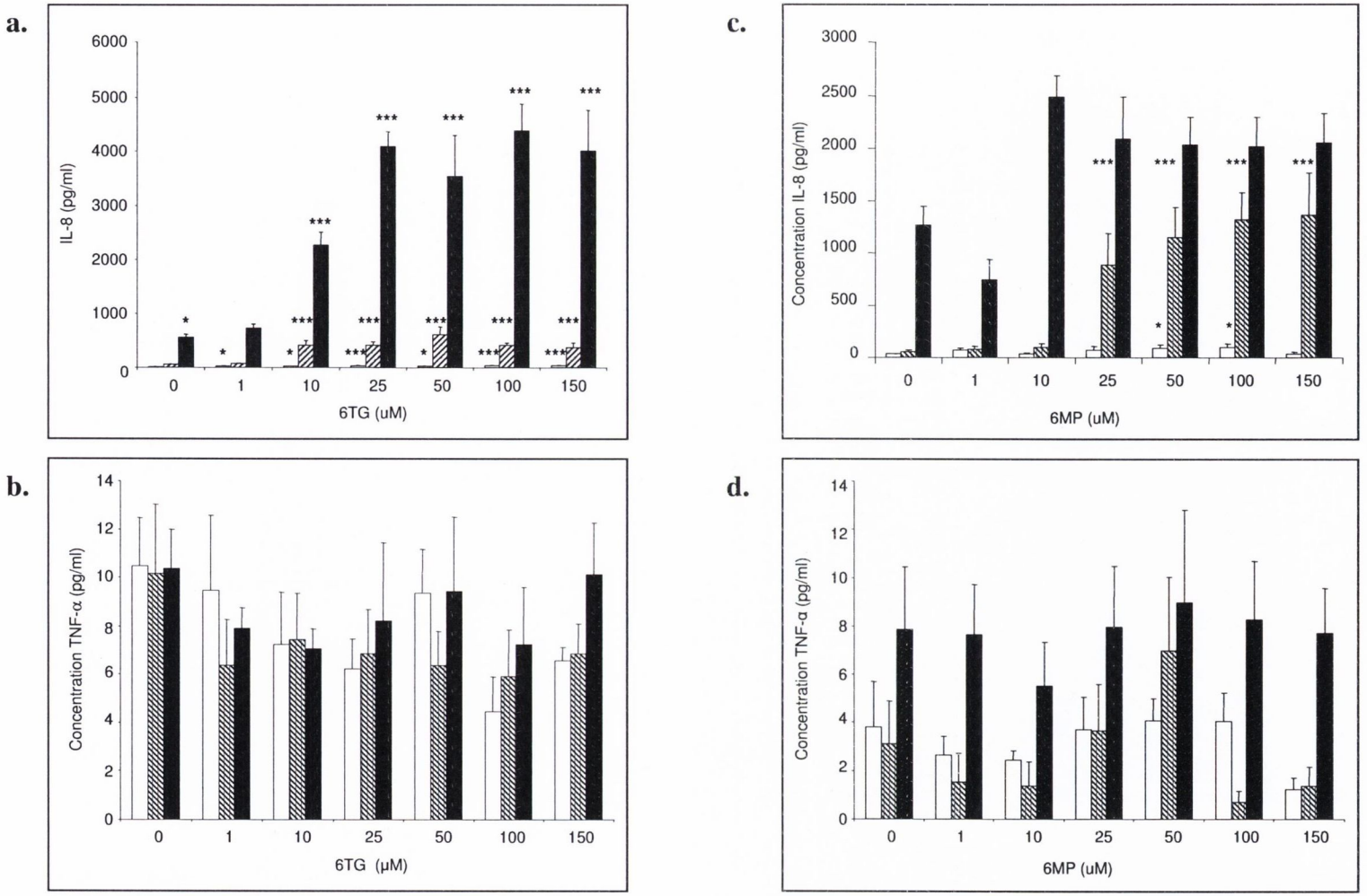


Figure 3.6 HepG2 Cytokine Response to 6TG or 6MP. . IL-8 (a and c) and TNF-α (b and d) levels in the supernatant were measured at 2 (□), 6 (▨) or 24 (■) hours, after cells ($1x10^6$) were incubated with 6TG (a and b) or 6MP (c and d). Results shown are the average + SEM of at least 3 independent experiments assayed in duplicate. Significance was determined by 2-way ANOVA; if this was significant ($P<0.05$), *a posteriori* comparison of treatment to untreated control at the same time point were made by LSD. * $P<0.5$, ** $P<0.01$, *** $P<0.001$.

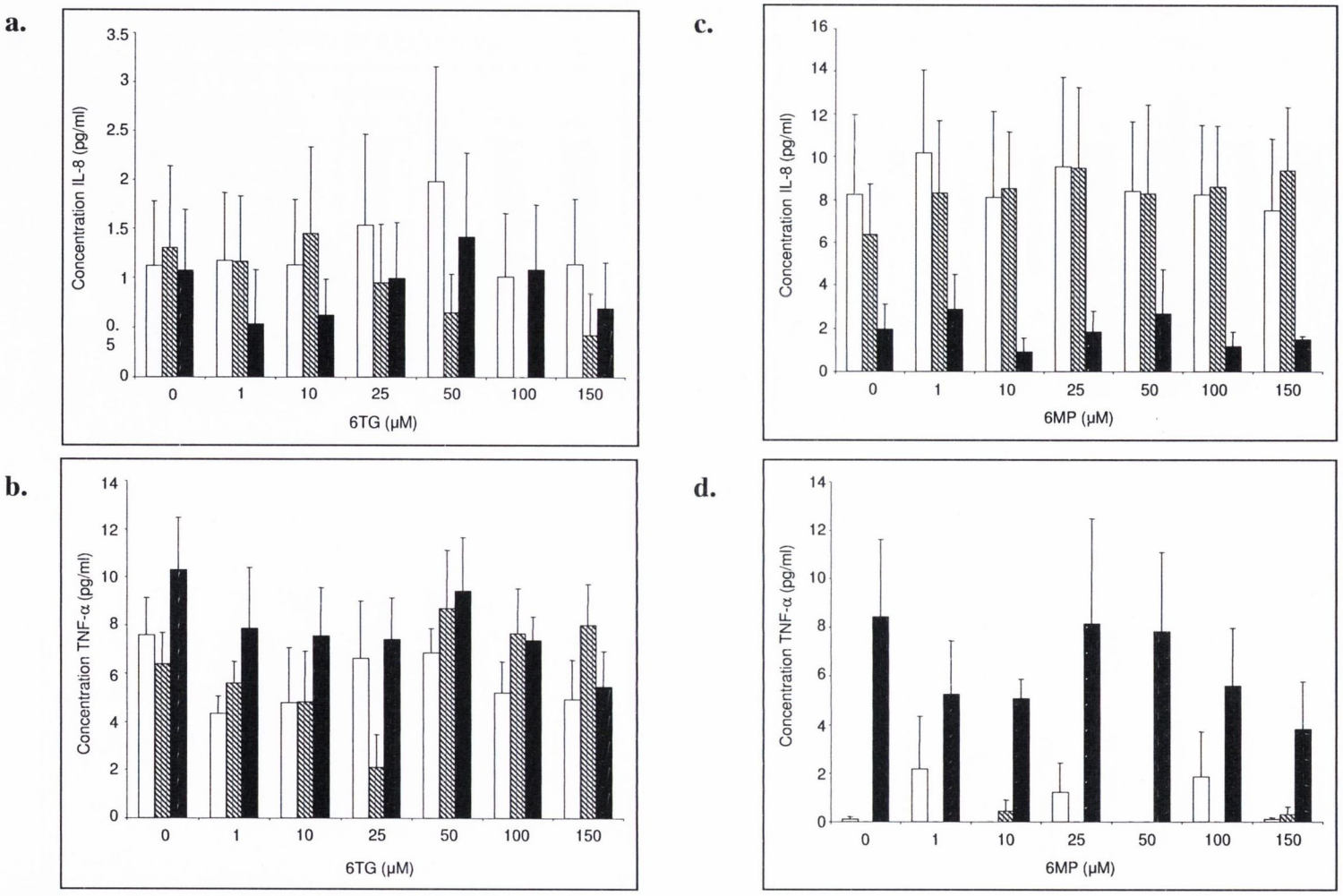


Figure 3.7 697 Cytokine Response to 6TG or 6MP. IL-8 (a and c) and TNF-α (b and d) levels in the supernatant were measured at 2 (□), 6 (▨) or 24 (■) hours, after cells ($1x10^6$) were incubated with 6TG (a and b) or 6MP (c and d). Results shown are the average + SEM of at least 3 independent experiments assayed in duplicate. Significance was determined by 2-way ANOVA; if this was significant ($P<0.05$), *a posteriori* comparison of treatment to untreated control at the same time point were made by LSD. * $P<0.5$, ** $P<0.01$, *** $P<0.001$.

3.3.2 Viability

Both THP1 (Figure 3.7a) and Jurkat E6.1 (Figure 3.8a) cells showed a significant ($P<0.001$), dose-dependent decrease in viability after incubation with 6TG for 24 hours. For both cell lines viability decreased with increasing concentration of 6TG until the 25 μM dose. The viability remained constant with increasing dose after that treatment. However, 6TG had a greater effect on Jurkat E6.1 cells, where the proliferative ability of the cells was reduced to approximately 50%, compared to 70% in THP1 cells.

The viability curves of 6MP treated cells showed a different effect than that seen with 6TG. As with 6TG treatment, the maximum decrease in proliferation occurred at the 25 μM treatment level. But as the dose increased, the cells recovered some of their proliferative ability. For example, in THP1 cells, as the dose increased from 25 to 50 μM of 6MP, the viability of the cells rose from 59% to 68%. In THP1 cells, there was a significant ($P<0.001$) decrease in viability at the 6 and 24 hour time points (Figure 3.7b). The viability of Jurkat E6.1 cells was only affected after 24 hours incubation with 6MP (Figure 3.8b). Neither HepG2 nor 697 cells showed any change in viability after treatment with 6TG or 6MP (Figure 3.9 and 3.10, respectively).

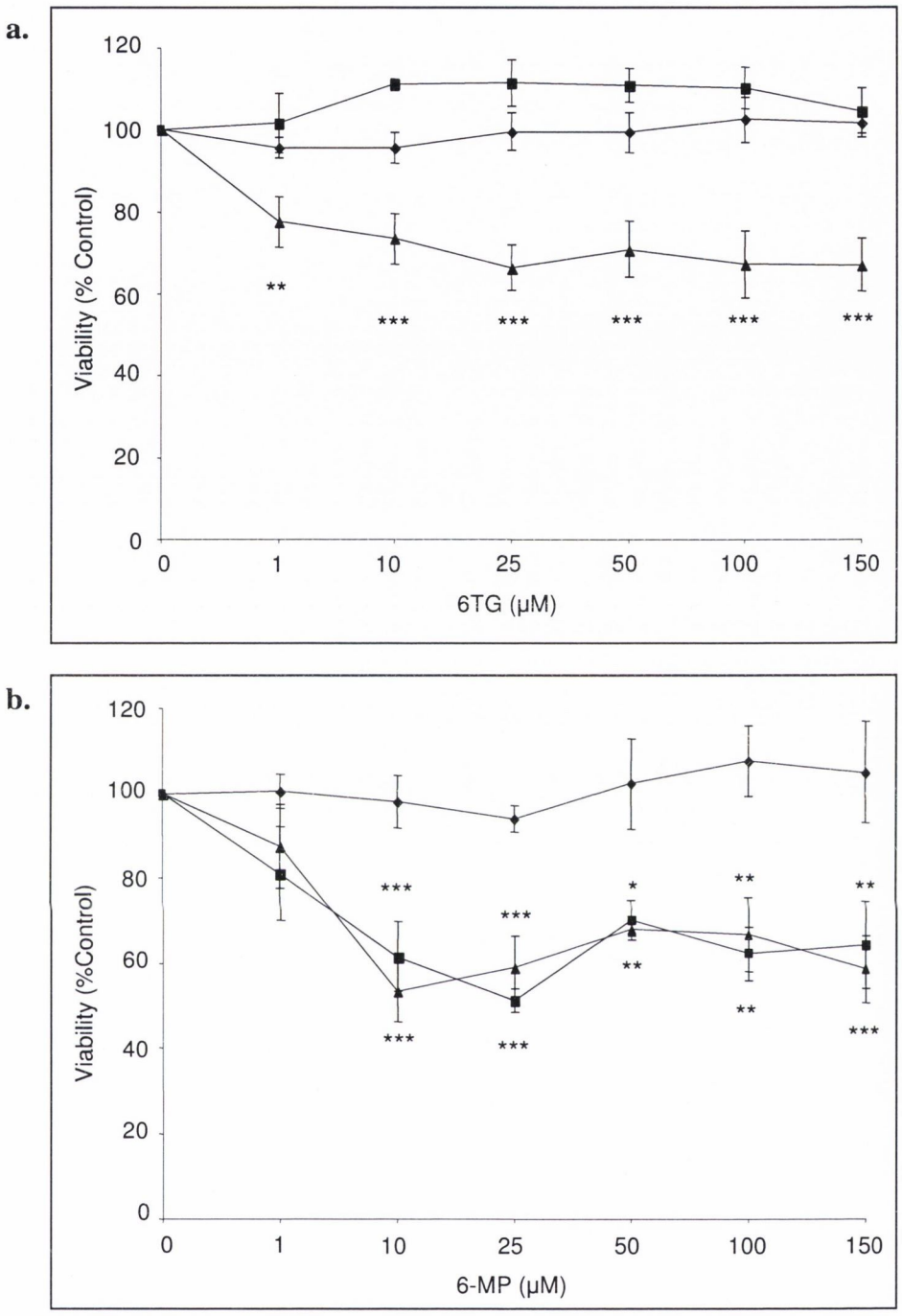


Figure 3.8 Viability of THP1 cells after treatment with 6TG or 6MP. Effect of 6TG (a) and 6MP (b) on the viability of THP1 cells was assessed after 2 (♦), 6 (■) and 24(▲) hour incubation with either drug. Viability was determined by measuring the cleavage of WST-1. Values are relative to the untreated control at the same time point, which was defined as 100% viable. Points shown are the mean ± SEM of at least three independent experiments assayed in duplicate. Data were analysed by 2-way ANOVA; if the ANOVA table was significant ($P<0.05$), post hoc comparisons of treatment to untreated control were made using LSD. * $P<0.5$, ** $P<0.01$, *** $P<0.001$.

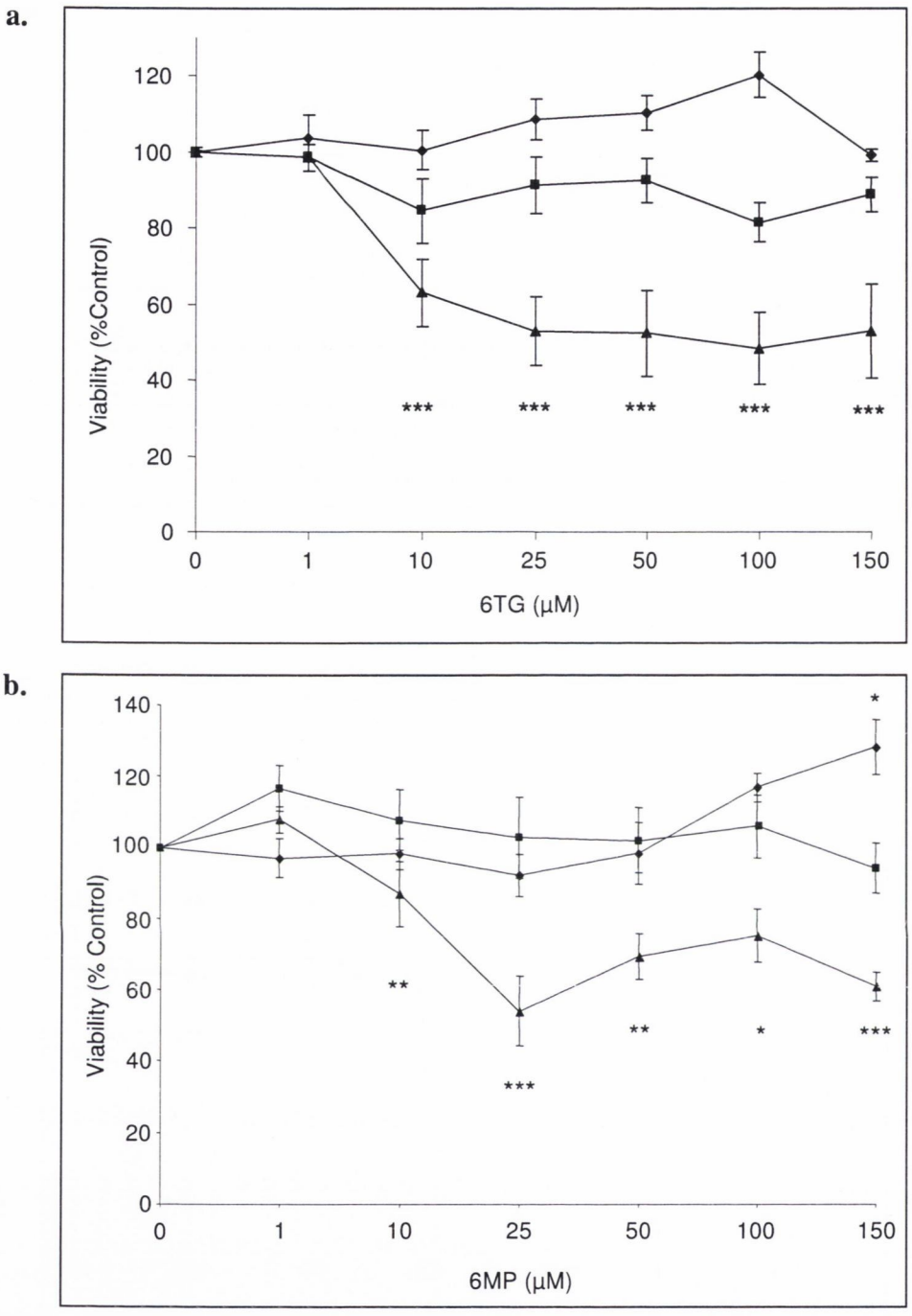


Figure 3.9 Viability of Jurkat E6.1 cells after treatment with 6TG or 6MP. Effect of 6TG (a) and 6MP (b) on the viability of Jurkat E6.1 cells was assessed after 2 (♦), 6 (■) and 24(▲) hour incubation with either drug. Viability was determined by measuring the cleavage of WST-1. Values are relative to the untreated control at the same time point, which was defined as 100% viable. Points shown are the mean ± SEM of at least three independent experiments assayed in duplicate. Data were analysed by 2-way ANOVA; if the ANOVA table was significant ($P<0.05$), post hoc comparisons of treatment to untreated control were made using LSD. * $P<0.5$, ** $P<0.01$, *** $P<0.001$.

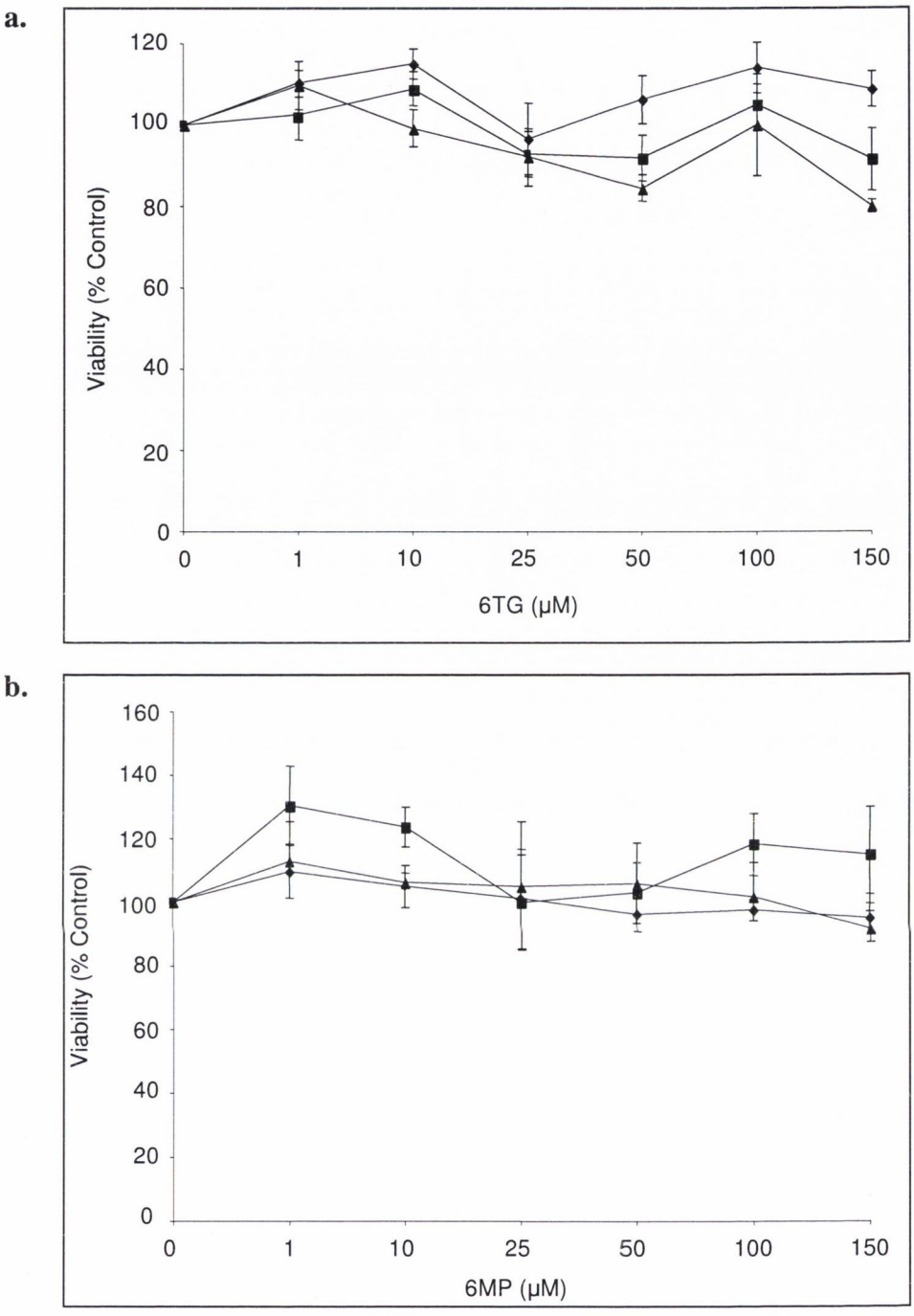


Figure 3.10 Viability of HepG2 cells after treatment with 6TG or 6MP. Effect of 6TG (a) and 6MP (b) on the viability of HepG2 cells was assessed after 2 (♦), 6 (■) and 24(▲) hour incubation with either drug. Viability was determined by measuring the cleavage of WST-1. Values are relative to the untreated control at the same time point, which was defined as 100% viable. Points shown are the mean ± SEM of at least three independent experiments assayed in duplicate. Data were analysed by 2-way ANOVA; if the ANOVA table was significant ($P<0.05$), post hoc comparisons of treatment to untreated control were made using LSD. * $P<0.5$, ** $P<0.01$, *** $P<0.001$.

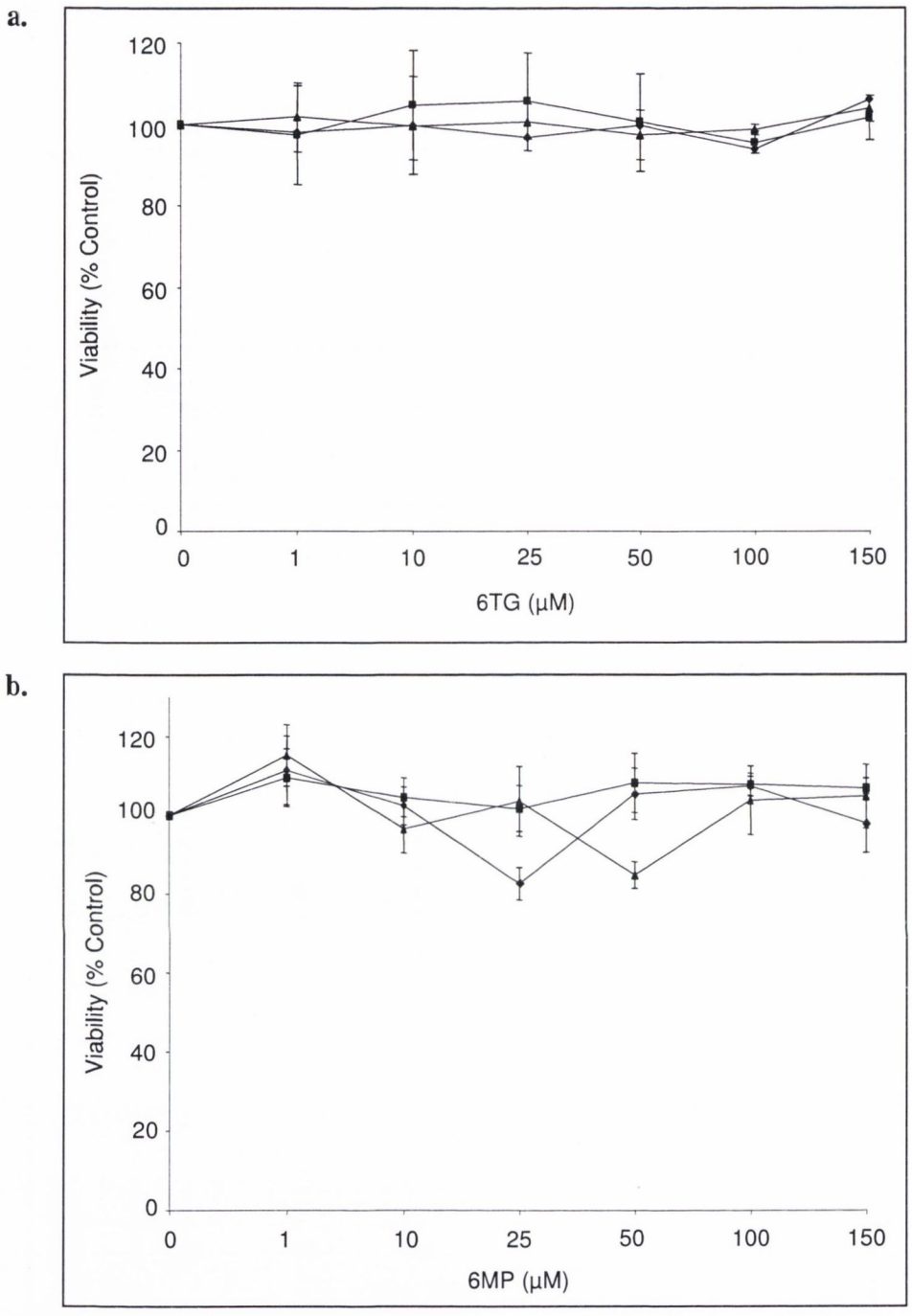


Figure 3.11 Viability of 697 cells after treatment with 6TG or 6MP. Effect of 6TG (a) and 6MP (b) on the viability of 697 cells was assessed after 2 (♦), 6 (■) and 24(▲) hour incubation with either drug. Viability was determined by measuring the cleavage of WST-1. Values are relative to the untreated control at the same time point, which was defined as 100% viable. Points shown are the mean ± SEM of at least three independent experiments assayed in duplicate. Data were analysed by 2-way ANOVA; if the ANOVA table was significant ($P<0.05$), post hoc comparisons of treatment to untreated control were made using LSD. * $P<0.5$, ** $P<0.01$, *** $P<0.001$.

3.3.3 Apoptosis

Both 6TG and 6MP increased apoptosis in Jurkat E6.1 cells (Figure 3.12). The greatest effect was seen in Jurkat E6.1 cells that had been exposed to 6TG; 25% of the cells analysed were apoptotic after 24 hour incubation with 25 μM 6TG and higher doses ($P<0.001$). For both drugs, apoptosis was significantly ($P<0.05$) increased at the 10μM treatment level. In THP1 cells, only 6TG elicited a significant ($P<0.001$) increase in apoptosis (Figure 3.11). As in Jurkat E6.1 cells, the increase began at the 10μM treatment level. HepG2 and 697 cells did not show any increase in apoptosis after treatment with 6TG or 6MP versus untreated control cells (Figure 3.13 and 3.14, respectively).

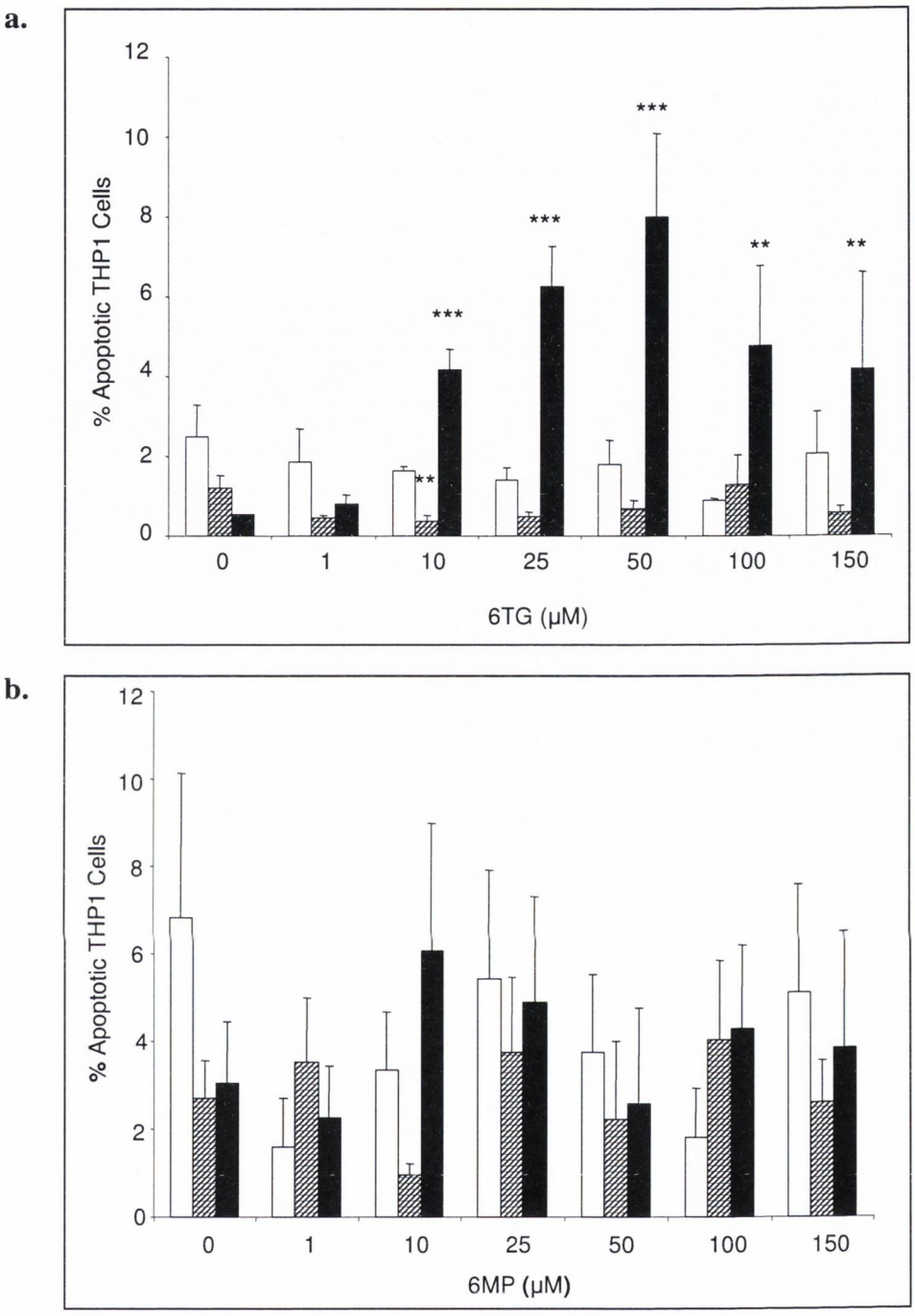


Figure 3.12 Apoptosis of THP1 cells after treatment with 6TG or 6MP. THP1 cells were incubated with 6TG (a) or 6MP (b) for 2 (□), 6 (▨) or 24 (■) hours. The number of apoptotic cells was measured by TUNEL staining and FACS. A minimum of 1000 events were collected for each sample. The values shown are the mean + SEM of at least three independent experiments. Data were analysed by 2-way ANOVA; if the ANOVA table was significant ($P<0.05$), post hoc comparisons of treatment to untreated control were made using LSD. * $P<0.5$, ** $P<0.01$, *** $P<0.001$.

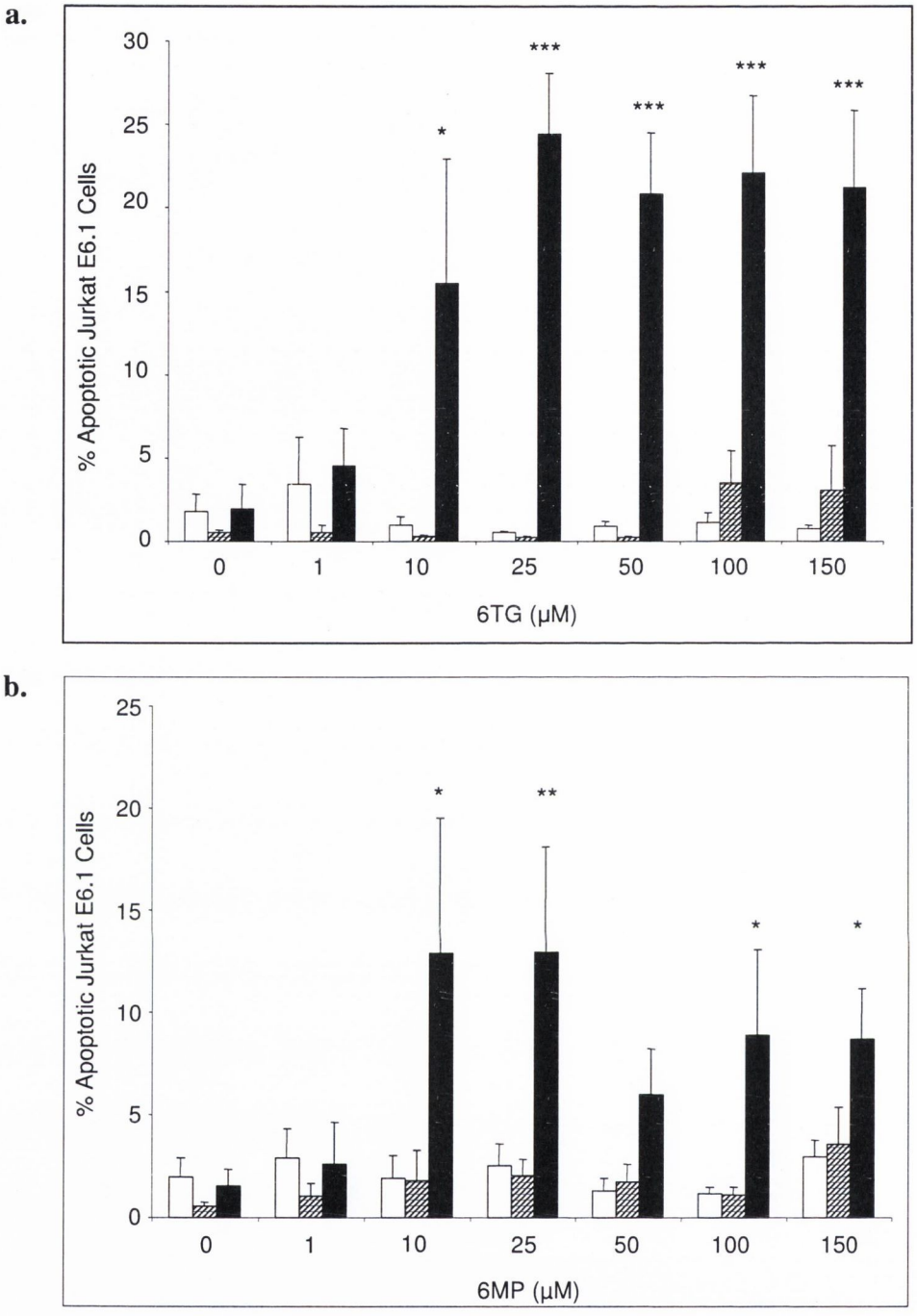


Figure 3.13 Apoptosis in Jurkat E6.1 cells after treatment with 6TG or 6MP. Jurkat E6.1 cells were incubated with 6TG (a) or 6MP (b) for 2 (□), 6 (▨) or 24 (■) hours. The number of apoptotic cells was measured by TUNEL staining and FACS. A minimum of 1000 events were collected for each sample. The values shown are the mean + SEM of at least three independent experiments. Data were analysed by 2-way ANOVA; if the ANOVA table was significant ($P<0.05$), post hoc comparisons of treatment to untreated control were made using LSD. * $P<0.5$, ** $P<0.01$, *** $P<0.001$.

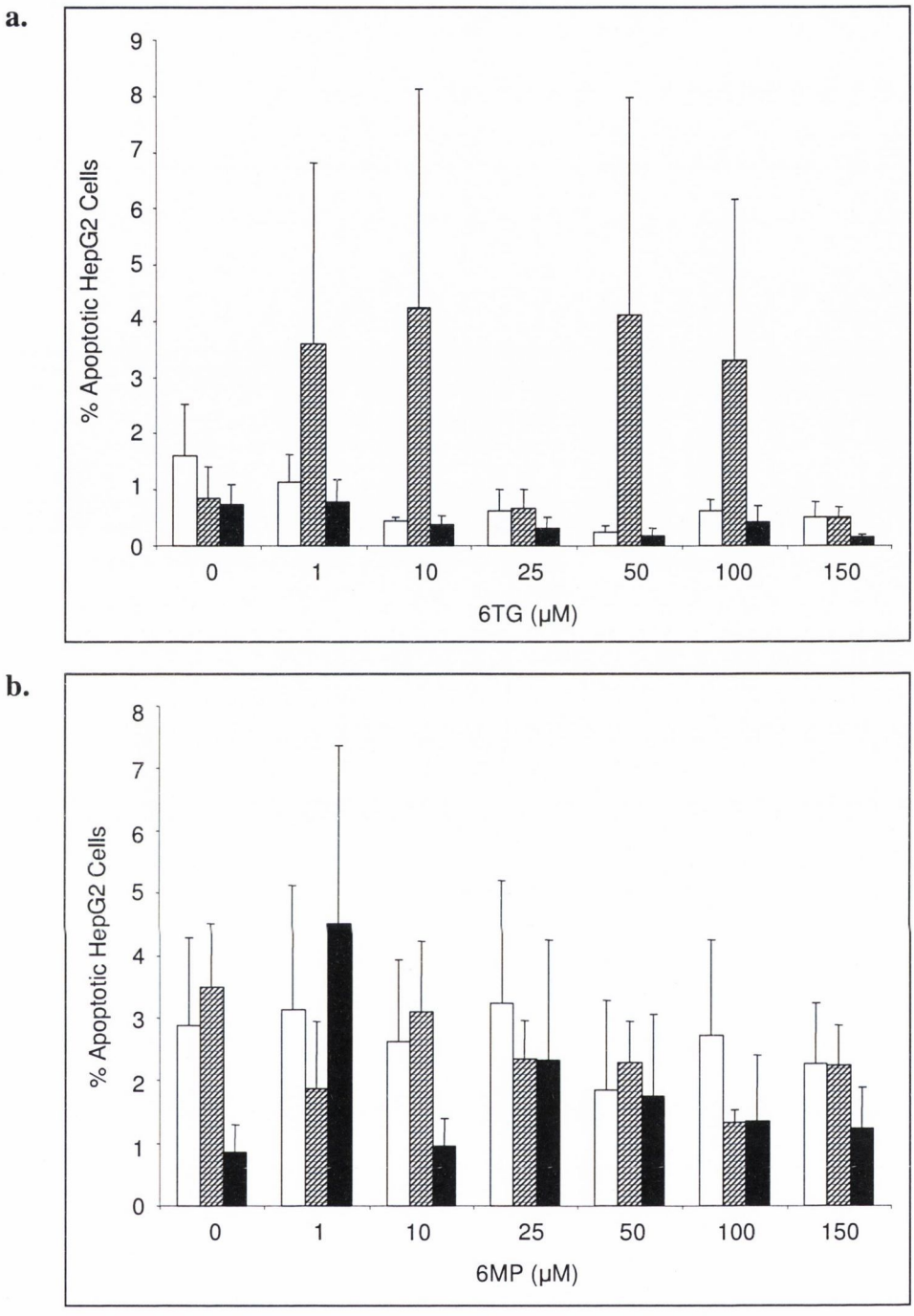


Figure 3.14 Apoptosis in HepG2 cells after treatment with 6TG or 6MP. HepG2 cells were incubated with 6TG (a) or 6MP (b) for 2 (□), 6 (▨) or 24 (■) hours. The number of apoptotic cells was measured by TUNEL staining and FACS. A minimum of 1000 events were collected for each sample. The values shown are the mean + SEM of at least three independent experiments. Data were analysed by 2-way ANOVA; if the ANOVA table was significant ($P<0.05$), post hoc comparisons of treatment to untreated control were made using LSD. * $P<0.5$, ** $P<0.01$, *** $P<0.001$.

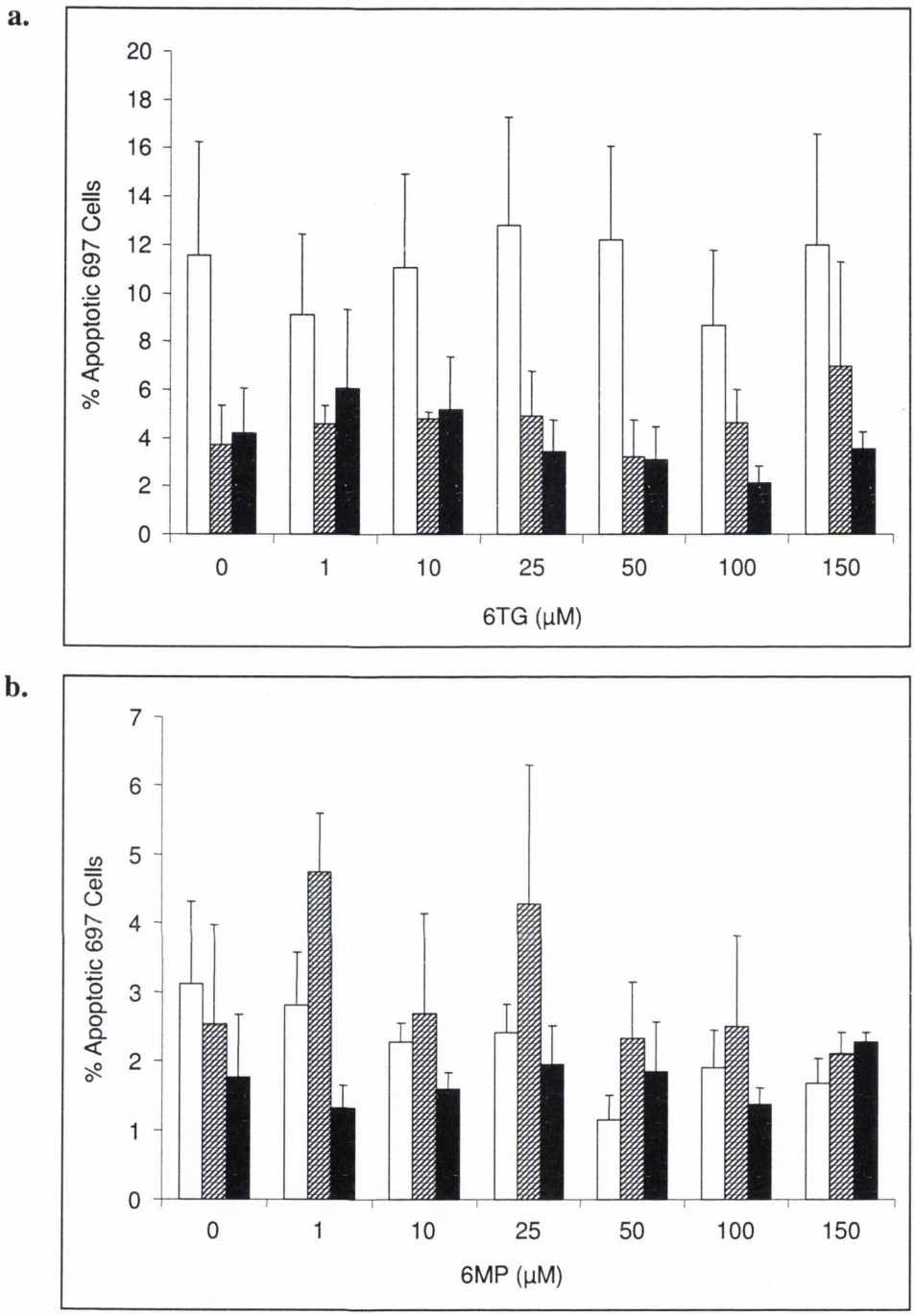


Figure 3.15 Apoptosis in 697 cells after treatment with 6TG or 6MP. 697 cells were incubated with 6TG (a) or 6MP (b) for 2 (□), 6 (▨) or 24 (■) hours. The number of apoptotic cells was measured by TUNEL staining and FACS. A minimum of 1000 events were collected for each sample. The values shown are the mean + SEM of at least three independent experiments. Data were analysed by 2-way ANOVA; if the ANOVA table was significant ($P<0.05$), post hoc comparisons of treatment to untreated control were made using LSD. * $P<0.5$, ** $P<0.01$, *** $P<0.001$.

3.3.4 TF Expression

THP1, HepG2 and Jurkat E6.1 cells all showed significant changes in TF expression after incubation with 6TG. In THP1 cells, there was a significant ($P<0.01$) decrease in TF expression (Figure 3.15). However, Jurkat E6.1 ($P<0.001$) and HepG2 ($P<0.01$) cells showed a significant increase in TF expression after exposure to 6TG (Figure 3.16 and 3.17, respectively). 6MP had no significant effect on THP1 TF expression levels, but in Jurkat E6.1 cells it caused a significant decrease ($P<0.001$) in cells surface expression of TF. In contrast, there was a significant increase ($P<0.05$) in TF expression in HepG2 cells after treatment with 6MP. 697 cells do not express TF on the cell surface as shown in Figure 3.18.

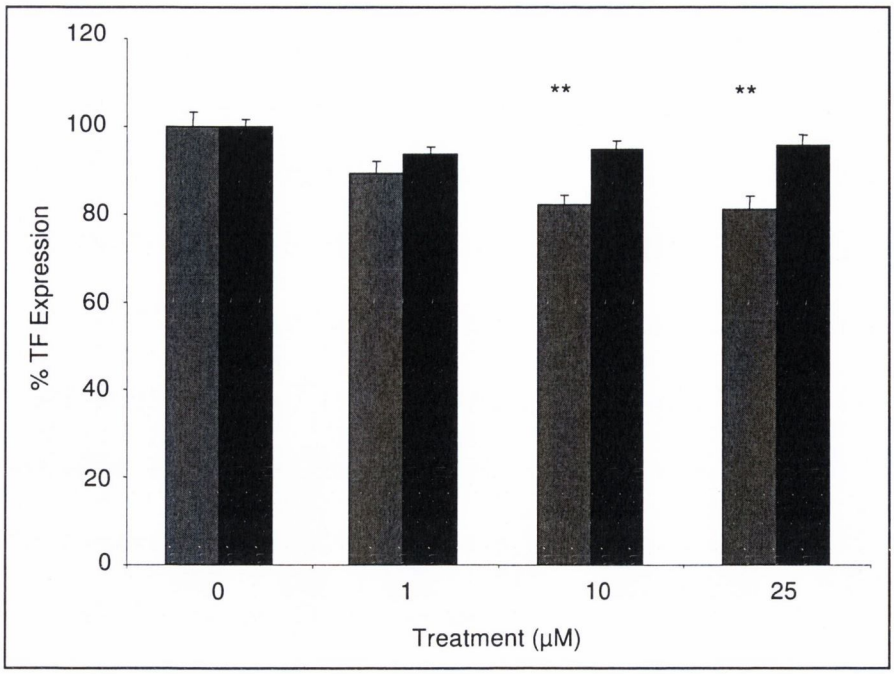


Figure 3.16 Effect of 6TG or 6MP on Tissue Factor Expression in THP1 cells. TF levels were measured after 6 hour incubation with either 6TG (■) or 6MP (■). Percentages are relative to untreated cells which were defined as 100% expression. Data shown are the mean of three separate experiments +SEM. Data were analysed by ANOVA; if significant ($P<0.05$), post hoc analysis was performed using Dunnett's test. * $P<0.05$, ** $P<0.01$, *** $P<0.001$.

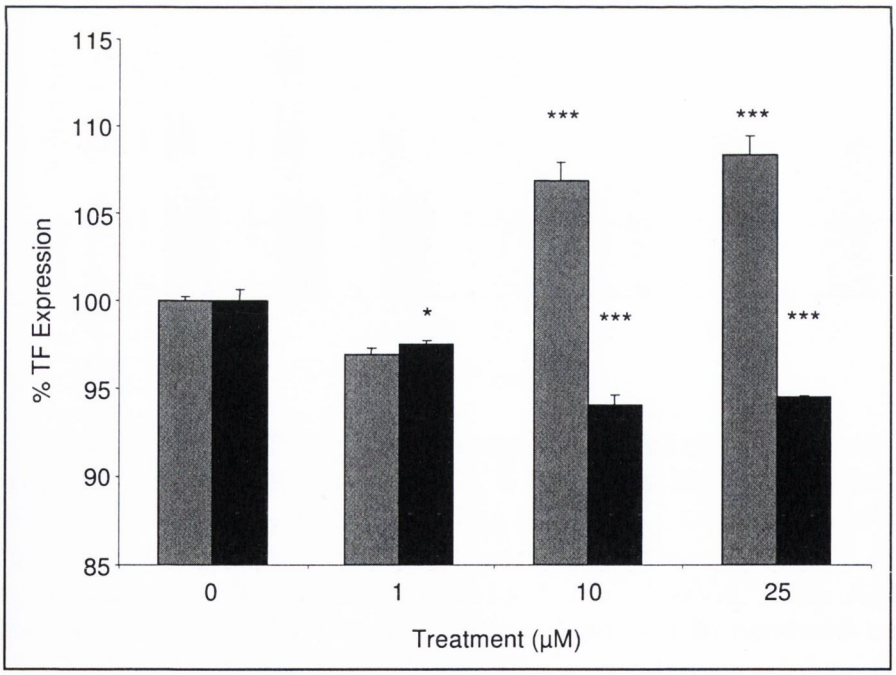


Figure 3.17 Effect of 6TG or 6MP on Tissue Factor Expression in Jurkat E6.1 cells. TF levels were measured after 6 hour incubation with either 6TG (■) or 6MP (■). Percentages are relative to untreated cells which were defined as 100% expression. Data shown are the mean of three separate experiments +SEM. Data were analysed by ANOVA; if significant ($P<0.05$), post hoc analysis was performed using Dunnett's test. * $P<0.05$, ** $P<0.01$, *** $P<0.001$.

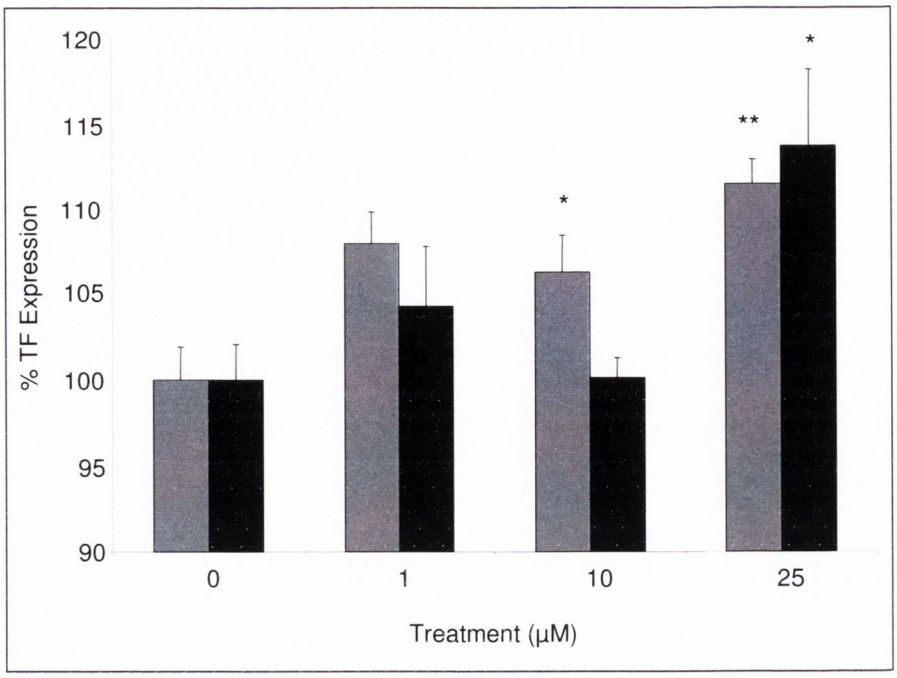


Figure 3.18 Effect of 6TG or 6MP on Tissue Factor Expression in HepG2 cells. TF levels were measured after 6 hour incubation with either 6TG (■) or 6MP (■). Percentages are relative to untreated cells which were defined as 100% expression. Data shown are the mean of three separate experiments +SEM. Data were analysed by ANOVA; if significant ($P<0.05$), post hoc analysis was performed using Dunnett's test. * $P<0.05$, ** $P<0.01$, *** $P<0.001$.

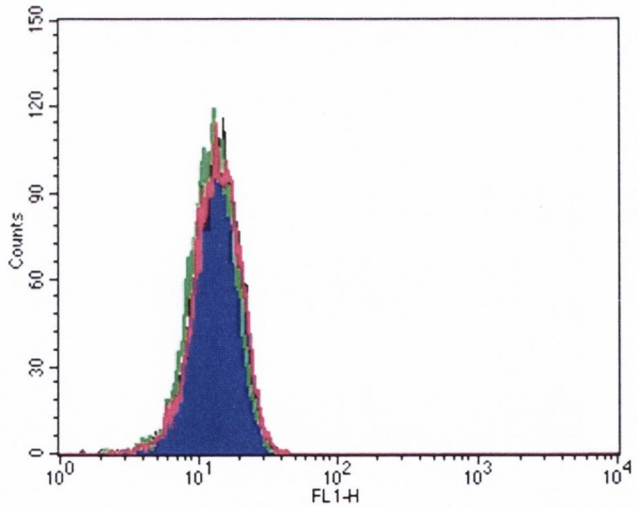


Figure 3.19 Histogram of Tissue Factor Expression in 697 cells. The histogram overlay confirms that 697 cells do not express TF on the cell surface. When there is no expression of a cell surface marker, the histograms of the stained cells is in line with the unstained cell sample histogram. Purple histogram, unstained cells. Pink histogram, TF stained cells. Green histogram, TF antibody isotype control.

3.3.5 TPMT Polymorphism

All four cell lines were homozygous wild-type for the three TPMT mutations tested. None of the DNA samples were amplified using the mutation-specific P2M primer, which showed that the G238C mutation was absent from all four cell lines (Figure 3.19). Incubation of the G460A PCR products with *Mwo*I resulted in two fragments, one at 267 bp and another at 98 bp (Figure 3.20). None of the A719G PCR products were digested after incubation with the *Acc*I (Figure 3.21).

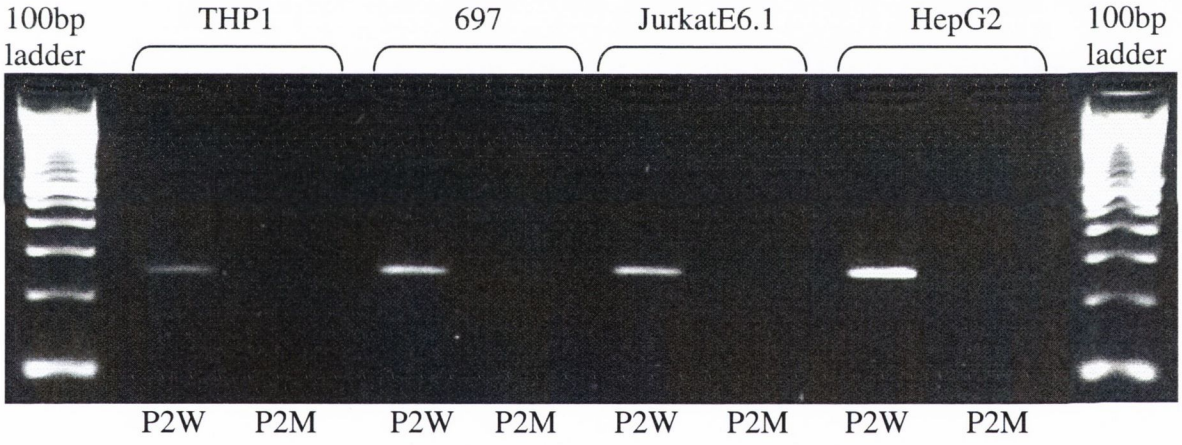


Figure 3.20 TPMT G238C Polymorphism. DNA samples were amplified with mutation specific primers. Primer P2W will only amplify the wild-type allele; primer P2M will only amplify the mutant allele. The top row of the figure lists the samples that were loaded into each lane of the gel. The bottom row lists the primer that was used to amplify the sample. All cells lines were homozygous wild-type for the G238C mutation.

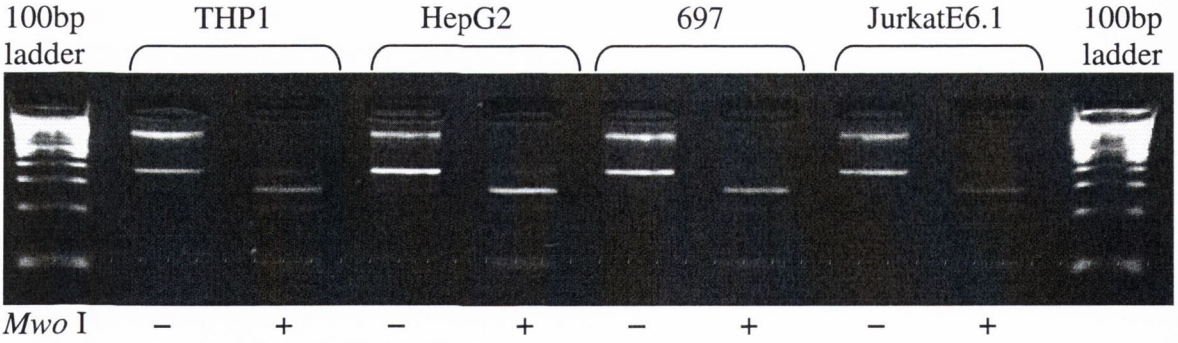


Figure 3.21 TPMT G460C Polymorphism. Amplification results in a PCR product that is 365 base pairs long. The wild-type sequence contains a recognition site for the restriction enzyme *Mwo*I, which will cleave the PCR product into a 267 bp and a 98 bp fragment. The G→C mutation removes the recognition site so the enzyme will not cleave the PCR product. All cell lines were homozygous wild type for the G460C mutation.

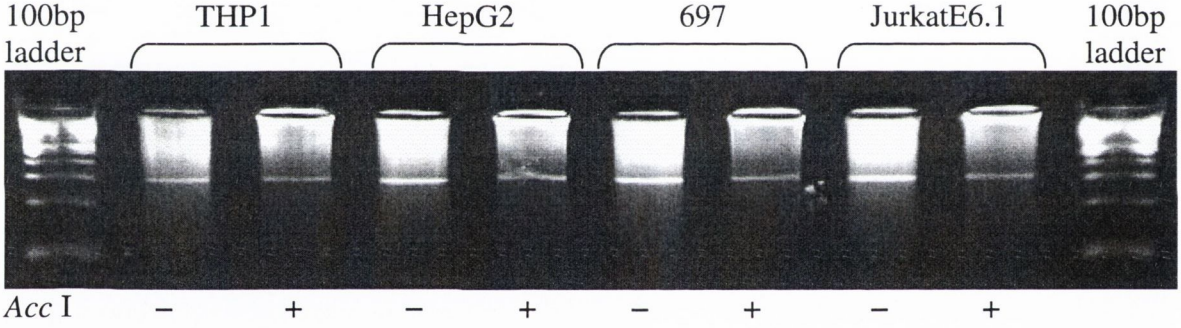


Figure 3.22 TPMT A719G Polymorphism. The PCR reaction results in a 293 bp fragment. The A→G mutation creates a recognition site for the restriction enzyme *Acc*I, which will cleave the product into a 207 bp and a 88 bp fragment. All the cell lines tested were homozygous wild-type for the A719G mutation.

3.4 DISCUSSION

Although 6TG and 6MP have been in routine clinical use for more that 50 years, their mechanism of action is still poorly understood. At present, it is believed that the thiopurines exert their cytotoxic activity by a combination of pro-apoptotic and anti-metabolic activity. Methylated ribonucleotides, one of the products of thiopurine metabolism, inhibit *de novo* purine synthesis, thereby causing the anti-metabolic effects. Incorporation of TGNs into DNA induces apoptosis in the affected cell *via* the MMR pathway (Cara, 2004).

6-Mercaptopurine is now the preferred drug of choice for maintenance therapy in most ALL protocols, while 6TG continues to be used during consolidation and remission induction protocols for AML. This usage pattern is based on historical precedent rather than pharmacological activity (Coulthard, 2002). A number of clinical trials are ongoing to determine the relative efficacies of 6MP and 6TG. Among these the MRC ALL97 study recommended that 6MP should be the principal thiopurine in ALL treatment protocols due to the liver toxicity that was associated with 6TG (Vora, 2006). In this study, 95 patients developed VOD, 82 (11% of all 6TG recipients) of whom were randomly assigned to 6TG treatment. The remaining 13 patients who developed VOD were also taking 6TG; one as non randomised treatment, and the other 12 as part of the intensification course of the treatment regimen after assignment to the 6MP arm of the protocol (12 patients). At long term follow up, 5% of 6TG recipients showed evidence of portal hypertension due to liver fibrosis or nodular regenerative hyperplasia (Vora, 2006).

Hepatic VOD is a pro-coagulant and pro-inflammatory syndrome. Low levels of Protein C (PC) and anti-thrombin (AT) have been noted in a number of studies of patients who develop VOD (Bearman, 2001). In addition, patients who develop VOD have significantly

elevated levels of the pro-inflammatory cytokines TNF-α (Bearman, 1995) and IL-8 (Coppell, 2003). We therefore investigated the effect of 6TG and 6MP on secretion levels of TNF-α and IL-8 in THP1, Jurkat E6.1, 697 and HepG2 cells. The pro-coagulant effect of 6TG and 6MP was investigated by measuring cell surface expression of TF, the initiator of blood coagulation, in THP1, Jurkat E6.1 and HepG2 cells.

To date, no studies have been published examining the effect of 6TG or 6MP on the secretion of inflammatory cytokines (based on searches of the NLM's PubMed databse up to October 2007). Our studies found that IL-8 was the predominant cytokine released after exposure to 6TG or 6MP. While IL-8 secretion levels were significantly increased in THP1 and HepG2 cells after treatment with either 6TG or 6MP (Figures 3.4 and 3.6, respectively), TNF-α levels were not significantly increased in any of the cells lines after treatment with either thiopurine. Neither Jurkat E6.1 cells nor 697 cells showed a significant change in TNF-α or IL-8 levels after 6TG or 6MP exposure (Figures 3.5 and 3.7, respectively).

It is interesting that TNF-α levels did not rise in a commensurate fashion with IL-8 levels, as TNF-α is a potent inducer of IL-8 secretion through transcriptional regulation of NF-κB (Gómez-Quiroz, 2003). Therefore, the thiopurines upregulation of IL-8 secretion may be independent of TNF-α. Further experiments are necessary to determine the precise mechanism of IL-8 induction.

IL-8 is the predominant chemo-attractant cytokine produced by hepatocytes (Rowell, 1997). Hepatocytes are capable of producing large amounts of IL-8 in response to specific stimuli (Gómez-Quiroz, 2003). Our results show that the 6TG and 6MP initiate the inflammatory response in this cell type. One possible explanation for the incidence of

VOD following 6TG and to a lesser extent 6MP treatment is that these drugs activate hepatocytes, which in turn produce and release IL-8. In turn, IL-8 provides the signal for chemo-attraction, infiltration and maturation of monocytes and other inflammatory cells into the area, ultimately creating an inflammatory microenviroment. Repeated administration of 6TG or 6MP would continually activate the hepatocytes and thereby induce an autocrine and paracrine loop that maintains high levels of fibrogenic cytokines in the liver.

The effect of 6TG and 6MP on TF expression has not been studied in any significant detail (NLM PubMed database searches up to October 2007). We show a significant increase in TF expression in HepG2 cells after treatment with 6TG or 6MP (Figure 3.18). This agrees with the results obtained from the cytokine experiments, where IL-8 was significantly increased by both drugs, and supports the pro-coagulant and pro-inflammatory hypothesis of VOD. However, in the AML cell line, THP1, TF expression decreased significantly after 6TG treatment but 6MP had no effect (Figure 3.16). In Jurkat E6.1 cells, 6TG increased TF expression while 6MP decreased TF expression (Figure 3.17). These results indicate that there is a varying expression of TF in the different cell types following thiopurine exposure and further investigation is warranted to elucidate this effect. Clearly, this has potential clinical implications as increases in TF expression are indicative of hypercoaguability following exposure to thiopurines.

Although 6MP has become the preferred thiopurine in acute leukaemia treatment, 6TG is a better anti-leukaemic drug *in vitro* and probably in patients as well. 6-thioguanine was more effective than 6MP in ALL patients with bone marrow and central nervous system (CNS) relapse (Gaynon, 2005). *In vitro* studies have shown that 6TG is 1 log more active than 6MP (Adamson, 1994). These experiments found that isolated paediatric ALL cells

were more susceptible to 6TG compared to 6MP, both in terms of the maximal cytotoxic dose and toxicity exposure times. Treatment with 6TG required four hour incubations to induce cytotoxicity, where as 6MP required 8 hours. The threshold for 6TG cytotoxicity was 0.05μM, with a maximum of 0.5μM. In contrast, 6MP treatment required doses of 1μM to induce cytotoxicity, with a maximum of 10μM (Adamson, 1994).

Cytotoxicity assays performed by Kaspers *et al* (2005) also found that much higher doses of 6MP than 6TG were required to induce cytotoxicity in relapsed paediatric lymphoblasts. In particular, they found that B cell precursor (BCP)-ALL blasts required very high doses of 6MP (median LC50 value 166.7μg/ml versus 8.7μg/ml for 6TG) (Kaspers, 2005). An earlier study of the several chemotherapeutic agents by da Silva *et al* (1996) also found that high doses of 6MP and long incubation times were required to have an effect on the viability of Jurkat or CEM T-lymphoblasts. 6TG was not investigated in this study (da Silva, 1996).

Our investigations found that the effect of the drug was dependent on the cell type used. The AML cell line THP1 was more susceptible to 6MP than 6TG (Figure 3.8). After 6 hours incubation with 10μM 6MP, viability was reduced to 60 percent compared to untreated control cells ($P<0.001$). Treatment with 6TG required 24 hours incubation before a significant decrease in viability was observed. For both drugs, the 25μM treatment exerted the maximal effect after which the decrease in viability plateaued.

As with the THP1 cells, the T lymphoblast cell line Jurkat E6.1 required 24 hours incubation with 6TG before a decrease in viability was observed (Figure 3.9a). The maximal effect was achieved at a concentration of 25μM, after which the viability curve plateaued. The Jurkat E6.1 cells showed a different response to 6MP treatment (Figure

3.9b). Again, 24 hours incubation with the drug was required before a reduction in viability was observed, and the maximal reduction in viability occurred at the 25μM dose. However, when the concentration of 6MP was increased above the 25μM dose, the drug had a reduced effect on the viability of the cells. This phenomenon has been noted previously in rat brain tumour cells treated with 6MP, and was termed 'paradoxical cell kill' by Matsumura *et al* (1983). One possible explanation for this phenomenon is saturation of the nucleoside transporters. Doses higher than 25μM may overload the transporters so that it is physically impossible for more 6MP to be transported into the cell even though the external concentration of 6MP increases.

Neither 6TG nor 6MP had an effect on the viability of the BCP-ALL cell line 697 within the concentration range tested (Figure 3.11). These results are in contrast to the results obtained by Kaspers *et al* (2005). However, they were using cells isolated from patients in their first relapse as opposed to cell lines. There was also a large range in the LC50 values obtained for each drug in the BCP-ALL cells (15.6-500μg/ml for 6MP, 1.56-50μg/ml for 6TG). The difference in the biology of an immortilised cell line versus an isolated cell population could account for the differences that have been observed between our study and Kaspers (2005).

The effect of the thiopurines on hepatocyte viability has also been studied in detail. Tapner *et al* (2004) studied the effect of 6MP on rat hepatocytes. They found that azathioprine (AZA, a precursor of 6MP), and 6MP significantly decreased hepatocyte viability both time and dose dependently after 48 hours of culture. This study used low doses of both drugs, ranging from 0.1 to 5.0 uM. However, an earlier study by Lee *et al* (2001) found that 6MP had no effect on HepG2 viability, even at doses as high as 1000 μM, after 16 hours. This is in agreement to our results with HepG2 cells, in which we found no

decrease in cell viability, even at high doses after 24 hours exposure (Figure 3.10). It is possible that the chemical differences between the rat hepatocyte and the cell line affect their susceptibility to thiopurines.

Thiopurines are also considered to be pro-apoptotic compounds. Experiments by da Silva *et al* (1996) found that 6MP had no apoptotic effect in Jurkat or CEM (a T ALL cell line) cells, however their study was limited in that the cells used were only treated with 1μm 6MP for 24 and 48 hours. Rat hepatocytes showed no increase in apoptosis after AZA treatment at low (0.1-5uM AZA, Tapner, 2004) or at high doses (0-250 μM, Lee, 2001). Neither 6TG nor 6MP were included in these studies, nor were there any other published studies of the apoptotic effect of these drugs on hepatocytes *in vitro* (NLM PubMed search November 2007).

Our results show that the apoptotic response to 6TG and 6MP varied with the cell type being studied. Apoptosis was significantly ($P<0.001$) increased in THP1 and Jurkat E6.1 after treatment with 6TG (Figures 3.12a and 3.13a, respectively). However, 6MP increased apoptosis in Jurkat E6.1 cells ($P<0.01$) but not THP1 cells. Apoptosis was not increased in either HepG2 or 697 cells after treatment with 6TG or 6MP (Figures 3.14 and 3.15, respectively). In agreement with da Silva *et al* (1996) we did not find a significant increase in apoptosis in the Jurkat E6.1 cell at 1μM doses for either drug. It was only at doses equal to or greater than 10μM that we found a significant increase in apoptosis.

It is important to note that the optimum activity of either drug was achieved in the range of 10 to 25 μM concentrations. For all the assays included herein, regardless of the cell type or drug, if there was a significant change it was observed at the 10μM treatment. At

therapeutic dosage levels (2-3 mg/kg body weight), the tissue concentrations are unlikely to exceed 10μM (Tapner, 2004).

Both 6TG and 6MP are prodrugs that require activation before they can exert their cytotoxic effect. Two of the enzymes that are involved in the activation of the thiopurines, HGPRT and TPMT, are polymorphic. Previous studies have shown that the polymorphisms in the TPMT gene affect expression levels of the enzyme, thereby affecting a patients' response to treatment. In particular, Lennard *et al.* (2006) found that the TPMT polymorphism was associated with the development of VOD in children with ALL. Children who developed VOD had significantly lower TPMT activity than those who did not. There was no difference in RBC TGN concentrations between the two patient groups (Lennard, 2006).

Thiopurines are proposed to act through a combination of pro-apoptotic and anti-metabolic activities. Incorporation of TGNs into newly synthesised DNA promotes apoptosis, while the anti-metabolic effects are due to inhibition of PDNS by methylated ribonucleotides. The TPMT enzyme is crucial to the balance between these two modes of action, because it controls the methylation of these compounds. When either drug is methylated by TPMT, it is no longer a substrate for HGPRT. HGPRT is the enzyme that converts 6TG and 6MP into TGNs (Figure 3.2).

Experimental evidence suggests that methylation has different consequences to the cytotoxic activity of 6TG and 6MP. The CCRF-CEM leukaemic cell line is thiopurine sensitive and constitutively expresses low levels of TMPT. CCRF-CEM cells that over-express TPMT (TPMT+) are less sensitive to 6TG than control cells (CCRF-CEM cells with normal TPMT expression); TPMT+ cells are more sensitive to 6MP than control cells.

TPMT+ cells exhibited increased concentration of methylthioguanine, decreased inhibition of PDNS as well as decreased TGN incorporation into DNA after 6TG treatment as compared to control cells. However, 6MP treatment of TPMT+ cells significantly increased the concentration of methylmercaptopurine and significantly increased inhibition of PDNS compared to control cells. Therefore, methylation of 6MP appears to increase its anti-metabolic effects while methylation inactivates 6TG (Dervieux, 2001). Experiments conducted by Coulthard *et al* (2002) in the embryonic kidney cell line 293 agree with the results obtained by Dervieux *et al* (2001).

In this study, all of the cell lines used were homozygous wild type for the three main polymorphisms found in Caucasian populations (Figures 3.20-3.22). All four cell lines were derived from Caucasian donors, therefore the other polymorphisms were not investigated. Cells that are homozygous wild-type for the TMPT polymorphism should have high TPMT enzyme activity (Collie-Duguid, 1999), however enzyme activity levels were not quantitated in this study. Based on the results obtained by Dervieux *et al* (2001) and Coulthard *et al* (2002), we would expect that cells with high TPMT activity would be more sensitive to 6MP treatment than 6TG treatment. This is not what we observed, which may be due to the quantitative difference in TPMT expression in the different cell line. The involvement of other enzymes such as HGPRT and XO must also be taken into account.

6-Mercaptopurine is the preferred thiopurine for the treatment of ALL due to the toxicity associated with 6TG. Our results confirm previous findings that 6TG is as potent as 6MP *in vitro*. The data also suggest that the effect of 6TG is pro-apoptotic, while 6MP is anti-metabolic. 6TG is more likely to induce a pro-inflammatory and pro-coagulant response, particularly in HepG2 cells. Taking into consideration the association between 6TG and

VOD, and the role of inflammation and coagulation in the development of VOD, the *in vitro* data presented here support the use of 6MP over 6TG in ALL treatment protocols.

CHAPTER 4

DESIGN AND DEVELOPMENT OF ASSAYS FOR THE INTRACELLULAR DETECTION OF 6-THIOGUANINE AND 6-MERCAPTOPURINE

4.1 INTRODUCTION

6-thioguanine (6TG) and 6-mercaptopurine (6MP) are small molecules structurally similar to endogenous purine nucleosides. Both 6TG and 6MP are prodrugs that require intracellular activation in order to exert their cytotoxic activity. The enzyme hypoxanthine guanine phosphoribosyl transferase (HGPRT) converts 6TG and 6MP into thioguanine nucleotides (TGN), which are then incorporated into DNA, and this is the proposed mechanism through which the thiopurines mediate their cytotoxic effects. 6-thioguanine and 6MP are also substrates for the enzyme thiopurine methyl transferase (TPMT), which converts the drugs into methylated ribonucleotides. These metabolic products are proposed to inhibit purine *de novo* synthesis (PDNS), inducing metabolic arrest (Cara, 2004).

Thiopurines have therapeutic activity in a variety of disease states, including leukaemia, inflammatory bowel disease, and dermatologic conditions. There are significant dose related toxicities associated with thiopurine treatment, in particular myelosuppresion (McLeod and Siva, 2002) and hepatic veno-occlusive disease (VOD) (Lennard, 2006). The inter-individual toxic effects of thiopurines can be explained in part by polymorphisms in the gene for TPMT that affect enzyme activity levels. Cells with a homozygous mutant genotype have low TPMT activity which favours the production of cytotoxic TGNs. However, there is significant inter-individual variation in the TPMT activity associated with genotype. Some heterozygous individuals display high enzyme activity while homozygous wild-type individuals show intermediate activity (McLeod and Siva, 2002).

Therefore, it is of clinical import to be able to efficiently assay the cellular uptake and metabolism of thiopurines.

At present, thioguanine metabolite concentrations are monitored by assaying the metabolite concentration in red blood cells (RBC) by high pressure liquid chromatography (HPLC). There are several different protocols (Keuzenkamp-Jansen, 1995; Dervieux, 1998), but the essential process involves lysis of the RBCs, removal of protein and acid extraction of ribonucleosides. The concentration of thiopurine metabolites are measured by injecting the sample onto a column and comparing the elution peaks in the sample to the elution peaks obtained from thiopurine standards. Protocols for the analysis of thiopurine metabolites in lymphoblasts use similar methods (Krynetski, 1995; Dervieux, 2002).

The HPLC methods for detecting thiopurine metabolites are time consuming and therefore not suitable for routine clinical use. For this reason we designed two different assays to detect the intracellular accumulation of thiopurines using a commercially available monoclonal antibody to 6TG and its metabolites. These assays allow analysis of larger number of samples in a shorter time period as they are both performed using a 96 well plate.

The first assay we developed was a competitive Enzyme Linked Immuno-Sorbent Assay (ELISA). An ELISA measures the amount of antigen in a sample using an antibody specific to the antigen in question. The antibody is linked to an enzyme so that it can be detected when a substrate is added to the sample. In this method, the anti-6TG antibody is added directly to the sample being assayed. An aliquot of the sample is then added to an ELISA plate that has been coated with the molecule of interest. Any antibody that has not bound to the target in the sample will bind to the target on the plate surface. Unbound

antibody is washed away, and the antibody bound to the plate is detected with a horse radish peroxidase (HRP) conjugated secondary antibody. Addition of substrate solution to each well produces a colour reaction that is quantitated at 450nm on a spectrophotometer. Since this is a competitive ELISA, the colour is inversely proportional to the target concentration. By including a standard curve on each plate, the amount of thiopurine in each sample can be calculated.

High Content Screening (HCS) was also used to as a screening method for the intracellular accumulation of thiopurines. It is a combination of the imaging qualities of fluorescence microscopy with the quantification capabilities of flow cytometry. Cells are plated in 96 well plates and treated with the substance of interest. After fixation and staining with fluorescent antibodies, the plate is loaded onto the workstation to be analysed. Images of the cells are acquired by a fluorescent microscope, which are then analysed using a specially designed computer program. The parameters of the algorithm that the computer uses to analyse the images have been set by the users to detect the features of interest. The parameters are set so that only suitable cells are included in the analysis. Some of the parameters include cell size, nuclear size, intensity of nuclear stain. The benefit of HCS versus the competitive ELISA is that the cells are imaged individually using fluorescent antibodies. This makes it possible to measure the concentration of the metabolites in the nucleus and the cytoplasm. The procedure involves fixing, permeabilising and staining the cells. Images of the cells are acquired and analysed on the KineticScan workstation using software that delineates between the nucleus and cytoplasm based on parameters that have been set by the user.

4.2 THIOPURINE ELISA EXPERIMENTAL DESIGN

4.2.1 ELISA Protocol

1. Conjugate 6TG to activated BSA. Coat an ELISA plate with a solution of BSA-6TG at 4°C overnight, 100µl per well.
2. Wash the plate three times with wash buffer (PBS + 0.05% Tween 20). Block the plate for 1 hour at room temperature with 300 µl block buffer (1% BSA in PBS) per well.
3. Lyse the samples to be assayed with the appropriate buffer. Incubate 200µl of the cell lysis solution with 200µl of the primary (1°) antibody solution for 1 hour at room temperature.
4. After the blocking step, wash the plate three times. Aliquot 100µl of sample to the appropriate well. All samples were assayed in duplicate. An 8 point standard was included on each plate. All dilutions were made using Reagent Diluent (PBS + 0.1% BSA + 0.05% Tween 20). Incubate the plate for 1 hour at room temperature.
5. Wash the plate three times. Add 100µl of a 1:1000 dilution of the HRP conjugated secondary antibody to each well. Incubate for 1 hour at room temperature.
6. Repeat the wash step three times. Add 100µl of substrate solution (1:1:2 solution of TMB:H_2O_2:H_2O) to each well. Stop the colour reaction after 15 minutes with 50µl of 2N H_2SO4 per well. Read the absorbance of each well at 450nm with a reference filter of 595nm. Construct a standard curve using the values from the 8 point standard, and use the equation of the standard curve to determine the concentration of thiopurines in the sample.

4.2.2 Primary Antibody Selection

A number of antibodies with different specificities for thioguanine, mercaptopurine, and their metabolites are commercially available from the Antibody Shop (Gentofte, Denmark). The antibodies vary in their specificity to thiopurine metabolites and their reactivity to free 6TG. For this assay, we wanted an antibody that was specific for 6TG, 6MP and their metabolites. The chosen antibody would also need to recognise these molecules when it had been attached to a carrier protein, which would bind the 6TG to the ELISA plate. Based on these parameters, the antibody HYB 138-07 was chosen. This mouse monoclonal antibody (subclass IgG_{2a}) was generated by linking 6TG to purified protein derivative of tuberculin (PPD). The specificity screening performed by the manufacturer determined that this clone was specific for 6TG and was also cross reactive with 6MP, methylmercaptopurine, 6-thioxanthine, 7-(carboxymethyl)-thioguanine, 8-methyl-thioguanine and thioinosine. The reactivity screening determined that HYB 138-07 bound strongly to 6TG coupled to a carrier protein *via* the sulphur atom at the 6 position, however the interaction could be inhibited with free 6TG. All of these characteristics made HYB 138-07 the best choice for the development of a competitive ELISA. The broad specificity meant that a wide range of metabolites would be detected in the assay. In addition, the reactivity profile meant that the antibody would be able to bind to free and conjugated 6TG, so that it would detect the unbound 6TG in a sample as well as the BSA-conjugated 6TG on the ELISA plate.

4.2.3 Generation of Plate Conjugate

The antibody chosen, HYB 138-07, was generated by conjugating 6TG to PPD. 6TG being a small molecule (Figure 3.1), it is a poor immunogen. However, conjugating it to a protein increases the surface area available for antibody access, while also enabling it to bind to the plate surface. The carrier protein for the assay must be different from the protein used for immunisation, to reduce non-specific binding of the antibody to the carrier protein. Bovine Serum Albumin was chosen as the conjugate protein as it was different from the immunisation protein and was available in pre-activated kits. BSA was pre-activated with a maleimide group, which reacts strongly with sulfhydryl groups at neutral pH (Figure 4.1). This reaction resulted in the conjugation of 6TG at the same position as the immunisation conjugate. The kit was used according to the manufacturer's instructions.

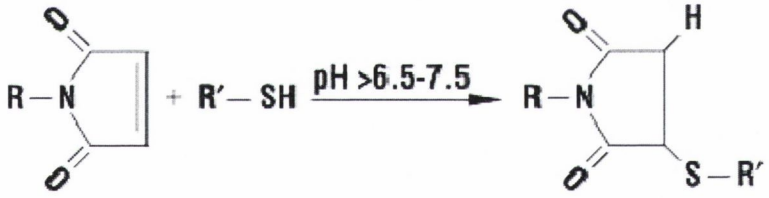


Figure 4.1 Maleimide Reaction. R = BSA, R' = 6TG. Taken from www.piercenet.com/proteomics.

The conjugation product was dialysed to remove excess unbound 6TG. During the dialysis procedure, the BSA-6TG solution was diluted, and therefore Bradford reaction was carried out to quantify the amount of protein in the conjugate solution. All samples and standards were assayed in duplicate. The standard curve for this Bradford reaction is shown in Figure 4.2. Prior to the dialysis procedure, the concentration of BSA was 1 mg/ml. The concentration of the plate conjugate was calculated using the equation of the Standard Curve as 0.66 mg/ml of protein after dialysis. This protein concentration value was used in all subsequent calculations for determining optimum plate conjugate concentration.

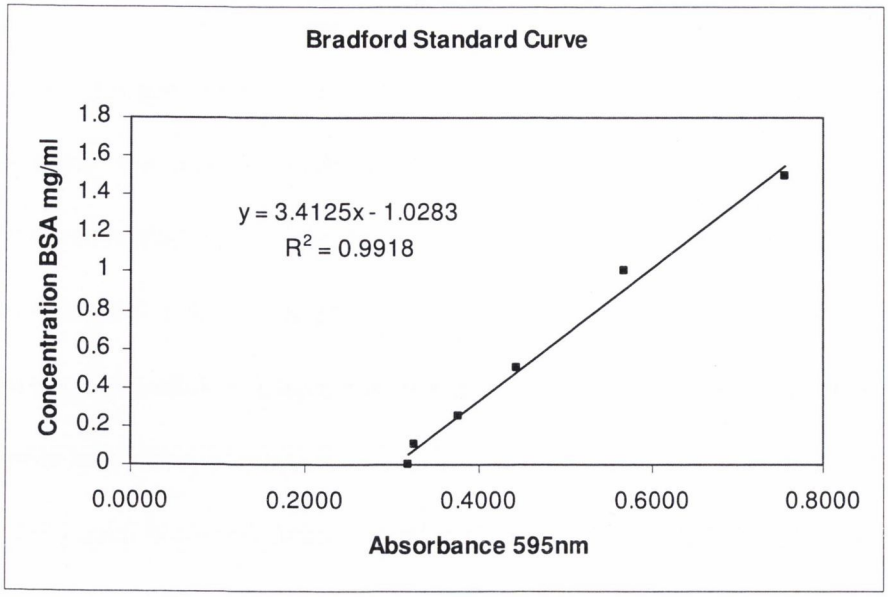


Figure 4.2 Bradford Reaction. Standard curve used to quantify the amount of protein in the conjugation reaction after dialysis of excess unbound 6TG.

4.2.4 Optimisation of Sample and Plate Preparation

Three different cell lysis solutions were assessed for use in the assay. The contents of the buffer are listed in Table 4.1. The protocol for sample preparation was as follows. A 1ml aliquot of cells ($1x10^6$ cells/ml) was centrifuged and washed twice with PBS. The supernatant was discarded and 500µl of the appropriate lysis solution was added to the tube. The sample was vortexed briefly, then sonicated on ice for 1 minute. At this stage, samples treated with Buffer 1 or Buffer 3 were centrifuged at 1000 rcf for 10 minutes at 4°C. Samples treated with Buffer 2 were incubated in a 50°C water bath for 30-60 minutes, then centrifuged at 1000rcf for 10 minutes at 4°C. After the centrifugation step, the supernatant from all samples was aliquoted into a new centrifuge tube and stored at -20°C for future analysis.

Table 4.1 Cell Lysis Buffer Formulations

Buffer 1	20mM Tris (pH 7.5) 150 mM NaCl 1mM EDTA 1% Triton X-100	Modified from Cell Signalling Technologies lysis buffer
Buffer 2	10mM Tris HCl (pH 8.0) 1mM EDTA 0.5mg/ml proteinase K	Protocol from Krynetski *et al.* (1995)
Buffer 3	50mM Tris HCl (pH 7.4) 150mM NaCl 1mM EDTA 1% Triton X-100 0.1% SDS	Modified RIPA buffer

The optimum concentration of plate conjugate and 1° antibody also had to be defined. The recommended initial concentration for the plate conjugate was 5µg/ml, therefore we tested solutions of 1, 5, and 10µg/ml. Primary antibody concentration range from 0.1 to 10µg/ml, therefore we tested solutions of 0.1, 1, 4, and 10µg/ml. Each of the lysis buffer solutions, as well as Reagent Diluent (zero), was also added to the plate to ensure that there was no cross reactivity between the components. Each sample was assayed in duplicate. Table 4.2 illustrates the layout of the plate for determining the optimum combination of plate conjugate, 1° antibody and lysis solution. The results of the optimisation ELISA are listed in Table 4.3.

Table 4.2 Illustration of the Optimisation Plate for the Thioguanine ELISA. The number in the table corresponds to the buffer listed in Table 4.1. Reagent Diluent is lysis solution 0.

		Plate Conjugate Concentration												
		1µg/ml				**5µg/ml**				**10µg/ml**				
Primary Antibody Concentration	**0.1 µg/ml**	**1**	**2**	**3**	**0**	**1**	**2**	**3**	**0**	**1**	**2**	**3**	**0**	**Lysis Solution**
	1µg/ml	**1**	**2**	**3**	**0**	**1**	**2**	**3**	**0**	**1**	**2**	**3**	**0**	
	4µg/ml	**1**	**2**	**3**	**0**	**1**	**2**	**3**	**0**	**1**	**2**	**3**	**0**	
	10µg/ml	**1**	**2**	**3**	**0**	**1**	**2**	**3**	**0**	**1**	**2**	**3**	**0**	

Table 4.3 Results of the Optimisation Plate for Thioguanine ELISA. The rows of highlighted (yellow) text detail the best combination of 1° antibody and plate conjugate. Conj. = Conjugate concentration (µg/ml); Ab = antibody concentration (µg/ml); Abs. = average absorbance of two samples at 450nm.

Buffer	Conj.	Ab	Abs.
1	1.0	0.1	0.1388
2	1.0	0.1	0.0097
3	1.0	0.1	0.1518
0	1.0	0.1	0.4469
1	5.0	0.1	0.4306
2	5.0	0.1	0.0236
3	5.0	0.1	0.4883
0	5.0	0.1	0.8215
1	10.0	0.1	0.6459
2	10.0	0.1	0.0484
3	10.0	0.1	0.6544
0	10.0	0.1	0.9121
1	1.0	1.0	0.6049
2	1.0	1.0	0.0501
3	1.0	1.0	0.6020
0	1.0	1.0	0.7637
1	5.0	1.0	0.9575
2	5.0	1.0	0.1464
3	5.0	1.0	0.9472
0	5.0	1.0	0.9965
1	10.0	1.0	1.0205
2	10.0	1.0	0.3035
3	10.0	1.0	1.0024
0	10.0	1.0	1.0190

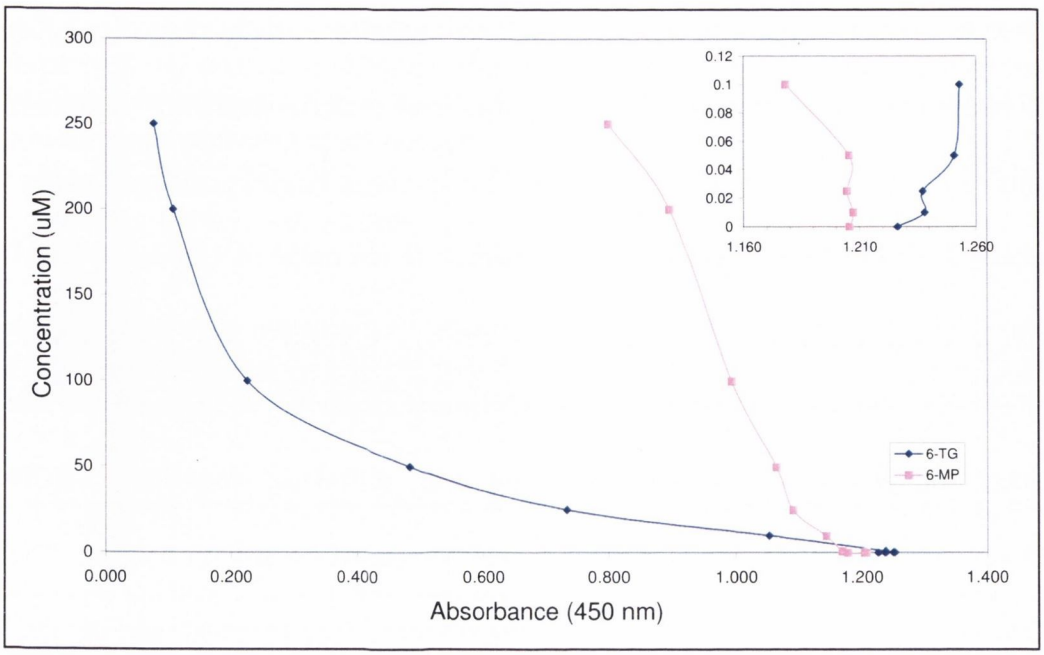
Buffer	Conj.	Ab	Abs.
1	1.0	4.0	0.7036
2	1.0	4.0	0.0731
3	1.0	4.0	0.7205
0	1.0	4.0	0.7927
1	5.0	4.0	0.9711
2	5.0	4.0	0.2520
3	5.0	4.0	0.9979
0	5.0	4.0	1.0175
1	10.0	4.0	0.9671
2	10.0	4.0	0.6221
3	10.0	4.0	0.9316
0	10.0	4.0	1.0044
1	1.0	10.0	0.7403
2	1.0	10.0	0.0505
3	1.0	10.0	0.7008
0	1.0	10.0	0.7132
1	5.0	10.0	0.9400
2	5.0	10.0	0.3345
3	5.0	10.0	0.9130
0	5.0	10.0	0.9643
1	10.0	10.0	0.9358
2	10.0	10.0	0.6411
3	10.0	10.0	0.8989
0	10.0	10.0	0.9903

The ideal combination of 1° antibody and plate conjugate will maximise sensitivity while also allowing for the maximal number of assays from the reagent. The effect of the extraction protocol on the assay must also be taken into account. The lysis solution should have the least amount of interference with the antibody binding (e.g. in comparison to Reagent Diluent). Based on these parameters, Lysis Buffer 1 had the least amount of interference with antibody binding. The best plate conjugate concentration was 5 or 10µg/ml BSA-6TG and the optimum antibody concentration was 1µg/ml.

4.2.5 Defining Limits of Sensitivity

The concentration range of 6TG that the assay could detect needed to be established. We also needed to confirm that the 1° antibody was cross reactive with 6MP. To determine the limits of sensitivity, THP1 cell pellets ($1x10^6$ cells) were lysed in cell lysis buffer that had contained 6TG or 6MP. Samples were produced in the range of 10nM to 250μM of each drug. The zero sample included lysis buffer only. All samples were assayed in duplicate. The standard curves from the inhibition experiment are shown in Figure 4.3 a. and b. The percent inhibition was calculated using the following formula: $((OD_{control} - OD_{sample})/OD_{control})*100$, OD being the optical density of the well at 450nm. The percent inhibition is shown in Figure 4.4. These experiments were repeated, and the results were similar to those shown in Figures 4.3 and 4.4. From the data obtained in both these experiments, we set the limits of sensitivity for this assay as 10μM to 200μM 6TG and 1μM to 250μM for 6MP.

a.



b.

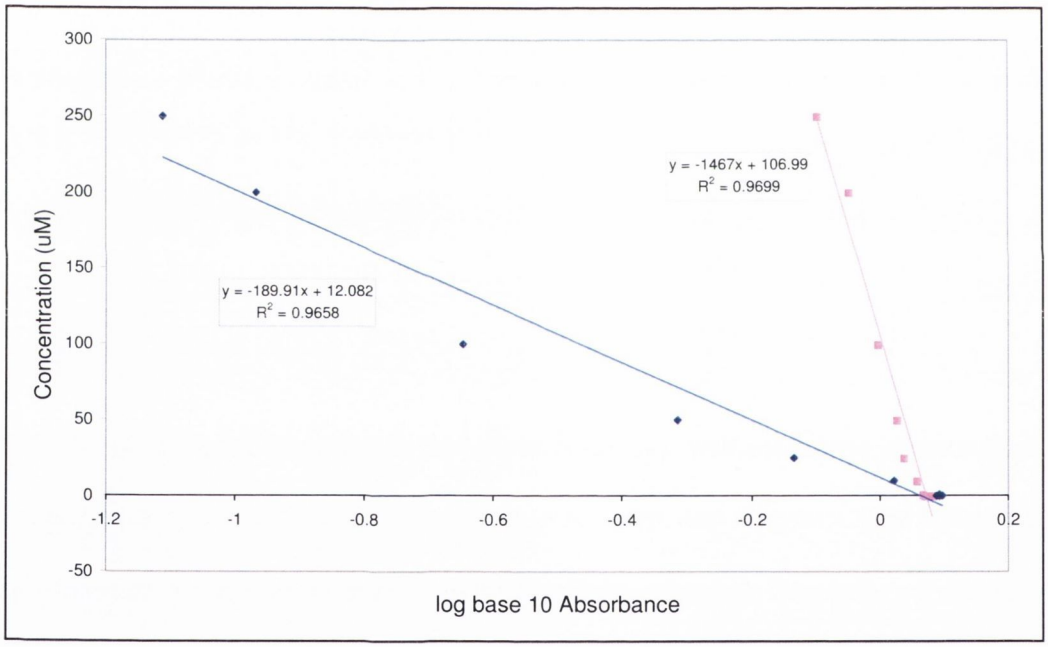


Figure 4.3 Inhibition Curve for 6TG and 6MP. This Experiment defined the limit of sensitivity of the antibody. Blue diamonds represent data points for 6TG; pink squares represent data points for 6MP. In Figure a, the inset detail magnifies the data from the 0μM to the 0.1μM dose range. The sensitivity range of the assay appears to be 100nM to 200μM based on this curve. In Figure b, the data have been log transformed so that a straight line standard curve could be generated. The blue line is the standard curve for 6TG; its equation is outlined in blue. The pink line is the standard curve for 6MP; the equation of this line is outline in pink. This was done for all experiments so the concentration of thiopurine in the unknown samples could be calculated from the equation of the standard curve. Samples with concentrations below 100nM could not be differentiated from one another.

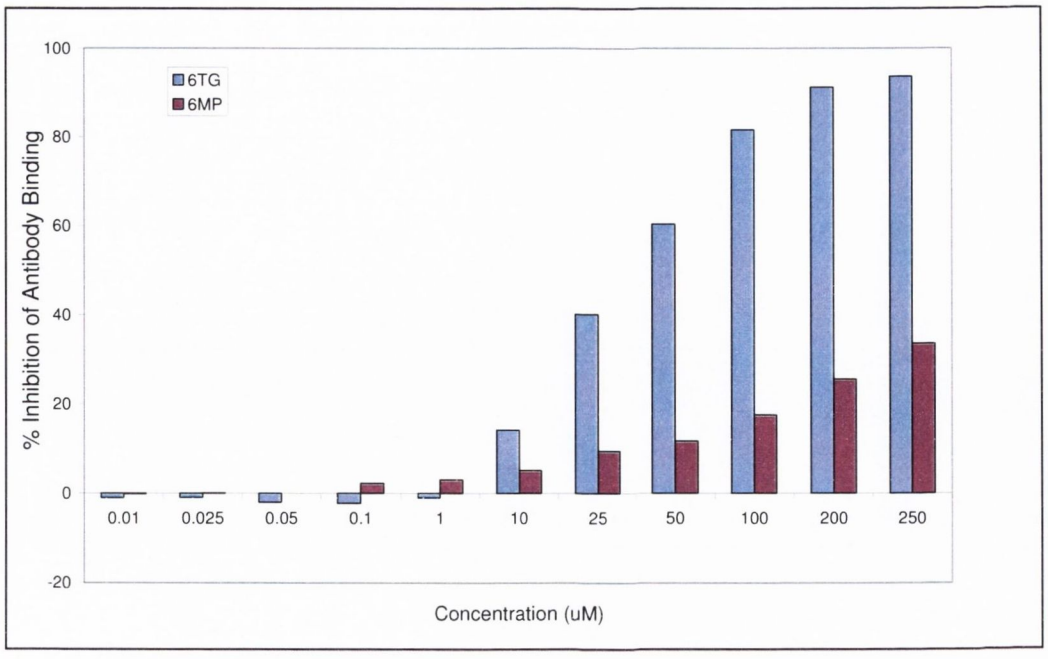


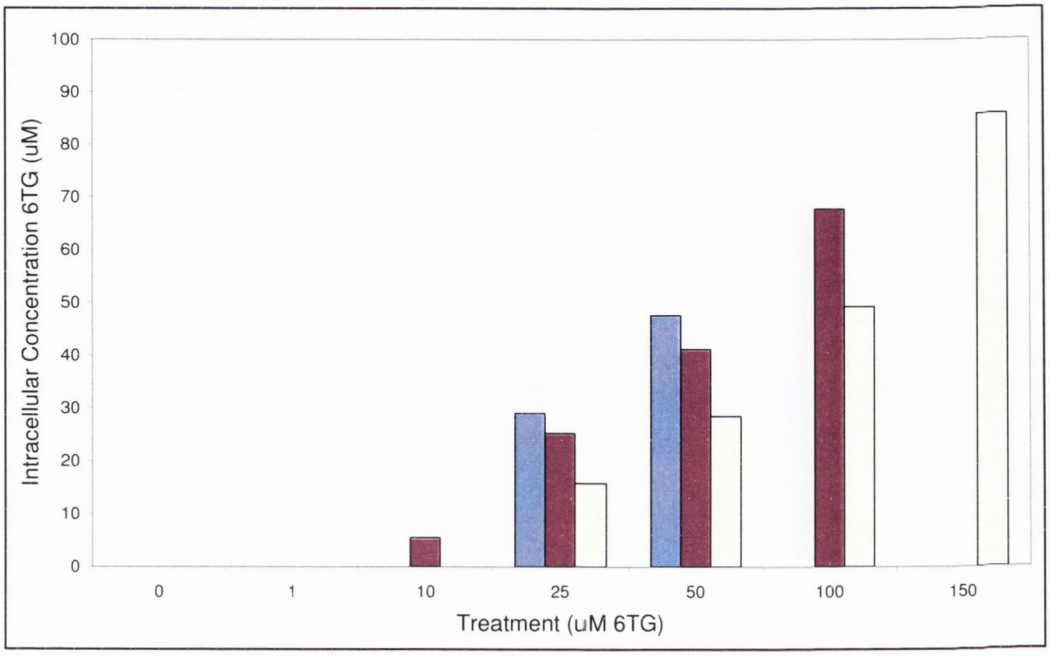
Figure 4.4 Percent Inhibition of Antibody Binding. % was calculated using the formula $((OD_{control} - OD_{sample})/OD_{control})*100$. From this data, the sensitivity of the assay is 10μM to 200μM for 6TG and 1μM to 250μM for 6MP. 6MP does not inhibit antibody binding as efficiently as 6TG, but it has increased sensitivity at low and high concentrations.

4.2.6 Quantitation of 6TG and 6MP in Experimental Samples

For quantitation of intracellular accumulation of 6TG or 6MP, experiments were carried out as previously described in Chapter 3.2. At the end of the incubation time, cells were removed from the tissue culture plate, washed twice in PBS, and then lysed as described in section 4.2.4. An 8 point standard curve for each drug was made in a concentration range from 1 to 200μM using lysis buffer as the diluent. The ELISA was conducted as described in section 4.2.1, with a 5μg/ml plate conjugate concentration, 1μg/ml 1° antibody solution and Lysis Buffer 1. Representative results for 6TG and 6MP are shown in Figure 4.5 a and b, respectively.

Higher concentrations of 6TG were detected relative to 6MP. Wide variations were detected in the 6MP treated samples. In order to exclude the possibility that a large number of cells had died or were lost during transfer, we added the additional step of measuring the protein content of each sample (in duplicate) after lysis. Protein content was determined by the Bradford Assay. The thiopurine concentration in the cell lysate was normalised to the protein content by dividing the thiopurine concentration by the protein content of the sample. The data are expressed as μM 6TG (or 6MP) per mg of protein. Representative results for THP1 cells treated with 6TG or 6MP are shown in Figure 4.6 a. and b., respectively.

a.



b.

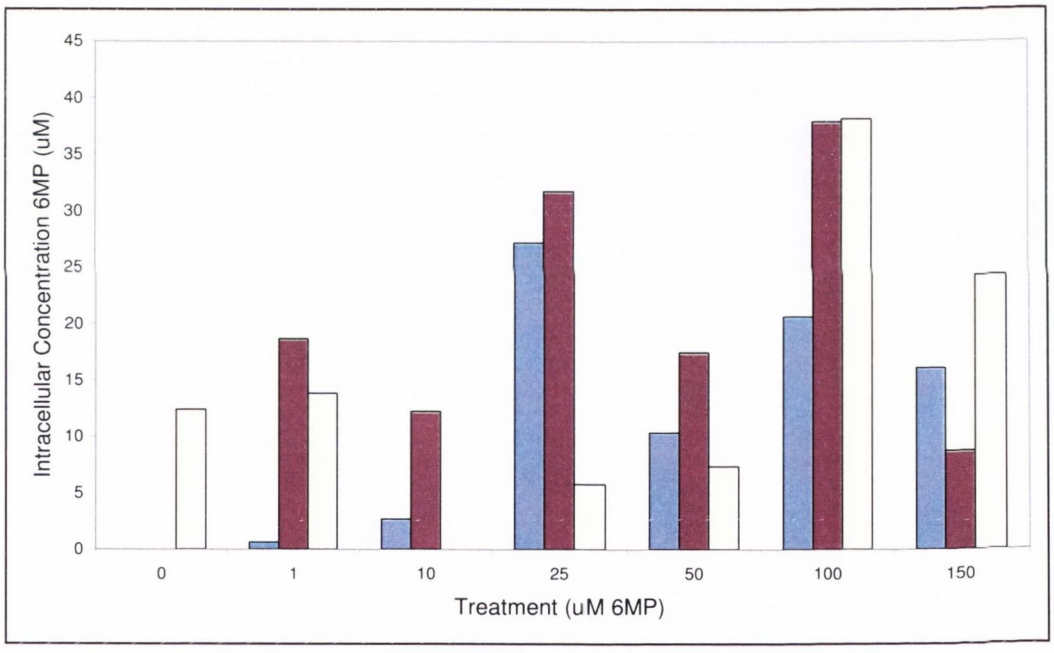
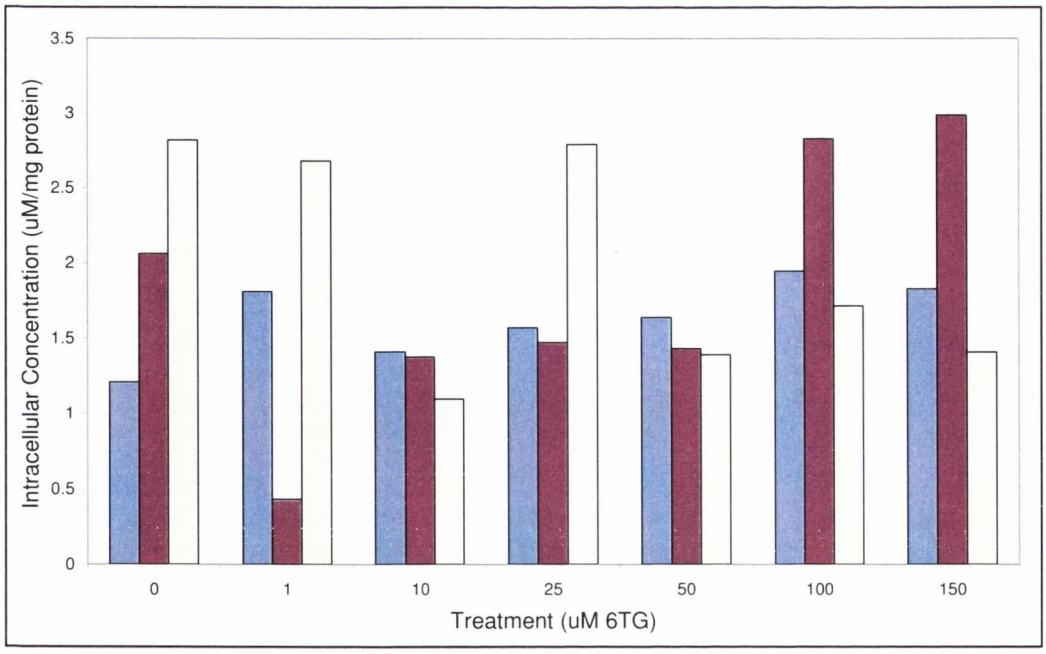


Figure 4.5 Quantitation of Intracellular Accumulation of 6TG and 6MP. Measurement of the intracellular concentration of 6TG (a) or 6MP (b) and are representative of several repeated experiments in THP1 cells. All samples were assayed in duplicate. (■) = 2 hour incubation, (■) = 6 hour incubation; (□) = 24 hour incubation.

a.



b.

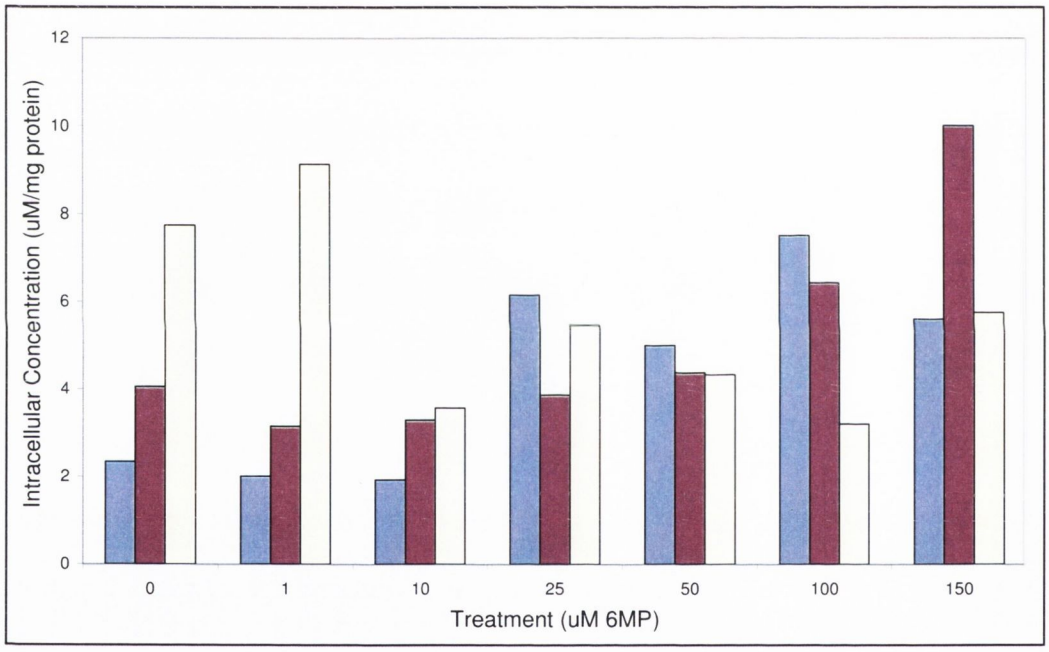


Figure 4.6 Intracellular Concentration of 6TG and 6MP Normalised to Protein Content of Sample. Measurement of the intracellular concentration of 6TG (a) or 6MP (b) normalised to the protein content of that sample. These data are representative of several repeated experiments in THP1 cells. All samples were assayed in duplicate for thiopurine concentration and protein concentration. (■) = 2 hour incubation, (■) = 6 hour incubation; (□) = 24 hour incubation. Normalised values were calculated by dividing the concentration of 6TG or 6MP in the sample by the total protein content of the sample. Protein content 6TG cells: average, 2.58mg, range 1.46 to 3.19mg; 6MP cells: average, 2.72mg, range 1.68 to 3.18mg.

4.3 INTRACELLULAR FLUORESCENT STAINING FOR 6TG and 6MP

4.3.1 Fluorescence Fixation and Staining Protocol

1. Incubate cells with appropriate treatment and time period.
2. Centrifuge tissue culture plate at 400rcf for 10 minutes and remove the supernatant, taking care not to disturb the cells on the plate. Wash the plate twice with PBS, centrifuging after each wash step.
3. Add 100µl 1% paraformaldehyde (PFA) to each well and incubate at room temperature for 10 minutes.
4. Wash cells once in PBS. Add 100µl 0.5% Triton X solution for 90 seconds.
5. Repeat the wash step two times, and add 50µl 1° antibody solution to each well. Incubate plate at room temperature for 1 hour.
6. Repeat the wash step twice, and add 50µl of the 2° antibody solution to each well. Incubate the plate at room temperature in the dark for 1 hour.
7. Wash plate twice, then aliquot 100µl of Hoechst 33342 (5µg/ml) to each well. Incubate the plate in the dark at room temperature for 10 minutes.
8. Wash plate twice, aliquot 200µl PBS to each well, and store sealed plate at 4°C for future analysis.

4.3.2 Optimisation of Assay Parameters

4.3.2.1 Antibody Concentration

For the purpose of fluorescent staining, the recommended concentration range for 1° antibodies is 0.5-5µg/ml and 1-10µg/ml for 2° antibodies. To determine the optimum combination of 1° and 2° antibodies for this assay, we labelled THP1 cells according to the plate layout in Table 4.4. Cells ($1x10^5$) were incubated with 150µM 6TG or 6MP for 12 hours prior to staining. The plate was analysed on the Cellomics KineticScan workstation.

Table 4.4 Plate Layout for 1° and 2° Antibody Concentration Optimisation. Well designations for each treatment are used for reference purposes.

	Primary Antibody Concentration					
	0.5µg/ml	1µg/ml	2µg/ml	5µg/ml		
6TG Treated Cells	A1	A2	A3	A4	1µg/ml	Secondary Antibody Concentration
	B1	B2	B3	B4	2µg/ml	
	C1	C2	C3	C4	5µg/ml	
	D1	D2	D3	D4	10µg/ml	
6MP Treated Cells	E1	E2	E3	E4	1µg/ml	
	F1	F2	F3	F4	2µg/ml	
	G1	G2	G3	G4	5µg/ml	
	H1	H2	H3	H4	10µg/ml	

Overall, the results from this experiment were inconsistent. Very few cells remained in any of the wells which made it difficult to accurately determine which combination of antibodies was the best. There was significant background signal in samples A1 and E1. The best results were from well D4.

This experiment was repeated, with similar loss of cell numbers. Several modifications were made to the protocol in an effort to increase the number of cells remaining at the end of the staining procedure. Firstly, the type of plate was changed from an Iwaki 96-well

tissue culture plate to a Nunc brand 96 well tissue culture plate. In order to assess whether the Nunc plates had better success at maintaining cell numbers throughout the staining process, untreated cells at a concentration of $4x10^6$ cells/ml were seeded onto the plate at 100µl per well and serially diluted. The cells were then fixed and permeabilised according to the protocol in Section 4.3.1. Following the permeabilisation step, the cells were washed repeatedly with PBS (maximum of 10 wash steps) and visualised under the light microscope with the 20X objective. The best retention of cell numbers was in the wells seeded with $2x10^5$ cells. All future experiments were performed with this cell density. The number of wash steps had already been reduced in an effort to limit cell loss, but were reduced further to one wash between the 1° and 2° antibody staining steps, and one wash between the 2° antibody and the Hoechst stain.

When the cell density and wash steps had been adjusted, the antibody concentration experiment was repeated. The best results were obtained with 5µg/ml solutions of both the 1° and 2° antibody. A typical field from that antibody pair is shown in Figure 4.7.

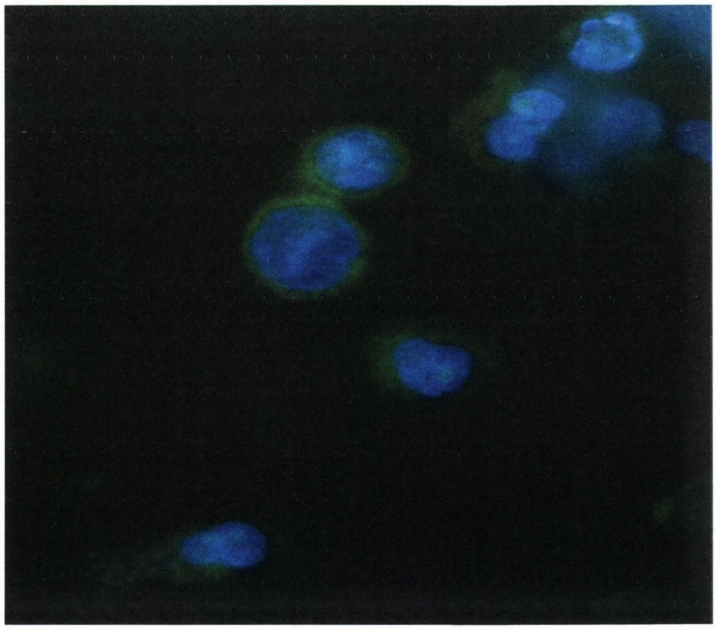


Figure 4.7 Optimisation of Antibody Concentrations for Fluorescent Staining. THP1 cells stained with 5µg/ml 1° antibody and 5µg/ml 2° antibody. Image captured using the 40X objective on the KineticScan workstation. Blue stain is the Hoechst 33342 nuclear stain; green stain is the Alexa488 antibody.

4.3.2.2 Blocking Experiments

Initial experiments with the optimised antibody concentrations revealed that there was a high degree of non-specific binding of one of the antibodies. The nuclear fluorescence intensity for the Hoechst stain was consistent across treatments (Figure 4.8). However, the fluorescence intensity of the cytoplasmic stain (anti-6TG antibody + Alexa 488 goat anti-mouse antibody) was within the same range for treated and untreated cells (Figure 4.9). Addition of NBMPR, a nucleoside transport inhibitor, did not significantly affect the level of cytoplasmic staining.

The source of the non-specific binding needed to be identified in order to improve the quality of the staining and the data that could be acquired. The KineticScan can be programmed to subtract the background fluorescence from the readings within that channel. The parameters are set by the user, and when the background intensity is very high, it overwhelms the intensity in the cells, resulting in poor resolution of the cytoplasmic compartment. This made it difficult to properly define the data collection parameters.

A series of experiments incorporating a blocking step were performed. A high background signal was hypothesised to be due to non-specific binding of the 2° antibody. The cells were blocked with increasing concentrations of normal goat serum (NGS) in PBS + 1% BSA as the 2° antibody was goat anti-mouse. To confirm the source of the background signal, we also included cells incubated with 1° antibody only and 2° antibody only. The results of the blocking experiments are detailed in Figure 4.10. The optimum results were obtained with a 1/100 dilution of NGS in the blocking solution with 1µg/ml of 1° and 2° antibodies.

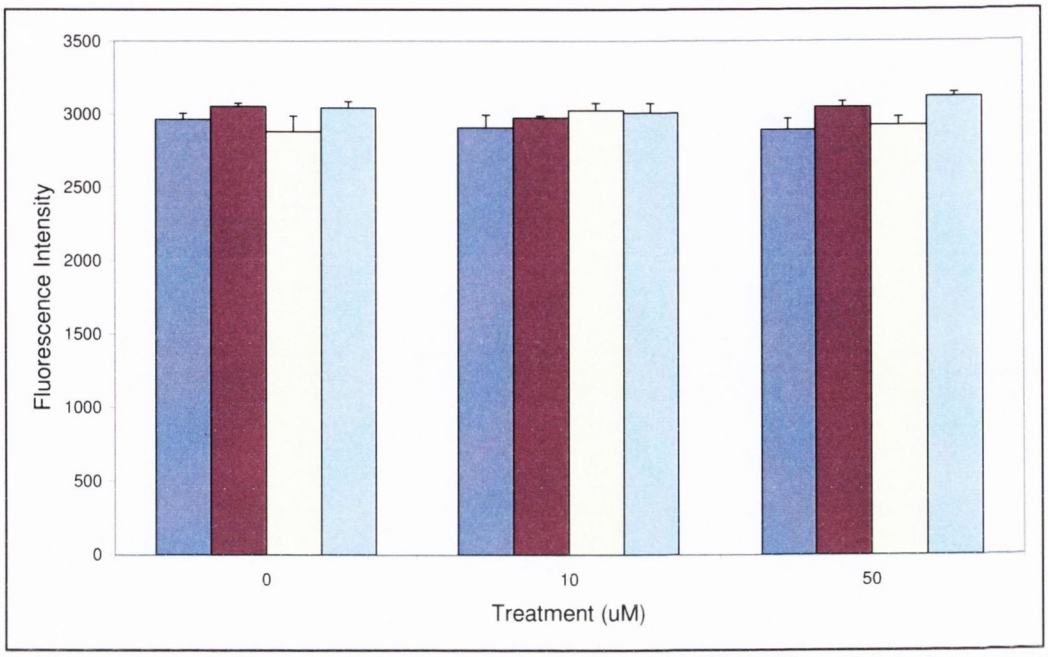


Figure 4.8 Intensity of the Hoechst 33342 stain in THP1 cells. Data shown are the average of values from three fields in the same well + SEM. Cells were treated with 6TG (■), 6TG + NBMPR (■), 6MP (□) or 6MP + NBMPR (□). Cells were treated with 100nM NBMPR or PBS prior to the addition of 6TG or 6MP. Cells were then incubated for a further 16 hours at 37°C before fixation and staining.

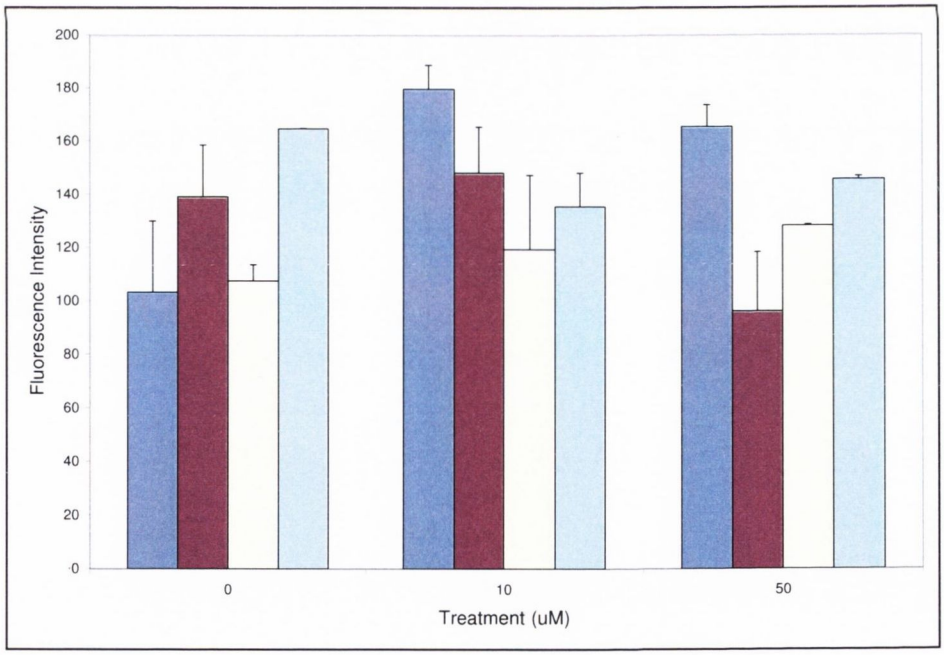


Figure 4.9 Intensity of Cytoplasmic stain in THP1 cells. Data shown are the average of values from three fields in the same well + SEM. Cells were treated with 6TG (■), 6TG + NBMPR (■), 6MP (□) or 6MP + NBMPR (□). Cells were treated with 100nM NBMPR or PBS prior to the addition of 6TG or 6MP. Cells were then incubated for a further 16 hours at 37°C before fixation and staining.

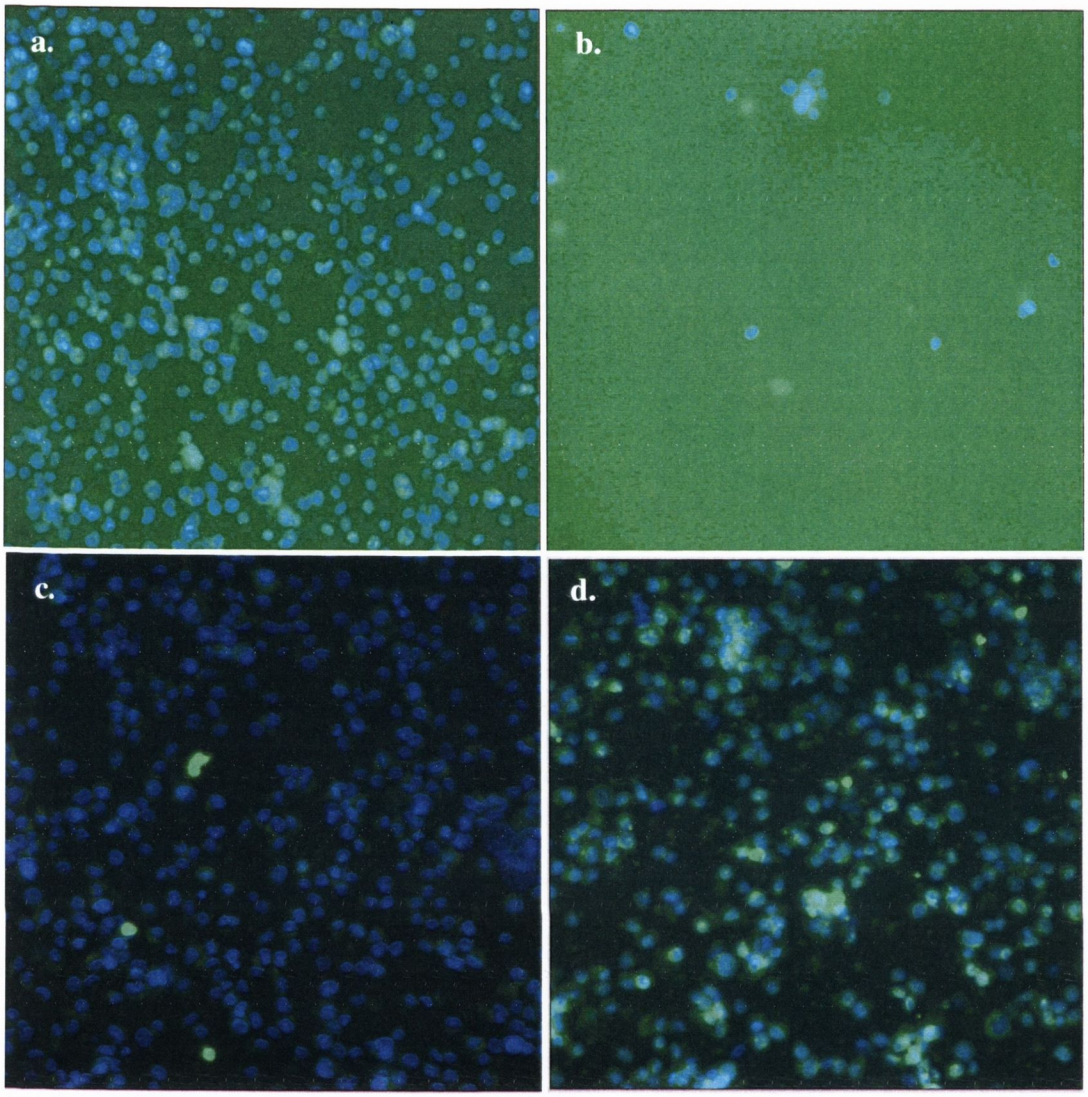


Figure 4.10 Results of Blocking Experiment. All staining experiments were conducted on untreated THP1 cells. Images were acquired with the 20X objective on the KineticScan platform. Pane a. No NGS in blocking solution and no 1° antibody; b. no NGS in blocking solution and no 2° antibody; c. 1/100 dilution of NGS, 1µg/ml 1° and 2° antibodies; d. 1/100 dilution of NGS, 5µg/ml 1° and 2° antibodies. Pane b. has high background because of the low signal due to the absence of a fluorophore in that excitation range.

4.3.3 Experimental Results

Figure 4.11 shows the results of an experiment to quantify the difference in thiopurine concentration between the nucleus and cytoplasm of THP1 cells. There was an increase in the fluorescence intensity in Channel 2 (green) between the untreated and treated cells. However, the ratio between the cytoplasmic and nuclear intensity was the same between the untreated and treated cells (1.2, 1.1, and 1.2, respectively).

Further experiments were conducted in THP1 cells, the results of which are shown in Figure 4.12. Cells treated with the nucleoside transport inhibitor NBMPR prior to the addition of 6TG or 6MP showed increased cytoplasmic and nuclear fluorescence compared to 6TG or 6MP treatment alone. As was observed previously, although the fluorescence intensity increased with certain treatments, the ratio of cytoplasmic to nuclear intensity remained constant between all treatments for both 6TG and 6MP

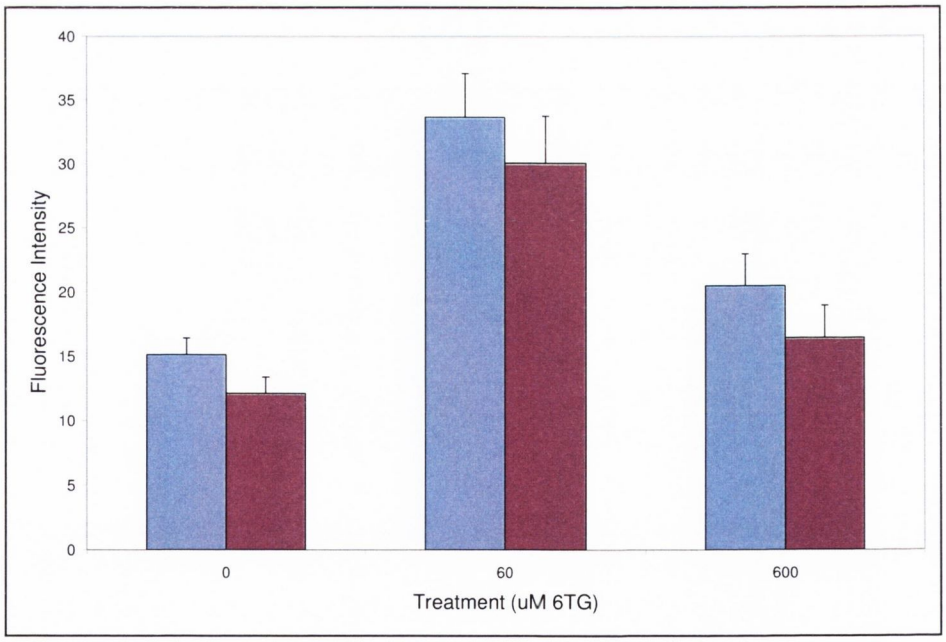
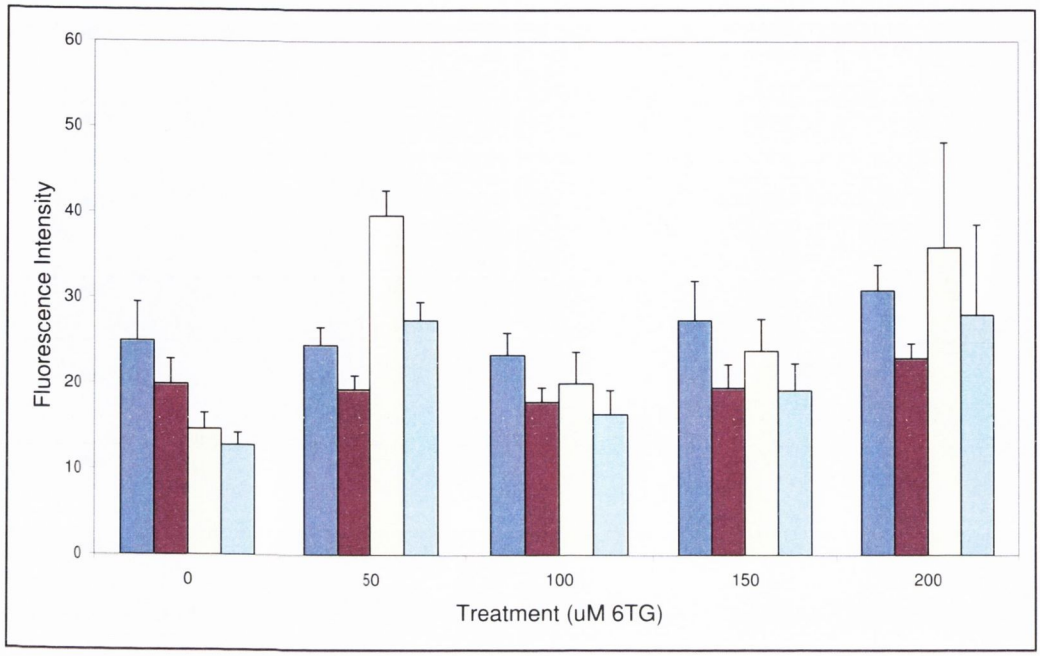


Figure 4.11 Cytoplasmic versus nuclear localisation of 6TG. THP1 cells were incubated with the 6TG for 4 hours at 37°C then fixed and stained for analysis on the KineticScan workstation. Data shown are the average of three fields + SEM. ▢ = cytoplasmic staining; ▢ = nuclear staining. Although the intensity increased, the ratio between cytoplasmic and nuclear fluorescence intensity was the same across the three treatments.

a.



b.

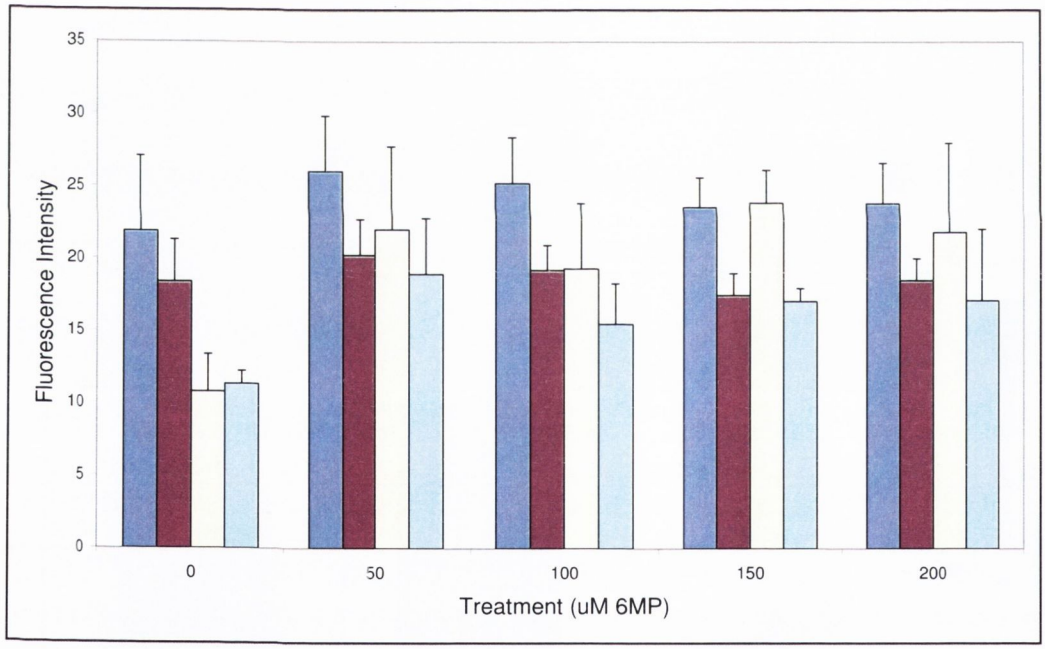


Figure 4.12 Cytoplasmic versus Nuclear localisation of 6TG or 6MP in THP1 cells with and without NBMPR. Data shown are the average of values from two fields in the same well + SEM. Figure a. shows 6TG results; b. shows 6MP results. Bars correspond to cytoplasmic fluorescence (■), nuclear fluorescence (■), cytoplasmic fluorescence + NBMPR (□) and nuclear fluorescence + NBMPR (□). Cells were treated with 100nM NBMPR or PBS 20 minutes prior to the addition of 6TG or 6MP. Cells were then incubated for a further 4 hours at 37°C before fixation and staining. Data was acquired on the KineticScan workstation.

4.4 DISCUSSION

In both methods, we encountered high signal levels in untreated cells. The antibody clone that we chose had very broad substrate specificity, and compounds structurally similar to thiopurines are ubiquitous within the cell. The antibody may be binding to the endogenous purines, creating a false positive. However if this were the case, we would expect to detect thiopurines in all of the samples, which we did not (Figure 4.5).

Other antibodies with a narrower range of specificity are also available. It may be possible to assay the thiopurine content in cells with a panel of antibodies with different reactivity. This would allow quantitation of the thiopurines and their metabolites individually. It would also provide a better image of the localisation of the drugs and their metabolites within the cell. While this would not be as efficient as using only one antibody, it would still allow multiple samples to be assayed on one plate.

The HYB 138-07 antibody has a higher affinity for 6TG than 6MP, therefore it was expected that 6MP would not inhibit antibody binding as strongly as 6TG did (Figure 4.4). These results agree with those obtained by Nerstrøm (1994) in experiments to characterise the antibody. The lower affinity of the antibody may also explain the lower levels of 6MP detected in the experimental samples (Figure 4.5). However, when the thiopurine concentration was normalised to protein content, there was more 6MP in the cells than 6TG (Figure 4.6), even though there was little variation in total protein content. Both 6TG and 6MP are substrates for the same nucleoside transporters. The cells used in these experiments were all from the same population, so there should be very little variation in the concentration and distribution of the transporters between cells. Over all of the experiments, there appears to be no pattern of detection. It is possible that a component of

the lysis buffer interferes with the antibody binding to its target. The variation observed between experiments is an issue that needs further exploration.

Another parameter that may have contributed to the non-specific signal is the plate conjugate concentration. If the plate conjugate concentration is too low, there will be uncoated areas on the plate surface, which would result in non-specific binding (Lav, 1996). The purpose of blocking buffer is to coat any empty areas on the plate surface after the incubation with the conjugate solution to prevent non-specific binding. The concentration of the plate conjugate and the blocking buffer were within the recommended ranges, but this is another area that could be examined to improve the quality of the assay.

We encountered a number of issues in developing the assay for the KineticScan platform. Firstly, we were unable to maintain cell numbers without sacrificing the quality of the images obtained. We reduced the number of washes in an effort to increase the number of cells remaining in the wells at the end of the fixation and staining protocol. However, this may have contributed to the background signal that we observed. Most protocols recommend two to three washes between staining steps to remove any unbound antibody. Any excess antibody in the wells could have contributed to the non-specific signal that we observed. Other investigators have used suspension cells successfully for HCS (Lövborg, 2004), however they used a plate washer for all washes and aspirations rather than manual pipetting as we did.

In an effort to reduce non-specific binding, we also decreased the concentration of both antibodies from 5µg/ml to 1µg/ml. This, along with the NGS blocking solution, appeared to eliminate the non-specific binding that we had observed previously (Figure 4.10c). Reducing the antibody concentrations also reduced the intensity of the signal emitted upon

excitation. To correct for this, we increased the exposure time to the maximal allowed (5 seconds). While this increased the signal from the labelled cells, it also increased the auto-fluorescence of the plates. This feedback from the plates made the background green, making it difficult to accurately define the cellular borders. Although the KineticScan workstation is automated, it operates using parameters which are set by the user based on values derived from control wells. Cells may have been missed, or alternatively included, in the capture phase due to faults in the parameters that we set. This would of course affect the subsequent analysis and the values that it produced.

Although neither of these assays has been fully optimised, there is still opportunity for their development. Analysis of the results obtained so far has pinpointed parameters that can be further investigated to improve the quality of the assays and the results that they provide. Specifically, the other antibodies to 6TG would be of interest in further efforts to develop these assays for clinical monitoring.

CHAPTER 5

PRO-INFLAMMATORY AND PRO-COAGULANT EFFECTS OF MYLOTARG

5.1 INTRODUCTION

Acute Myelogenous Leukemia is one of the most common forms of acute leukemia in adults, affecting 3.4 individuals per 100,000 annually in the United States (SEER 2002). The incidence increases with age, rising from approximately 1 case per 100,000 individuals in the 30 to 34 year old age group, to 1 case per 10,000 in persons between the ages of 65 and 69 (Leukemia and Lymphoma Society, 2007). Traditional cytotoxic therapies can induce remission in 70 to 80% of patients, but these individuals typically relapse within 2 years (van Der Velden, 2001). In addition to the high relapse rate, there is also significant toxicity associated with traditional chemotherapeutic regimens, especially in older populations.

Over 90% of AML blast cells express the Cluster of Differentiation 33 (CD33) antigen. This antigen is expressed on normal myeloid progenitor cells, but not on pluripotent stem cells or non-haematopoietic cells or tissues (Applebaum, 2001). This makes it an ideal therapeutic target for AML, since a monoclonal antibody specific for this antigen can deliver the cytotoxic agent to the affected cells without damaging normal cells. Another characteristic of CD33 that makes it an ideal target is that new antigens are rapidly expressed when the CD33 complex is internalised. This creates a new population of antigens to which the drug can bind (van der Velden, 2004).

CD33 is a member of the sialic acid binding Ig-like lectins (siglecs) receptor family. CD33 shares a high degree of sequence similarity with other siglecs in both the intracellular and extracellular region. This group of molecules are known as CD33-related siglecs. These

molecules also express two conserved immunoreceptor tyrosine-based inhibitory motifs (ITIM) in their cytoplasmic tails. CD33-related siglecs are differentially expressed on the cells of the haematopoietic system. Their cellular expression pattern and the two ITIMs suggest that the CD33-related siglecs play a role in regulating cellular activation in the immune system most likely as inhibitory receptors (Crocker, 2001). Disruption of either of the ITIMs affects the internalisation of CD33, further emphasising their importance (Walter, 2005).

Gemtuzumab ozogamicin (Mylotarg®; GO) consists of a humanised anti-CD33 murine monoclonal antibody conjugated to the cytotoxic antibiotic calicheamicin (Figure 5.1).

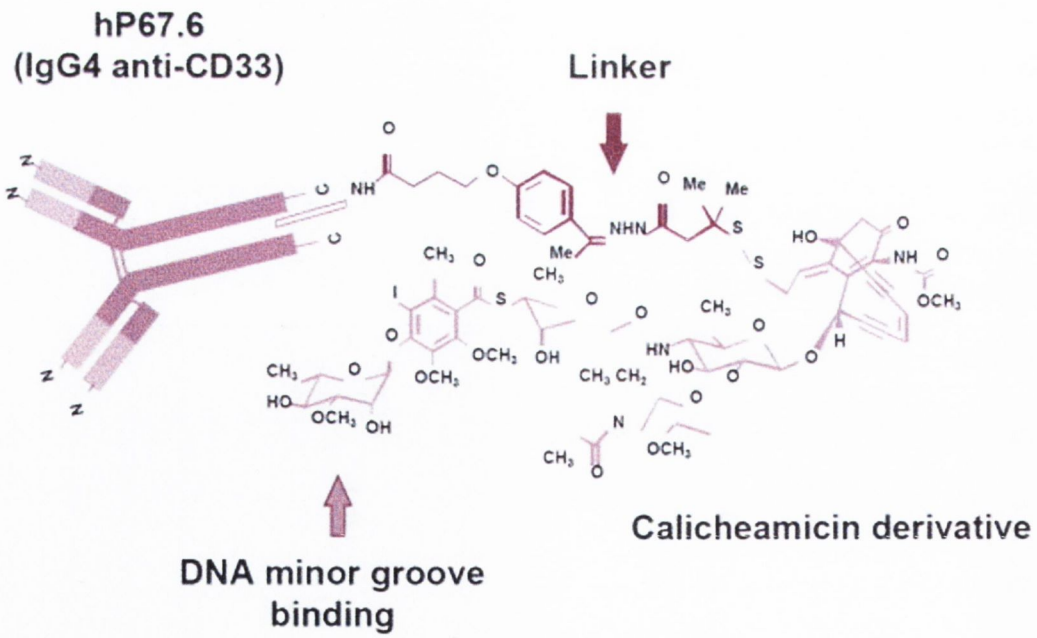


Figure 5.1 Structure of Gemtuzumab Ozogamicin. Two - three calicheamicin molecules are conjugated to each antibody. Taken from Amadori *et al*, Best Prac & Research Clin Haem; 2006, 19(4): 715-736.

When the monoclonal antibody binds to the CD33 antigen, the antigen-antibody complex is internalised. The link between the antibody and the antibiotic includes two labile bonds, a hydrazone and a sterically hindered di-sulfide. The hydrazone bond between the antibody and the cytotoxic antibiotic is cleaved by acid hydrolysis inside the lysosome, releasing the calicheamicin molecule to bind to DNA (Wu, 2005). Calicheamicin binds to DNA in a sequence-specific manner, causing double strand breakage and apoptosis (Sievers, 2001). One of the distinguishing features of this drug is that it saturates the target within 30 minutes, which reduces the likelihood of the antibody-drug bond being cleaved before the molecule has been internalised (Wu, 2005).

Calicheamicin is an enediyne derived from the soil organism *Micromonospora echinospora* ssp.*Calichensis*. It is a very potent tumour antibiotic, more than 5000 times as potent as adriamycin, however it lacks tumour specificity. Calicheamicin exerts its cytotoxic activity *via* oxidative double strand scission of DNA (Ahlert, 2002). Inside the cell, calicheamicin is reduced by glutathione. Once calicheamicin is reduced, the enediyne ring cyclises, creating the reactive biradical intermediate (Amadori, 2006). This reactive compound binds to the minor groove of DNA in a sequence specific manner at 3'-TCCT-5'. When bound to DNA, the reactive intermediate extracts hydrogen from the deoxyribose backbone causing double strand breaks in the structure, which ultimately leads to cell death (Frankel, 2003).

Calicheamicin is conjugated to a humanised anti-CD33 antibody (hP67.6) to target delivery of the agent to AML blast cells. The antibody was humanised by grafting the antigen specific regions of the original murine antibody onto a human immunoglobulin isotype G4 (IgG4) scaffold. The IgG4 isotype was chosen because it has fewer Fc dependent functions than other Ig subtypes, therefore it is less likely to cause an

immunogenic response in the patient (Frankel, 2003). A hydrazone bond links calicheamicin to hP67.6 *via* lysine residues on the antibody. The hydrazone bond releases the cytotoxic calicheamicin at the low pH found in the lysosomes, where, the antibody conjugate is routed once internalised by the cell (Hamann, 2002a). Previous studies have shown that the hydrazone bond is required to maintain the selectivity and potency of the antibody-calicheamicin conjugate (Hamann, 2002b).

Cellular response to GO depends on the expression of multi-drug resistance proteins (MDRs). Multi-drug resistance proteins are membrane bound proteins that pump drugs out of the cell. Permeability glycoprotein (Pgp), is a member of this family of proteins that is associated with resistance to chemotherapeutic drugs (Tallman, 2005a). Permeability glycoprotein is expressed mainly in healthy tissues, but it is also prevalent in older patients and individuals with relapsed or refractory AML. Permeability glycoprotein expression has been found on the blast cells of 19 to 75% patients with *de novo* AML (Walter, 2003).

The side effects of Mylotarg treatment are limited compared to traditional chemotherapy regimens for AML. Patients experience transient neutropenia and thrombocytopenia, as the antigen is expressed on myeloid precursor cells, but not on the more primitive haematopoietic stem cells. Reversible increases in bilirubin and transaminase levels have also been noted.

5.2 MATERIALS AND METHODS

5.2.1 Materials

Mylotarg, calicheamicin and unconjugated hP67.6 antibody were kindly provided by Wyeth (Cambridge, Massachusetts, USA). Mylotarg and hP67.6 were reconstituted in sterile PBS. Calicheamicin was reconstituted in 20% Ethanol in sterile PBS. Once reconstituted, all solutions were immediately aliquoted and stored at -80°C. All other materials used were as per Chapter 2.1.

5.2.2 Methods

Experiments were performed as described in Chapter 3.2 with minor alterations. *In vitro* exposure to Mylotarg must be limited to a maximum of 4 hours. Longer incubation times increase the likelihood that calicheamicin will be hydrolytically released from the antibody in the supernatant (Bianca Goemans, Amsterdam, the Netherlands, personal communication). To exclude the effects of free calicheamicin, experiments were performed as described in Chapter 3.2, but after 1.5 hours incubation, cells were washed twice in pre-warmed medium and resuspended in 1ml of pre-warmed medium. The washed cells were returned to the incubator for the remainder of designated time period. All cytokine assays were performed on supernatant collected after the wash step.

5.3 RESULTS

5.3.1 CD33 Expression

CD33 was expressed on THP1 cells (Figure 5.2) but not on HepG2 cells (Figure 5.3). A small proportion (8%) of the THP1 cell population expressed low levels of CD33 on the cells surface.

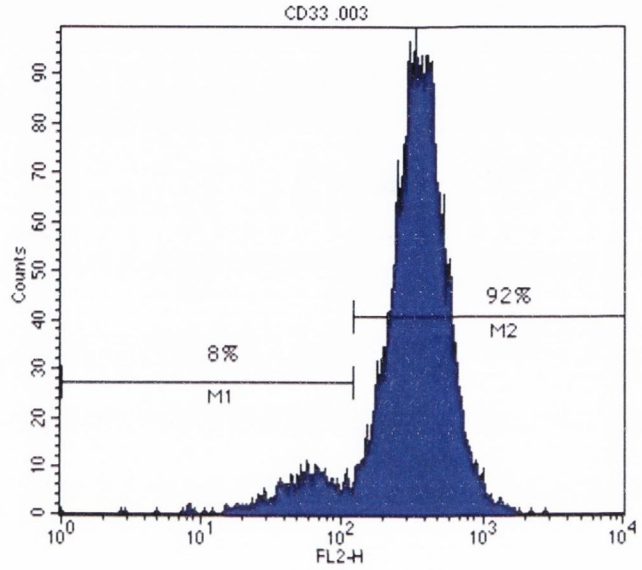


Figure 5.2 CD33 Expression in THP1 cells. There were two distinct populations of cells based on CD33 expression; CD33 dim (8%) and CD33 bright (92%).

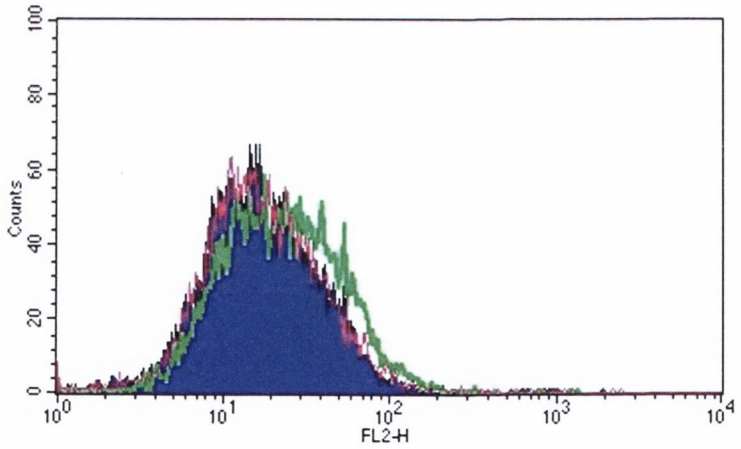
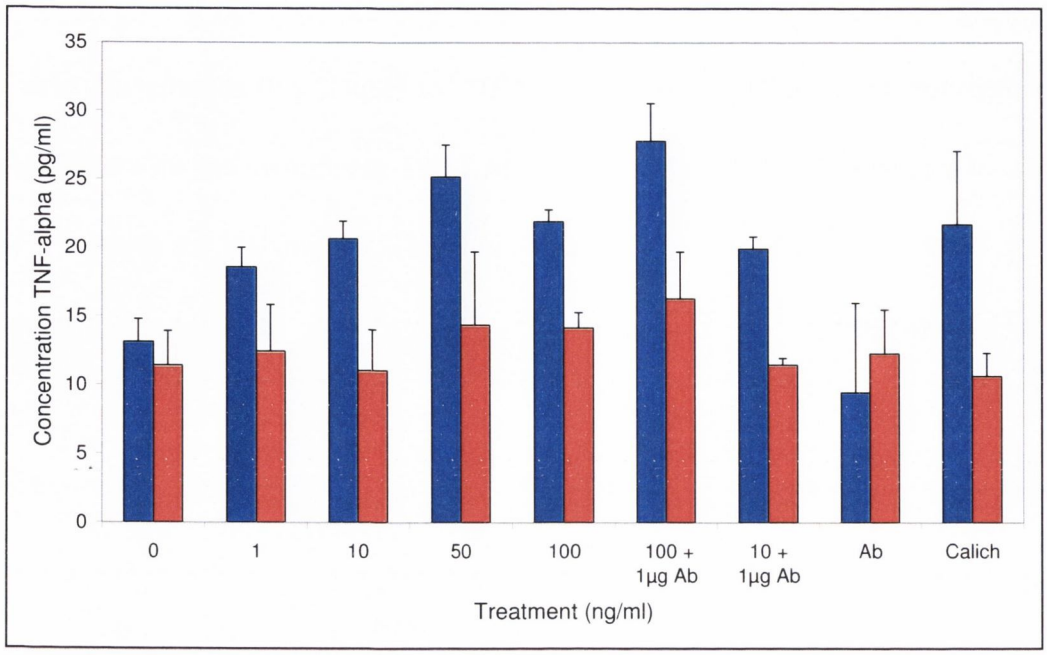


Figure 5.3 CD33 Expression in HepG2 cells. No CD33 antigen was detected on the surface of HepG2 cells. Purple histogram, unstained cells. Pink histogram, CD33 stained cells. Green histogram, isotype control stained cells.

5.3.2 Cytokine Release

Mylotarg, calicheamicin or the unconjugated hP67.6 antibody did not significantly affect the secretion levels of TNF-α or IL-8 in THP1 or HepG2 cell supernatants after 6 or 24 hours of treatment. TNF-α and IL-8 levels in THP1 supernatant are shown in Figure 5.4 a and b, respectively. TNF-α and IL-8 levels in HepG2 supernatant are shown in Figure 5.5 a and b, respectively.

a.



b.

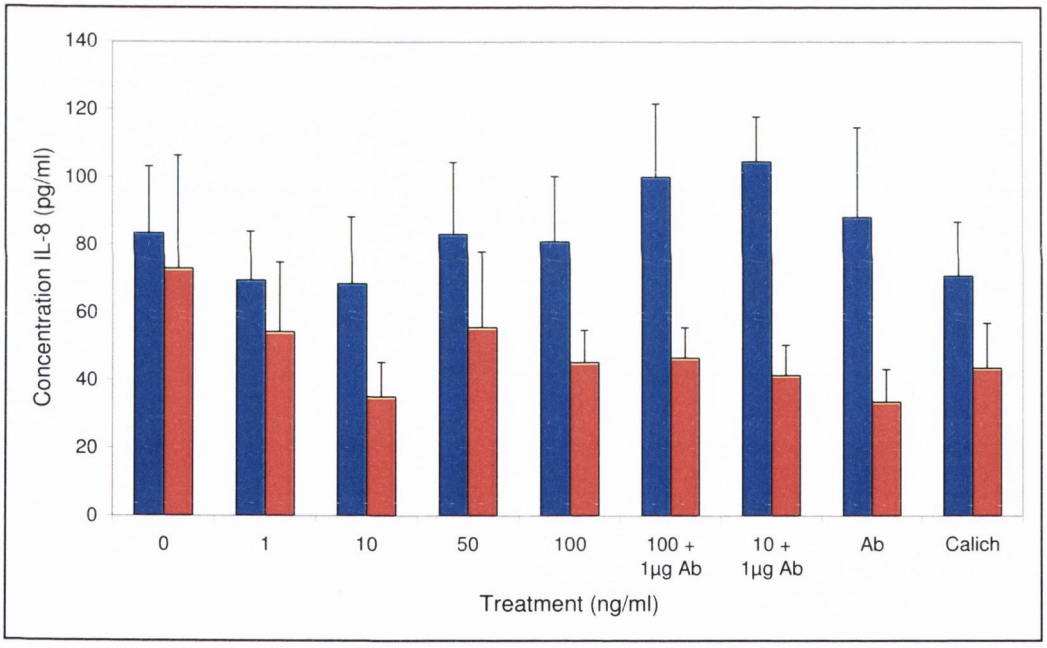
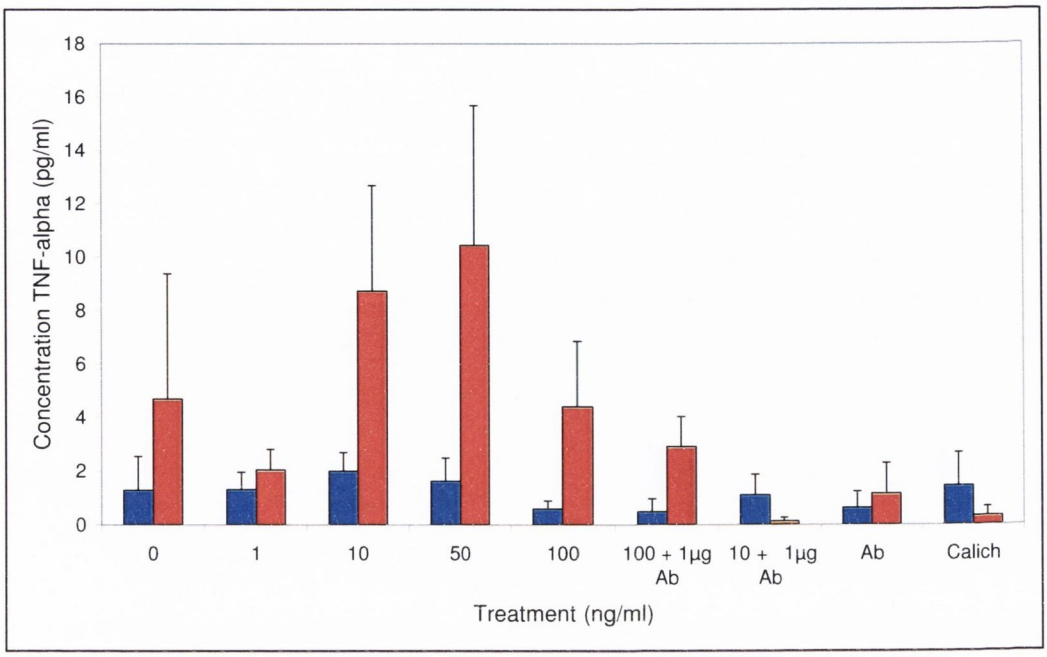


Figure 5.4 Cytokine Release in THP1 cells after treatment with Mylotarg. TNF-α (a) and IL-8 (b) levels were measured in the cell supernatant after 6 (■) or 24 (■)hours incubation with GO, calicheamicin, or unconjugated hP67.6 antibody. Results shown are the mean + SEM of at least 3 independent experiments assayed in duplicate. Data were analysed by two-way repeated measures ANOVA. If the ANOVA was significant (P <0.05), *a posteriori* comparisons of treatment to untreated control at the same time point were made by Least Significant Difference. *, P<0.05; **, P<0.01; ***, P<0.001.

a.



b.

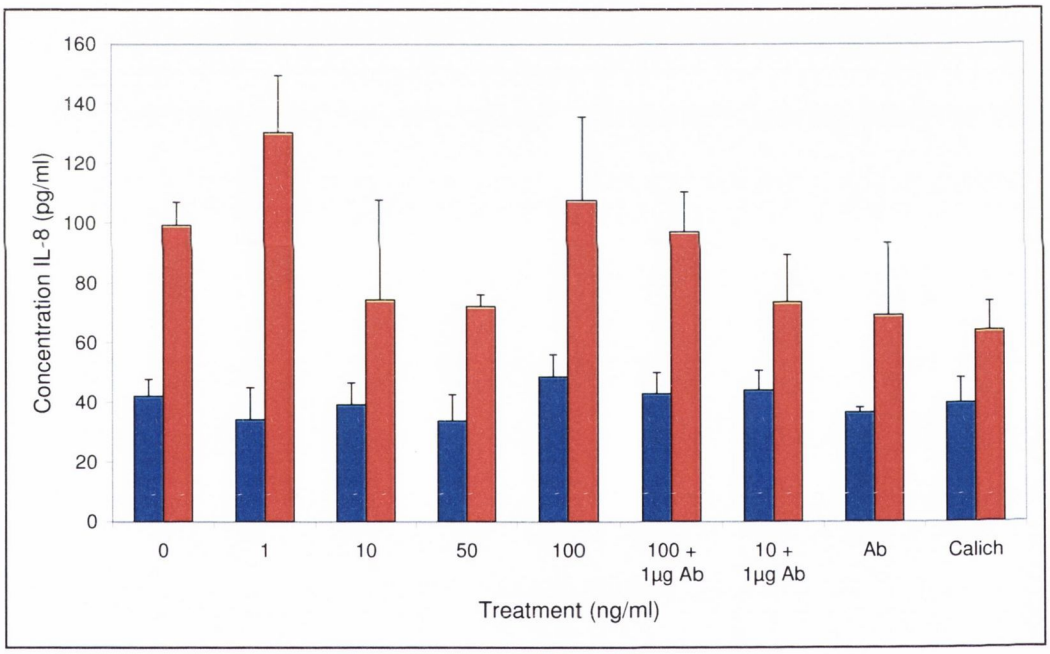


Figure 5.5 Cytokine Release in HepG2 cells after treatment with Mylotarg. TNF-α (a) and IL-8 (b) levels were measured in the cell supernatant after 6 (■) or 24 (■) hours incubation with GO, calicheamicin, or unconjugated hP67.6 antibody. Results shown are the mean + SEM of at least 3 independent experiments assayed in duplicate. Data were analysed by two-way repeated measures ANOVA. If the ANOVA was significant ($P < 0.05$), *a posteriori* comparisons of treatment to untreated control at the same time point were made by Least Significant Difference. *, $P<0.05$; **, $P\leq0.01$; ***, $P\leq0.001$.

5.3.3 Viability

Mylotarg, calicheamcin or hP67.6 did not have any significant effect on the viability of THP1 or HepG2 cells. Results for THP1 cells are shown in Figure 5.6. The results for HepG2 cells are shown in Figure 5.7.

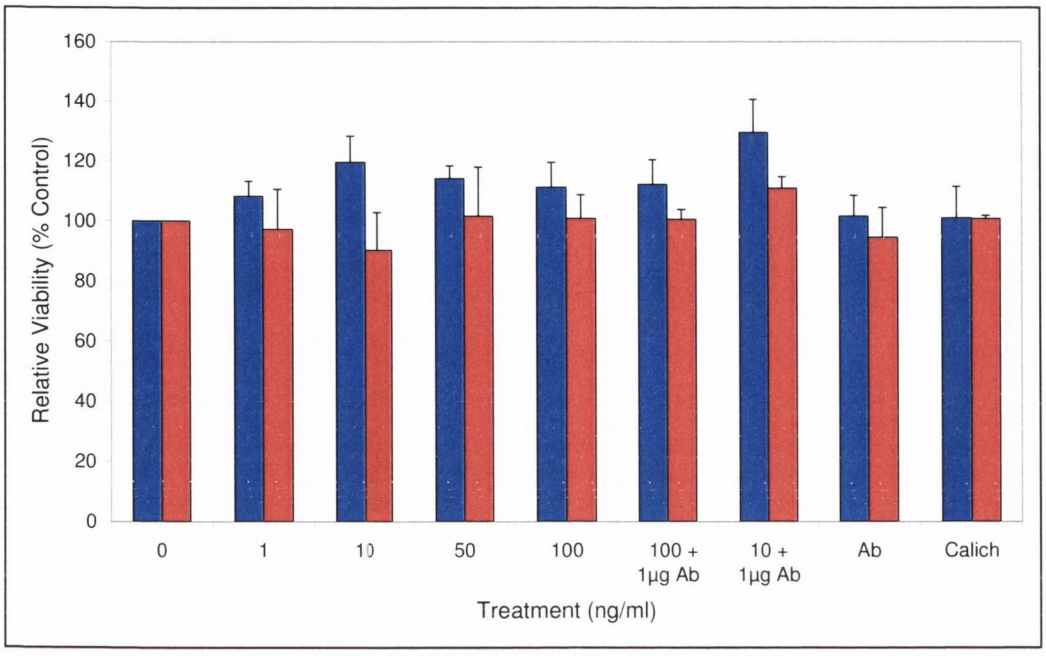


Figure 5.6 Viability of THP1 cells after treatment with Mylotarg. Viability was measured by the WST-1 assay after 6 (■) or 24 (■) hours incubation. Percentages are relative to untreated cells from the same time point which were defined as 100% viable. Data shown are the mean of at least three separate experiments +SEM. Data were analysed by two-way repeated measures ANOVA.

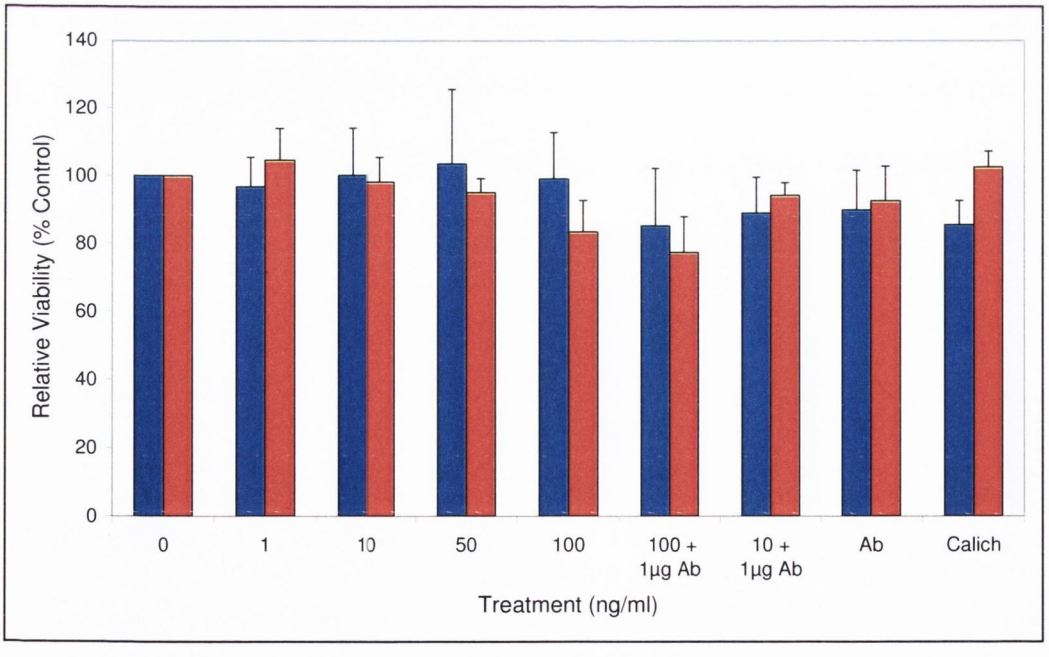


Figure 5.7 Viability of HepG2 cells after treatment with Mylotarg. Viability was measured by the WST-1 assay after 6 (■) or 24 (■) hours incubation. Percentages are relative to untreated cells from the same time point which were defined as 100% viable. Data shown are the mean of at least three separate experiments +SEM. Data were analysed by two-way repeated measures ANOVA.

5.3.4 Tissue Factor

Mylotarg (GO) induced a significant increase in TF expression in THP1 cells after 24 hours (Figure 5.8). The increase was observed at the maximal dose of 100ng/ml ($P \leq 0.01$), and 100ng/ml GO plus 1μg/ml unconjugated antibody ($P \leq 0.001$). There was no significant increase in TF expression on HepG2 cells after 6 or 24 hours of treatment with GO or its components (Figure 5.9).

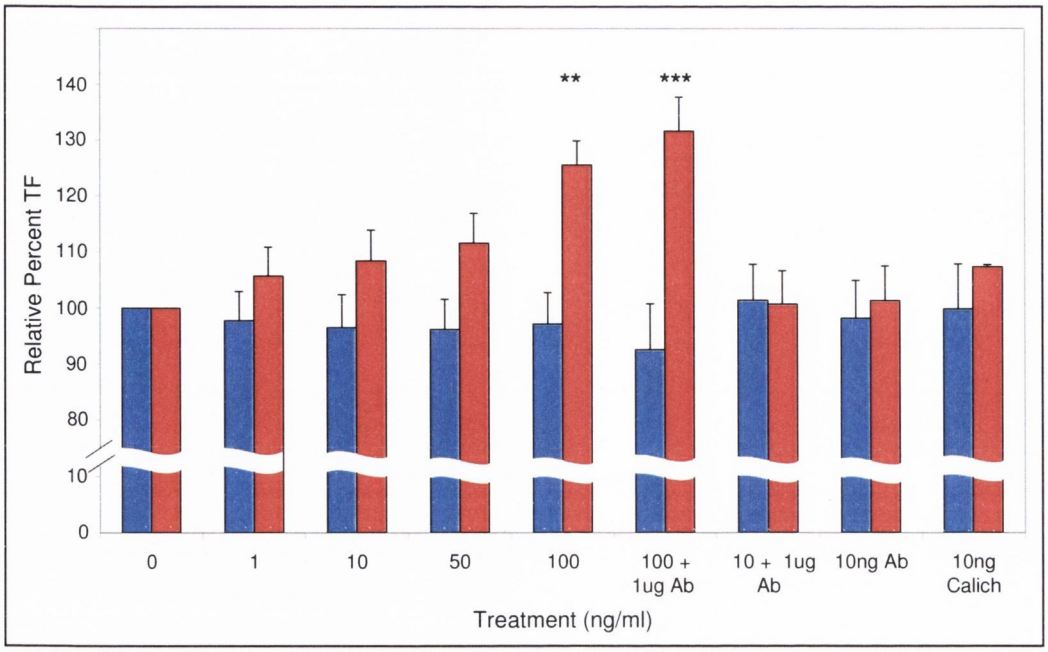


Figure 5.8 Tissue Factor Expression in THP1 cells after treatment with GO. TF levels were measured after 6 (■) or 24 (■) hours incubation. Percentages are relative to untreated cells which were defined as 100% expression. Data shown are the mean of at least three separate experiments +SEM. Data were analysed by two-way repeated measures ANOVA; if significant ($P<0.05$), *a posteriori* comparisons of treatment to untreated control at the same time point were made using Least Significant Difference.
* $P<0.05$, ** $P<0.01$, *** $P<0.001$.

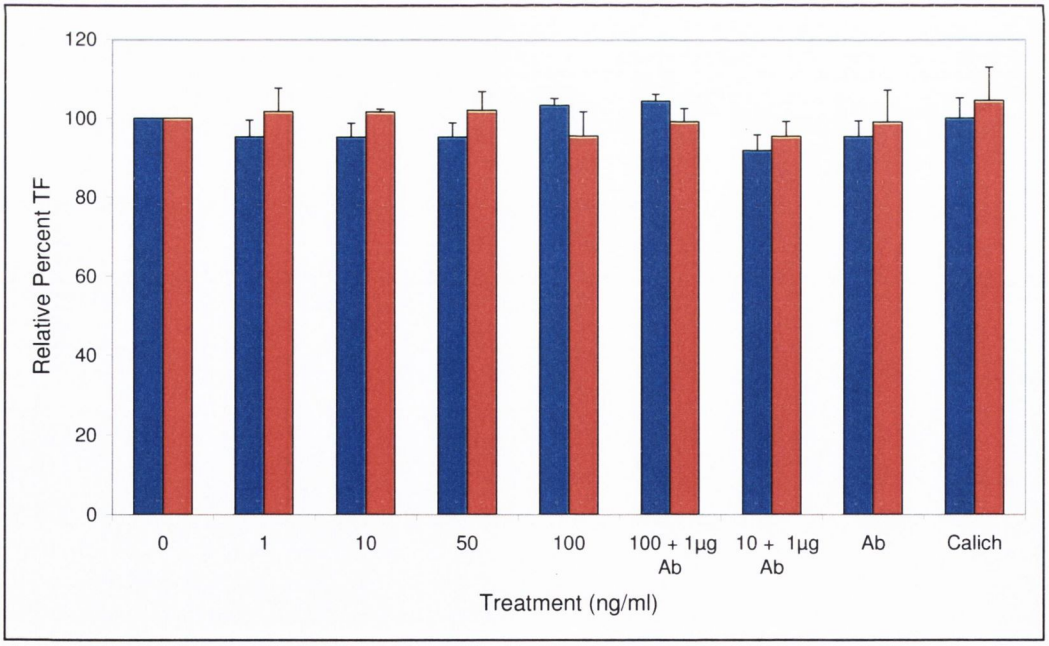


Figure 5.9 Tissue Factor Expression in HepG2 cells after treatment with GO. TF levels were measured after 6 (■) or 24 (■) hours incubation. Percentages are relative to untreated cells which were defined as 100% expression. Data shown are the mean of at least three separate experiments +SEM. Data were analysed by two-way repeated measures ANOVA; if significant ($P<0.05$), *a posteriori* comparisons of treatment to untreated control at the same time point were made using Least Significant Difference.
* P<0.05, ** P<0.01, *** $P<0.001$.

5.4 DISCUSSION

Mylotarg (Gemtuzumab ozogamicin,GO) delivers the cytotoxic compound calicheamicin directly to cells bearing the CD33 antigen *via* a CD33 specific antibody. This reduces the incidence of treatment related side effects because the haematopoietic stem cells are not irreversibly affected. However, GO treatment is more frequently associated with the development of VOD than any other drug in this patient group, particularly at the highest dose of 9 mg/m^2. Our results indicate that GO induces a pro-coagulant response at high doses, which may predispose an individual to developing VOD.

GO induced a significant increase ($P < 0.01$) in TF expression in the CD33+ AML cell line THP1 at the highest dose studied (100 ng/ml) (Figure 5.8). Treatment of THP1 cells with the unconjugated antibody hP67.6 (1µg/ml) and GO (100ng/ml) elicited a further increase in TF expression in THP1 cells ($P < 0.001$). This synergistic effect is most likely due to the continuous renewal of CD33 on the cell surface that was observed *in vitro* by van der Velden *et al.* (2001). When CD33 is bound by an antibody, the complex is internalised and new CD33 antigens are rapidly expressed on the cell surface. This prompt turnover provides more sites for the drug conjugated antibody to bind. Therefore, although the unbound antibody does not have any direct cytotoxic activity *per se*, it may augment the effect of the calicheamicin-antibody conjugate.

HepG2 cells did not show an increase in TF expression after incubation with GO, most likely due to their lack of CD33 expression (Figure 5.9). There have been conflicting reports of the importance of CD33 expression for GO induced toxicity. Jedema *et al.* (2004) found that there was no clear correlation between CD33 expression on leukaemic blasts and response to GO *in vivo*. In addition, they demonstrated incomplete inhibition of the cytotoxic effects of GO in cells pre-treated with unconjugated hP67.6 *in vitro*. Based

on these results, they proposed that at high doses, GO has a CD33 independent mode of internalisation. While this alternative mechanism does not involve CD33, it must still have some degree of specificity otherwise major toxicity would be observed (Jedema, 2004).

In contrast to these results, Walter *et al.* (2005) found that CD33 expression *in vitro* affected response to GO. Also, it has been demonstrated that GO is active against CD33+ ALL both *in vitro* and *in vivo* (Golay, 2005). Further evidence of the role of CD33 in the effectiveness of GO treatment comes from the experiments manipulating ITIMs. The ITIMs are crucial for the internalisation of CD33 when the antigen is bound to antibody. Introducing point mutations into the ITIMs impairs the internalisation of CD33. Cells that express the mutated ITIMs also show decreased response to GO. (Walter, 2005). Without internalisation, the calicheamicin will not be delivered into the cell. Impaired internalisation will also affect the presentation of new CD33 antigens on the cell surface for other drug molecules to bind. Therefore, the evidence to date supports the importance of CD33 expression in the activity of GO.

While high CD33 expression may improve response to GO *in vitro*, the reverse appears to be true *in vivo*. High CD33 expression on peripheral blood cells has been reported as a negative prognostic indicator for response to treatment (van der Velden, 2004). The authors hypothesise that high expression of CD33 on cells in the circulation sequesters GO in the periphery, limiting the amount of drug that reaches the bone marrow. If there is insufficient penetration of GO into the bone marrow, the leukaemic blast cells will not be affected by the treatment regimen. The leukaemic blast cells are the true target of treatment; if they are not eradicated the treatment will have reduced efficacy.

Our investigations found no change in the viability of THP1 or HepG2 cells after treatment with GO (Figures 5.6 and 5.7, respectively). Experiments by Morris *et al.* in AML blast cells showed a dose-dependent decrease in proliferation after 96-102 hours incubation with GO (1, 10, 100 and 1000ng/ml) (Morris, 2006). Naito *et al.* (2000) reported a dose dependent increase in GO induced cytotoxicity in CD33+ cells after 48 hours incubation. However, they also found that CD33+ cells expressing Pgp were insensitive to the effects of GO (Naito, 2000).

Investigation of MDR expression in four AML cell lines showed that THP1 cells had the highest expression of MDR1 on the cell surface, but this study did not find a correlation between MDR1 expression and susceptibility to GO *in vitro*. The researchers also reported that THP1 cells were resistant to the pro-apoptotic effects of GO, but showed a 60% decrease in viability after treatment with 1000ng/ml GO for 48 hrs (Amico, 2003).

Expression of Pgp is also correlated with a poorer clinical response to GO. Reduced complete remission (CR) and survival rates have been reported in patients with Pgp positive AML, both with traditional treatment regimens and GO (Walter, 2003). Achievement of CR was associated with low Pgp activity (Linenberger, 2001). *In vitro* assays of CD33+ AML blast cells showed that Pgp expression conferred resistance to GO (Walter, 2003). Morris et al (2006) demonstrated a significant difference ($P < 0.04$) in *in vitro* sensitivity to 10ng/ml GO between Pgp positive and negative AML blasts. The study revealed an inverse correlation between GO sensitivity and Pgp function, but not between GO sensitivity and Pgp expression (Morris, 2006). Results published by Matsui *et al.* (2002) also found an inverse correlation between Pgp activity and cytotoxic activity of GO on AML blasts *in vitro*. They also reported an inverse correlation between cellular Pgp expression levels and GO sensitivity (Matsui, 2002).

There are several agents that modulate the drug efflux capacity of Pgp. Cyclosporine (CSA), a Pgp inhibitor, improved the *in vitro* response of CSA sensitive AML blast cells to Mylotarg. A higher proportion of samples from non-responders were CSA-sensitive, and showed less drug induced apoptosis *in vitro* in the absence of CSA (Linenberger, 2001). PS833, a non-immunosuppresive analogue of CSA, significantly increased the cytotoxic effects of GO in AML blasts (Matsui, 2002).

Although other researchers report a decrease in THP1 viability after GO treatment (Amico, 2003), their experiments used a much higher dose of GO for a longer time period than ours. This, along with the high activity of Pgp in THP1 cells, may explain the difference in our results with those reported by Amico *et al.* (2003). HepG2 cells also express Pgp, which has been shown to decrease the cytotoxic activity of other chemotherapeutic agents in this cell line (Marguerite, 2007). The lack of response by HepG2 cells is most likely due to their CD33- status, but may well be due to the expression of Pgp.

To date, there have been no publications investigating the inflammatory effects of GO *in vitro* (Search of NLM's PubMed database, November 2007). We did not find a significant change in the secretion of TNF-α or IL-8 in THP1 or HepG2 cells after treatment with GO (Figures 5.4 and 5.5, respectively). However, this may be a result of the reduced cytocidal capacity of GO in these cell lines. It is clear from the current literature that Pgp expression and activity play a role in the cytotoxic effect of GO. It is possible that Pgp also modulates other cellular responses to GO exposure. Further experiments are needed to examine the effect of Pgp status on the inflammatory and coagulant response to GO.

Several studies have demonstrated high saturation levels of peripheral CD33 antigen sites at therapeutic doses of GO. Sievers *et al* (1999) reported near complete saturation of CD33 sites in peripheral blood 30 min after the start of infusion. The near complete saturation was confirmed by van der Velden *et al* (2001), however they measured the amount of GO binding to AML blasts, monocytes and granulocytes at 3 and 6 hours after the start of the infusion (van der Velden, 2001). Another investigation found 75% saturation of peripheral CD33+ cells in patients treated with 6mg/m^2 GO; at the 9mg/m^2 dose, 80% saturation of peripheral CD33+ cells was detected (Treish, 2000). In this study there was a large variation in interpatient and intrapatient pharmacokinetic profiles. The interpatient variability was most likely due to differences in CD33 expression between patients. The intrapatient variability could be due to a reduction in CD33+ cell numbers after the first dose of GO (Treish, 2000).

The plasma half life of GO is 72 hours. If the recommended treatment schedule of 2 doses 14 days apart is followed, it is possible that GO will still be present in the blood at the start of the second infusion (van der Velden, 2001). The average serum concentration of GO in patients after their first infusion was 2.86µg/ml, which increased to 3.67µg/ml after the second infusion (Dowell, 2001). Taking into account the pharmacokinetics of GO and the peripheral CD33 saturation levels after the 6 and 9mg/m^2 dosages of GO may help explain the increased incidence of VOD in patients treated with 9mg/m^2 GO. High doses of GO may exert a pro-coagulant state *in vivo*, as it does *in vitro*, predisposing the patient to the development of VOD.

After the first infusion, there will be a reduction in the number of CD33+ cells in the blood, and some GO penetration into the bone marrow. At the time of the second infusion, there will have been a reduction in the number of peripheral CD33+ cells, and a small

amount of GO will remain in the circulation. The increased concentration of GO will provide more drug molecules to bind to CD33+ cells in the bone marrow, but there will also be excess GO transported to the liver. This increased concentration may activate the liver by a CD33 independent manner, as was proposed by Jedema *et al* (2004). It is also possible that the excess GO binds to CD33+ targets in the liver, such as the Kupffer cells, the resident macrophages of the liver. Once activated, the Kupffer cells could provide the molecular signals necessary to initiate inflammation and fibrosis that leads to the development of VOD. Further studies are needed to determine the cell type in the liver that is targeted by Mylotarg.

CHAPTER 6

CONCLUSIONS AND FUTURE WORK

The results included herein demonstrate that the thiopurines 6-thioguanine (6TG) and 6-mercaptopurine (6MP) have a significant effect on both the target leukaemic cells and the liver. Jurkat E6.1 cells are particularly susceptible to the effect of both 6TG and 6MP, while THP1 cells are more sensitive to 6TG. Neither agent had any effect on 697 cells, which is in agreement with the previous clinical studies that B cell precursor acute lymphoblastic leukaemia (BCP-ALL) requires very high drug concentration in order to elicit an effect *in vitro*. Both 6TG and 6MP have been shown to be pro-inflammatory and pro-coagulant, particularly in hepatocytes. Interleukin (IL)-8 is the predominant chemo-attractant secreted by the hepatocytes, and would provide the signal for infiltration and maturation of monocytes. IL-8 also initiates autocrine and paracrine loops in the injured liver that perpetuate inflammation and lead to the development of fibrosis.

Interleukin 8 is a critical factor in the development of VOD. Secretion of IL-8 by hepatocytes activates Kupffer cells, increasing the expression and secretion of inflammatory mediators TNF-α, IL-1, and IL-6 as well as the fibrogenic cytokine transforming growth factor β1 (TGF-β1). These cytokines will create autocrine and paracrine loops in the injured liver, sustaining high levels of the fibrogenic cytokines. The autocrine loop upregulates cytokine production by the Kupffer cells, while the paracrine loop stimulates the hepatic stellate cells (HSC) (Rojkind, 2001). HSCs are responsible for the deposition of matrix proteins in the sinusoids. They also have contractile ability, which restricts fluid flow through the sinusoids. Upon activation, HSC release monocyte chemotactic peptide-1 (MCP-1) and macrophage colony stimulating factor (M-CSF) which serve as signals for the infiltration and maturation of monocytes. They also release the inflammatory cytokines IL-6 and TGF-β1 (Marra, 1999).

For a single liver insult, the cycle of HSC activation is self-limiting; activated HSC show an increased susceptibility to apoptosis and express decreased levels of bcl-2, an anti-apoptotic protein (Li, 2001). However, repeat or continuous injury will perpetuate the inflammatory response through autocrine and paracrine loops. The cytokines TGF-β and TNF-α inhibit apoptosis in activated HSC, promoting the survival of fibrinogenic stellae cells. Continued production of these cytokines will perpetuate the deposition of the matrix proteins (Li, 2001).

Mylotarg (Gemtuzumab Ozogamicin, GO) elicited a pro-coagulant response it THP1 cells at the highest dose studied (100ng/ml), but did not affect the secretion of Tumour Necrosis Factor (TNF) α or IL-8. This could explain the clinical findings that patients treated with 9 mg/m^2 of GO are more likely to develop VOD than those treated with lower doses (3 or 6 mg/m^2). High doses of GO may exert a pro-coagulant state *in vivo*, as it does *in vitro*, predisposing the patient to the development of VOD.

In contrast to the thiopurines, GO had no effect on HepG2 cells. Mylotarg is a CD33 specific drug, and HepG2 cells do not express CD33. Hepatocytes may be involved in the development of VOD, but they are not the site of initiation with this drug. It is possible that the Kupffer cells, the resident macrophages of the liver, are activated by GO. Once activated, the Kupffer cells could provide the molecular signals necessary to initiate inflammation and fibrosis that leads to the development of VOD. Further studies are needed to determine the liver cell type that is targeted by GO.

VOD is more common in patients treated with 9 mg/m^2 of Mylotarg rather than 6mg/m^2 (Rajvanshi, 2002). This is most likely due to the fact that the 6mg/m^2 dose is sufficient to saturate the CD33 antigens on peripheral blast cells. Any additional drug will remain in

the circulation, travelling to the liver where it will bind to and activate the Kupffer cells. This serves as the initiation signal for fibrosis. Upon repeat administration of the drug, the majority of the blast cells will have been eliminated from the marrow, leaving more molecules free to act on the liver, perpetuating the fibrogenic cascade and leading to the development of VOD.

In addition to studying the cellular effect of the thiopurines, my thesis involved the design and optimisation of methods to detect the intracellular accumulation of thiopurines. Traditionally, thiopurines and their metabolites have been assayed by high pressure liquid chromatography (HPLC) analysis of red blood cells. However, these methods are time consuming and have not been standardised. The aim was to develop a high throughput assay so that intracellular accumulation of thiopurines and their metabolites could be measured quickly and easily in order to optimise patient treatment regimens. A competitive ELISA and a High Content Screening (HCS) assay were developed. During the development of both assays, all parameters were optimised. Briefly, the competitive ELISA procedure involves adding a thiopurine-specific antibody to the sample being assayed. An aliquot of the sample is added to a well on a 96-well plate that has been coated with Bovine Serum Albumin (BSA) conjugated to 6TG. The remaining antibody that has not bound to the thiopurines in the sample will bind to the 6TG on the test plate. The anti-6TG antibody is detected with an enzyme conjugated secondary antibody that will cause a colour change when substrate is added to the well. The colour is quantitated on a spectrophotometer and the concentration of the sample calculated by comparison to a set of standards.

Unfortunately, due to the structural similarity between the thiopurines and naturally occurring bases, the ELISA assay had a high degree of non-specific binding. I was unable

to find the right combination of parameters to optimise the signal difference between the untreated control cells and the treated cells. Other antibodies with a narrower range of specificity are commercially available. It may be possible to design an assay that would screen for 6TG and 6MP individually, as well as their metabolites; however it was beyond the scope of this project to test these as well.

The benefit of the HCS assay versus the competitive ELISA is that the cells are imaged individually using fluorescent antibodies. It is a combination of the imaging qualities of fluorescence microscopy with the quantification capabilities of flow cytometry. Images of the cells are acquired on the Cellomics KineticScan workstation and analysed using software that delineates between the nucleus and the cytoplasm based on parameters that have been set by the user. My aim was to measure the overall accumulation of the thiopurine metabolites, but to also track the transport of the metabolite into the nucleus. This method had very high non-specific binding as well, even though a number of different blocking solutions and antibody concentrations were tested. In addition, it was difficult to maintain cell numbers throughout the number of wash steps that were required. The platform is optimised for adherent cells, so considerable experimentation was required to find the optimum computational parameters. Further experiments with other antibody sets are required in order for this assay to be optimised for use with patient samples.

There are many elements of this study that have scope for continued research. Mylotarg has been shown to elicit a pro-coagulant response in CD33+ cells. It has been implicated in the development of VOD in the clinical setting. The results that we have generated do not identify the site in the liver that is activated by GO, therefore future work with Kupffer cells and co-culturing Kupffer cells and hepatocytes are necessary. In addition, further work with multi-drug resistance proteins will provide vital information on the development

of cellular resistance in patients and how best to overcome it in order to improve treatment outcomes.

The thiopurines 6TG and 6MP both significantly increase IL-8 production in the absence of TNF-α, one of the main regulators of IL-8. Further investigation of the signalling pathways involved in this upregulation is required. Identifying the signalling pathways that the thiopurines induce will provide better insight into their mechanism of action and provide more information on how to avoid their side effects.

In line with improving the knowledge of the intracellular effects of the thiopurines is a better understanding of their absorption. Clinicians in a variety of disciplines would be better equipped to manage treatment regimens if they had more data on the accumulation of the thiopurines and their metabolites *in vivo*. While I was unable to optimise the assay protocols during this project, I believe that with the proper resources they will be successfully optimised and will prove beneficial for monitoring maintenance therapy regimens.

REFERENCES

Adamson, P.C., Poplack, D.G. & Balis, F.M. (1994) The cytotoxicity of thioguanine vs mercaptopurine in acute lymphoblastic leukemia. *Leuk Res,* **18,** 805-810.

Ahlert, J., Shepard, E., Lomovskaya, N., Zazopoulos, E., Staffa, A., Bachmann, B.O., Huang, K., Fonstein, L., Czisny, A., Whitwam, R.E., Farnet, C.M. & Thorson, J.S. (2002) The calicheamicin gene cluster and its iterative type I enediyne PKS. *Science,* **297,** 1173-1176.

Amadori, S. & Stasi, R. (2006) Monoclonal antibodies and immunoconjugates in acute myeloid leukemia. *Immune Therapy in Haematological Malignancies,* **19,** 715-736.

Amico, D., Barbui, A.M., Erba, E., Rambaldi, A., Introna, M. & Golay, J. (2003) Differential response of human acute myeloid leukemia cells to gemtuzumab ozogamicin in vitro: role of Chk1 and Chk2 phosphorylation and caspase 3. *Blood,* **101,** 4589-4597.

Appelbaum, F.R., Rowe, J.M., Radich, J. & Dick, J.E. (2001) Acute myeloid leukemia. *Hematology (Am Soc Hematol Educ Program),* 62-86.

Arceci, R.J., Sande, J., Lange, B., Shannon, K., Franklin, J., Hutchinson, R., Vik, T.A., Flowers, D., Aplenc, R., Berger, M.S., Sherman, M.L., Smith, F.O., Bernstein, I. & Sievers, E.L. (2005) Safety and efficacy of gemtuzumab ozogamicin in pediatric patients with advanced CD33+ acute myeloid leukemia. *Blood %R 10.1182/blood-2004-10-3821,* **106,** 1183-1188.

Baldwin, S.A., Mackey, J.R., Cass, C.E. & Young, J.D. (1999) Nucleoside transporters: molecular biology and implications for therapeutic development. *Mol Med Today,* **5,** 216-224.

Bearman, S.I. (1995) The syndrome of hepatic veno-occlusive disease after marrow transplantation. *Blood,* **85,** 3005-3020.

Bearman, S.I. (2000) Veno-occlusive disease of the liver. *Curr Opin Oncol,* **12,** 103-109.

Bearman, S.I. (2001) Avoiding hepatic veno-occlusive disease: what do we know and where are we going? *Bone Marrow Transplant,* **27,** 1113-1120.

Cara, C.J., Pena, A.S., Sans, M., Rodrigo, L., Guerrero-Esteo, M., Hinojosa, J., Garcia-Paredes, J. & Guijarro, L.G. (2004) Reviewing the mechanism of action of thiopurine drugs: towards a new paradigm in clinical practice. *Med Sci Monit,* **10,** RA247-254.

Carreras, E. (2000) Veno-occlusive disease of the liver after hemopoietic cell transplantation. *Eur J Haematol,* **64,** 281-291.

Collie-Duguid, E.S., Pritchard, S.C., Powrie, R.H., Sludden, J., Collier, D.A., Li, T. & McLeod, H.L. (1999) The frequency and distribution of thiopurine methyltransferase alleles in Caucasian and Asian populations. *Pharmacogenetics,* **9,** 37-42.

Coppell, J., Brown, S. & Perry, D. (2003) Veno-occlusive disease: cytokines, genetics, and haemostasis. *Blood Reviews,* **17,** 63-70.

Coulthard, S. & Hogarth, L. (2005) The thiopurines: An update. *Invest New Drugs,* **23,** 523-532.

Coulthard, S.A., Hogarth, L.A., Little, M., Matheson, E.C., Redfern, C.P., Minto, L. & Hall, A.G. (2002) The effect of thiopurine methyltransferase expression on sensitivity to thiopurine drugs. *Mol Pharmacol,* **62,** 102-109.

Crocker, P.R. & Varki, A. (2001) Siglecs in the immune system. *Immunology,* **103,** 137-145.

da Silva, C.P., de Oliveira, C.R., da Conceicao, M. & de Lima, P. (1996) Apoptosis as a mechanism of cell death induced by different chemotherapeutic drugs in human leukemic T-lymphocytes. *Biochem Pharmacol,* **51,** 1331-1340.

Dahlback, B. (2000) Blood coagulation. *The Lancet,* **355,** 1627-1632.

de Boer, N.K., Reinisch, W., Teml, A., van Bodegraven, A.A., Schwab, M., Lukas, M., Ochsenkuhn, T., Petritsch, W., Knoflach, P., Almer, S., van der Merwe, S.W., Herrlinger, K.R., Seiderer, J., Vogelsang, H. & Mulder, C.J. (2006) 6-Thioguanine treatment in inflammatory bowel disease: a critical appraisal by a European 6-TG working party. *Digestion,* **73,** 25-31.

Dervieux, T., Blanco, J.G., Krynetski, E.Y., Vanin, E.F., Roussel, M.F. & Relling, M.V. (2001) Differing contribution of thiopurine methyltransferase to mercaptopurine versus thioguanine effects in human leukemic cells. *Cancer Res,* **61,** 5810-5816.

Dowell, J.A., Korth-Bradley, J., Liu, H., King, S.P. & Berger, M.S. (2001) Pharmacokinetics of gemtuzumab ozogamicin, an antibody-targeted chemotherapy agent for the treatment of patients with acute myeloid leukemia in first relapse. *J Clin Pharmacol,* **41,** 1206-1214.

Esmon, C.T. (2001) Role of coagulation inhibitors in inflammation. *Thromb Haemost,* **86,** 51-56.

Esmon, C.T. (2004) Crosstalk between inflammation and thrombosis. *Maturitas,* **47,** 305-314.

Estlin, E.J. (2001) Continuing therapy for childhood acute lymphoblastic leukaemia: clinical and cellular pharmacology of methotrexate, 6-mercaptopurine and 6-thioguanine. *Cancer Treat Rev,* **27,** 351-363.

Faioni, E.M. & Mannucci, P.M. (1997) Venocclusive disease of the liver after bone marrow transplantation: the role of hemostasis. *Leuk Lymphoma,* **25,** 233-245.

Frankel, A.E., Powell, B.L., Estey, E. & Tallman, M.S. (2003) Drug Immunoconjugate Therapy of Acute Myeloid Leukemia. In: *Biologic Therapy of Leukemia* (ed. by M. Kalaycio), pp. 43-58. Humana Press Inc., Totowa, N.J.

Gaynon, P.S. (2005) Childhood acute lymphoblastic leukaemia and relapse. *British Journal of Haematology,* **131,** 579-587.

Giles, F.J., Kantarjian, H.M., Kornblau, S.M., Thomas, D.A., Garcia-Manero, G., Waddelow, T.A., David, C.L., Phan, A.T., Colburn, D.E., Rashid, A. & Estey, E.H. (2001) Mylotarg (gemtuzumab ozogamicin) therapy is associated with hepatic venoocclusive disease in patients who have not received stem cell transplantation. *Cancer,* **92,** 406-413.

Gisbert, J.P., Gonzalez-Lama, Y. & Mate, J. (2007) Thiopurine-Induced Liver Injury in Patients With Inflammatory Bowel Disease: A Systematic Review. *Am J Gastroenterol.*

Golay, J., Di Gaetano, N., Amico, D., Cittera, E., Barbui, A.M., Giavazzi, R., Biondi, A., Rambaldi, A. & Introna, M. (2005) Gemtuzumab ozogamicin (Mylotarg) has therapeutic activity against CD33 acute lymphoblastic leukaemias in vitro and in vivo. *Br J Haematol,* **128,** 310-317.

Gomez-Quiroz, L., Bucio, L., Souza, C., Escobar, C., Farfan, B., Hernandez, E., Konigsberg, M., Vargas-Vorackova, F., Kershenobich, D. & Gutierrez-Ruiz, M.C. (2003) Interleukin 8 response and oxidative stress in HepG2 cells treated with ethanol, acetaldehyde or lipopolysaccharide. *Hepatology Research,* **26,** 134-141.

Grem, J.L. & Keith, B. (2002) Mechanism of Action of Cancer Chemotherapeutic Agents: Antimetabolites. In: *The Cancer Handbook* (ed. by M.R. Alison), Vol. 2, pp. 1271-1293. Nature Publishing Group, London.

Hamann, P.R., Hinman, L.M., Beyer, C.F., Lindh, D., Upeslacis, J., Flowers, D.A. & Bernstein, I. (2002a) An anti-CD33 antibody-calicheamicin conjugate for treatment of acute myeloid leukemia. Choice of linker. *Bioconjug Chem,* **13,** 40-46.

Hamann, P.R., Hinman, L.M., Hollander, I., Beyer, C.F., Lindh, D., Holcomb, R., Hallett, W., Tsou, H.R., Upeslacis, J., Shochat, D., Mountain, A., Flowers, D.A. & Bernstein, I. (2002b) Gemtuzumab ozogamicin, a potent and selective anti-CD33 antibody-calicheamicin conjugate for treatment of acute myeloid leukemia. *Bioconjug Chem,* **13,** 47-58.

Iguchi, A., Kobayashi, R., Yoshida, M., Kobayashi, K., Matsuo, K., Kitajima, I. & Maruyama, I. (2001) Vascular endothelial growth factor (VEGF) is one of the cytokines causative and predictive of hepatic veno-occlusive disease (VOD) in stem cell transplantation. *Bone Marrow Transplant,* **27,** 1173-1180.

Jedema, I., Barge, R.M., van der Velden, V.H., Nijmeijer, B.A., van Dongen, J.J., Willemze, R. & Falkenburg, J.H. (2004) Internalization and cell cycle-dependent killing of leukemic cells by Gemtuzumab Ozogamicin: rationale for efficacy in CD33-negative malignancies with endocytic capacity. *Leukemia,* **18,** 316-325.

Kaspers, G.J., Wijnands, J.J., Hartmann, R., Huismans, L., Loonen, A.H., Stackelberg, A., Henze, G., Pieters, R., Hahlen, K., Van Wering, E.R. & Veerman, A.J. (2005) Immunophenotypic cell lineage and in vitro cellular drug resistance in childhood relapsed acute lymphoblastic leukaemia. *Eur J Cancer,* **41,** 1300-1303.

Keuzenkamp-Jansen, C.W., De Abreu, R.A., Bokkerink, J.P. & Trijbels, J.M. (1995) Determination of extracellular and intracellular thiopurines and methylthiopurines by high-performance liquid chromatography. *J Chromatogr B Biomed Appl,* **672,** 53-61.

Krynetski, E.Y., Krynetskaia, N.F., Gallo, A.E., Murti, K.G. & Evans, W.E. (2001) A Novel Protein Complex Distinct from Mismatch Repair Binds Thioguanylated DNA. *Mol Pharmacol,* **59,** 367-374.

Krynetski, E.Y., Krynetskaia, N.F., Yanishevski, Y. & Evans, W.E. (1995) Methylation of mercaptopurine, thioguanine, and their nucleotide metabolites by heterologously expressed human thiopurine S-methyltransferase. *Mol Pharmacol,* **47,** 1141-1147.

Kuby, J. (1997) *Immunology.* W.H. Freeman, New York.

Law, B., Malone, M.D. & Biddlecombe, R.A. (1996) Enzyme-linked immunosorbent assay (ELISA) development and optimisation In: *Immunoassay: A Practical Guide* (ed. by B. Law), pp. 127-149. CRC Press.

Lee, A.U. & Farrell, G.C. (2001) Mechanism of azathioprine-induced injury to hepatocytes: roles of glutathione depletion and mitochondrial injury. *J Hepatol.,* **35,** 756-764.

Lennard, L., Richards, S., Cartwright, C.S., Mitchell, C., Lilleyman, J.S. & Vora, A. (2006) The thiopurine methyltransferase genetic polymorphism is associated with thioguanine-related veno-occlusive disease of the liver in children with acute lymphoblastic leukemia. *Clin Pharmacol Ther,* **80,** 375-383.

Li, D.a.F.S.L. (2001) Hepatic Stellate Cells: Morphology, Function and Regulation. In: *The Liver: biology and pathobiology* (ed. by F.V.C. Irwin L Boyer, Nelson Fausto, David Schachter, David A Shafritz), pp. 455-468. Lippincott Williams and Wilkins, Philadelphia

Linenberger, M.L., Hong, T., Flowers, D., Sievers, E.L., Gooley, T.A., Bennett, J.M., Berger, M.S., Leopold, L.H., Appelbaum, F.R. & Bernstein, I.D. (2001) Multidrug-resistance phenotype and clinical responses to gemtuzumab ozogamicin. *Blood,* **98,** 988-994.

Lovborg, H., Nygren, P. & Larsson, R. (2004) Multiparametric evaluation of apoptosis: effects of standard cytotoxic agents and the cyanoguanidine CHS 828. *Mol Cancer Ther,* **3,** 521-526.

Marguerite, V., Beri-Dexheimer, M., Ortiou, S., Guéant J-L & Merten, M. (2007) Cobalamin Potentiates Vinblastine Cytotoxicity Through Downregulation of mdr-1 Gene Expression in HepG2 Cells. *Cellular Physiology and Biochemistry,* **20,** 967-976.

Marra, F. (1999) Hepatic stellate cells and the regulation of liver inflammation. *J Hepatol,* **31,** 1120-1130.

Matsui, H., Takeshita, A., Naito, K., Shinjo, K., Shigeno, K., Maekawa, M., Yamakawa, Y., Tanimoto, M., Kobayashi, M., Ohnishi, K. & Ohno, R. (2002) Reduced effect of gemtuzumab ozogamicin (CMA-676) on P-glycoprotein and/or CD34-positive leukemia cells and its restoration by multidrug resistance modifiers. *Leukemia,* **16,** 813-819.

Matsumura, S., Hoshino, T., Weizsaecker, M. & Deen, D. (1983) Paradoxical behavior of 6-mercaptopurine as a cytotoxic agent: decreasing cell kill with increasing drug dose. *Cancer TReat Rep,* **67,** 475-480.

McKoy, J.M., Angelotta, C., Bennett, C.L., Tallman, M.S., Wadleigh, M., Evens, A.M., Kuzel, T.M., Trifilio, S.M., Raisch, D.W., Kell, J., Deangelo, D.J. & Giles, F.J. (2007) Gemtuzumab ozogamicin-associated sinusoidal obstructive syndrome (SOS): An overview from the research on adverse drug events and reports (RADAR) project. *Leuk Res,* **31,** 599-604.

McLeod, H.L. & Siva, C. (2002) The thiopurine S-methyltransferase gene locus -- implications for clinical pharmacogenomics. *Pharmacogenomics,* **3,** 89-98.

Morris, J.D., Harris, R.E., Hashmi, R., Sambrano, J.E., Gruppo, R.A., Becker, A.T. & Morris, C.L. (1997) Antithrombin-III for the treatment of chemotherapy-induced organ dysfunction following bone marrow transplantation. *Bone Marrow Transplant,* **20,** 871-878.

Nabhan, C., Rundhaugen, L., Jatoi, M., Riley, M.B., Boehlke, L., Peterson, L.C. & Tallman, M.S. (2004) Gemtuzumab ozogamicin (MylotargTM) is infrequently associated with sinusoidal obstructive syndrome/veno-occlusive disease. *Ann Oncol,* **15,** 1231-1236.

Naito, K., Takeshita, A., Shigeno, K., Nakamura, S., Fujisawa, S., Shinjo, K., Yoshida, H., Ohnishi, K., Mori, M., Terakawa, S. & Ohno, R. (2000) Calicheamicin-conjugated humanized anti-CD33 monoclonal antibody (gemtuzumab zogamicin, CMA-676) shows cytocidal effect on CD33-positive leukemia cell lines, but is inactive on P-glycoprotein-expressing sublines. *Leukemia,* **14,** 1436-1443.

Nerstrom, V.M., Henriksen, U., Nielsen, P.E., Buchardt, O., Schmiegelow, K. & Koch, C. (1994) Monoclonal antibodies to thioguanine: influence of coupling position on fine specificity. *Bioconjug Chem,* **5,** 357-363.

O'Brien, V. & Brown, R. (2006) Signalling cell cycle arrest and cell death through the MMR System. *Carcinogenesis %R 10.1093/carcin/bgi298,* **27,** 682-692.

Rajvanshi, P., Shulman, H.M., Sievers, E.L. & McDonald, G.B. (2002) Hepatic sinusoidal obstruction after gemtuzumab ozogamicin (Mylotarg) therapy. *Blood,* **99,** 2310-2314.

Ritzel, M.W., Ng, A.M., Yao, S.Y., Graham, K., Loewen, S.K., Smith, K.M., Ritzel, R.G., Mowles, D.A., Carpenter, P., Chen, X.Z., Karpinski, E., Hyde, R.J., Baldwin, S.A., Cass, C.E. & Young, J.D. (2001) Molecular identification and characterization of novel human and mouse concentrative Na+-nucleoside cotransporter proteins (hCNT3 and mCNT3) broadly selective for purine and pyrimidine nucleosides (system cib). *J Biol Chem,* **276,** 2914-2927.

Roberts, H.R. & Tabares, A.H. (1995) Overview of the Coagulation Reactions. In: *Molecular Basis of Thrombosis and Hemostasis* (ed. by K.A. High & H.R. Roberts), pp. 35-51. Marcel Dekker, New York.

Roberts, R.L., Barclay, M.L., Gearry, R.B. & Kennedy, M.A. (2004) A multiplexed allele-specific polymerase chain reaction assay for the detection of common thiopurine S-methyltransferase (TPMT) mutations. *Clin Chim Acta,* **341,** 49-53.

Rojkind, M.a.G.P. (2001) Pathophysiology of liver fibrosis. In: *The Liver: biology and pathobiology* (ed. by F.V.C. Irwin L Boyer, Nelson Fausto, David Schachter, David A Shafritz), pp. 721-738. Lippincott Williams and Wilkins, Philadelphia.

Rottman, J.B. (1999) Key role of chemokines and chemokine receptors in inflammation, immunity, neoplasia, and infectious disease. *Vet Pathol,* **36,** 357-367.

Rowell, D.L., Eckmann, L., Dwinell, M.B., Carpenter, S.P., Raucy, J.L., Yang, S.K. & Kagnoff, M.F. (1997) Human hepatocytes express an array of proinflammatory cytokines after agonist stimulation or bacterial invasion. *Am J Physiol Gastrointest Liver Physiol,* **273,** G322-332.

Russmann, S., Zimmermann, A., Krahenbuhl, S., Kern, B. & Reichen, J. (2001) Veno-occlusive disease, nodular regenerative hyperplasia and hepatocellular carcinoma after azathioprine treatment in a patient with ulcerative colitis. *Eur J Gastroenterol Hepatol,* **13** 287-290.

Sievers, E.L., Appelbaum, F.R., Spielberger, R.T., Forman, S.J., Flowers, D., Smith, F.O., Shannon-Dorcy, K., Berger, M.S. & Bernstein, I.D. (1999) Selective ablation of acute myeloid leukemia using antibody-targeted chemotherapy: a phase I study of an anti-CD33 calicheamicin immunoconjugate. *Blood,* **93,** 3678-3684.

Sievers, E.L., Larson, R.A., Stadtmauer, E.A., Estey, E., Lowenberg, B., Dombret, H., Karanes, C., Theobald, M., Bennett, J.M., Sherman, M.L., Berger, M.S., Eten, C.B., Loken, M.R., van Dongen, J.J., Bernstein, I.D. & Appelbaum, F.R. (2001) Efficacy and safety of gemtuzumab ozogamicin in patients with CD33-positive acute myeloid leukemia in first relapse. *J Clin Oncol,* **19,** 3244-3254.

Somerville, L., Krynetski, E.Y., Krynetskaia, N.F., Beger, R.D., Zhang, W., Marhefka, C.A., Evans, W.E. & Kriwacki, R.W. (2003) Structure and dynamics of thioguanine-modified duplex DNA. *J Biol Chem,* **278,** 1005-1011.

Song, D.K., Zhao, J. & Zhang, L.R. (2006) TPMT genotype and its clinical implication in renal transplant recipients with azathioprine treatment. *J Clin Pharm Ther,* **31,** 627-635.

Sparrow, M.P., Hande, S.A., Friedman, S., Lim, W.C., Reddy, S.I., Cao, D. & Hanauer, S.B. (2005) Allopurinol safely and effectively optimizes tioguanine metabolites in inflammatory bowel disease patients not responding to azathioprine and mercaptopurine. *Aliment Pharmacol Ther,* **22,** 441-446.

Stalnikowitz, D.K. & Weissbrod, A.B. (2003) Liver fibrosis and inflammation: A review. *Annals of Hepatology,* **2,** 159-163.

Stoneham, S., Lennard, L., Coen, P., Lilleyman, J. & Saha, V. (2003) Veno-occlusive disease in patients receiving thiopurines during maintenance therapy for childhood acute lymphoblastic leukaemia. *Br J Haematol,* **123,** 100-102.

Swann, P.F., Waters, T.R., Moulton, D.C., Xu, Y.-Z., Zheng, Q., Edwards, M. & Mace, R (1996) Role of Postreplicative DNA Mismatch Repair in the Cytotoxic Action of Thioguanine. *Science %R 10.1126/science.273.5278.1109,* **273,** 1109-1111.

Tang, W., Ziring, D., Gershman, G. & French, S. (2003) Role of macrophages and stellate cells in the pathogenesis of veno-occlusive disease: an electron microscopic case study. *Exp Mol Pathol,* **75,** 201-209.

Tapner, M.J., Jones, B.E., Wu, W.M. & Farrell, G.C. (2004a) Toxicity of low dose azathioprine and 6-mercaptopurine in rat hepatocytes. Roles of xanthine oxidase and mitochondrial injury. *J Hepatol,* **40,** 454-463.

Tapner, M.J., Jones, B.E., Wu, W.M. & Farrell, G.C. (2004b) Toxicity of low dose azathioprine and 6-mercaptopurine in rat hepatocytes. Roles of xanthine oxidase and mitochondrial injury. *J Hepatol,* **40,** 454-463.

Treish, I.M. (2000) Targeting leukemia cells with gemtuzumab ozogamicin. *Cancer Pract,* **8,** 254-257.

van der Velden, V.H., Boeckx, N., Jedema, I., te Marvelde, J.G., Hoogeveen, P.G., Boogaerts, M. & van Dongen, J.J. (2004) High CD33-antigen loads in peripheral blood limit the efficacy of gemtuzumab ozogamicin (Mylotarg) treatment in acute myeloid leukemia patients. *Leukemia,* **18,** 983-988.

van Der Velden, V.H., te Marvelde, J.G., Hoogeveen, P.G., Bernstein, I.D., Houtsmuller, A.B., Berger, M.S. & van Dongen, J.J. (2001) Targeting of the CD33-calicheamicin immunoconjugate Mylotarg (CMA-676) in acute myeloid leukemia: in vivo and in vitro saturation and internalization by leukemic and normal myeloid cells. *Blood,* **97,** 3197-3204.

Vora, A., Mitchell, C.D., Lennard, L., Eden, T.O., Kinsey, S.E., Lilleyman, J. & Richards, S.M. (2006) Toxicity and efficacy of 6-thioguanine versus 6-mercaptopurine in childhood lymphoblastic leukaemia: a randomised trial. *Lancet,* **368,** 1339-1348.

Wadleigh, M., Richardson, P.G., Zahrieh, D., Lee, S.J., Cutler, C., Ho, V., Alyea, E.P., Antin, J.H., Stone, R.M., Soiffer, R.J. & DeAngelo, D.J. (2003) Prior gemtuzumab ozogamicin exposure significantly increases the risk of veno-occlusive disease in patients who undergo myeloablative allogeneic stem cell transplantation. *Blood,* **102,** 1578-1582.

Walter, R.B., Raden, B.W., Hong, T.C., Flowers, D.A., Bernstein, I.D. & Linenberger, M.L. (2003) Multidrug resistance protein attenuates gemtuzumab ozogamicin-induced cytotoxicity in acute myeloid leukemia cells. *Blood,* **102,** 1466-1473.

Walter, R.B., Raden, B.W., Kamikura, D.M., Cooper, J.A. & Bernstein, I.D. (2005) Influence of CD33 expression levels and ITIM-dependent internalization on gemtuzumab ozogamicin-induced cytotoxicity. *Blood,* **105,** 1295-1302.

Yan, T., Berry, S.E., Desai, A.B. & Kinsella, T.J. (2003) DNA Mismatch Repair (MMR) Mediates 6-Thioguanine Genotoxicity by Introducing Single-strand Breaks to Signal a G2-M Arrest in MMR-proficient RKO Cells. *Clin Cancer Res,* **9,** 2327-2334.

Yates, C.R., Krynetski, E.Y., Loennechen, T., Fessing, M.Y., Tai, H.L., Pui, C.H., Relling, M.V. & Evans, W.E. (1997) Molecular diagnosis of thiopurine S-methyltransferase deficiency: genetic basis for azathioprine and mercaptopurine intolerance. *Ann Intern Med,* **126,** 608-614.

Zaza, G., Cheok, M., Yang, W., Panetta, J.C., Pui, C.H., Relling, M.V. & Evans, W.E. (2005) Gene expression and thioguanine nucleotide disposition in acute lymphoblastic leukemia after in vivo mercaptopurine treatment. *Blood,* **106,** 1778-1785.